CRCLEME
Cooperative Research Centre for
Landscape Evolution & Mineral Exploration

CSIRO
EXPLORATION
AND MINING

AMIRA
Australian Mineral Industries Research Association Limited ACN 004 448 266

OPEN FILE
REPORT
SERIES

EXPLORATION GEOCHEMISTRY ABOUT THE MT. GIBSON GOLD DEPOSITS, WESTERN AUSTRALIA

Progress to 31 March 1989

R.R. Anand, R.E. Smith, J. Innes and H.M. Churchward

CRC LEME OPEN FILE REPORT 35

October 1998

(CSIRO Division of Exploration Geoscience Report 20R, 1989.
Second impression 1998)

CRC LEME is an unincorporated joint venture between The Australian National University, University of Canberra, Australian Geological Survey Organisation and CSIRO Exploration and Mining, established and supported under the Australian Government's Cooperative Research Centres Program.

CRC

AMIRA
Australian Mineral Industries Research Association Limited ACN 004 448 266

CRCLEME
Cooperative Research Centre for Landscape Evolution & Mineral Exploration

CSIRO
EXPLORATION AND MINING

EXPLORATION GEOCHEMISTRY ABOUT THE MT. GIBSON GOLD DEPOSITS, WESTERN AUSTRALIA

Progress to 31 March 1989

R.R. Anand, R.E. Smith, J. Innes and H.M. Churchward

CRC LEME OPEN FILE REPORT 35

October 1998

(CSIRO Division of Exploration Geoscience Report 20R, 1989.
Second impression 1998)

CRC LEME is an unincorporated joint venture between The Australian National University, University of Canberra, Australian Geological Survey Organisation and CSIRO Exploration and Mining
Headquarters: CRC LEME c/o CSIRO Exploration and Mining, Private Bag, PO Wembley, Western Australia, 6014

RESEARCH ARISING FROM CSIRO/AMIRA REGOLITH GEOCHEMISTRY PROJECTS 1987-1993

In 1987, CSIRO commenced a series of multi-client research projects in regolith geology and geochemistry which were sponsored by companies in the Australian mining industry, through the Australian Mineral Industries Research Association Limited (AMIRA). The initial research program, "Exploration for concealed gold deposits, Yilgarn Block, Western Australia" (1987-1993) had the aim of developing improved geological, geochemical and geophysical methods for mineral exploration that would facilitate the location of blind, buried or deeply weathered gold deposits. The program included the following projects:

P240: Laterite geochemistry for detecting concealed mineral deposits (1987-1991). Leader: Dr R.E. Smith.
Its scope was development of methods for sampling and interpretation of multi-element laterite geochemistry data and application of multi-element techniques to gold and polymetallic mineral exploration in weathered terrain. The project emphasised viewing laterite geochemical dispersion patterns in their regolith-landform context at local and district scales. It was supported by 30 companies.

P241: Gold and associated elements in the regolith - dispersion processes and implications for exploration (1987-1991). Leader: Dr C.R.M. Butt.
The project investigated the distribution of ore and indicator elements in the regolith. It included studies of the mineralogical and geochemical characteristics of weathered ore deposits and wall rocks, and the chemical controls on element dispersion and concentration during regolith evolution. This was to increase the effectiveness of geochemical exploration in weathered terrain through improved understanding of weathering processes. It was supported by 26 companies.

These projects represented "an opportunity for the mineral industry to participate in a multi-disciplinary program of geoscience research aimed at developing new geological, geochemical and geophysical methods for exploration in deeply weathered Archaean terrains". This initiative recognised the unique opportunities, created by exploration and open-cut mining, to conduct detailed studies of the weathered zone, with particular emphasis on the near-surface expression of gold mineralisation. The skills of existing and specially recruited research staff from the Floreat Park and North Ryde laboratories (of the then Divisions of Minerals and Geochemistry, and Mineral Physics and Mineralogy, subsequently Exploration Geoscience and later Exploration and Mining) were integrated to form a task force with expertise in geology, mineralogy, geochemistry and geophysics. Several staff participated in more than one project. Following completion of the original projects, two continuation projects were developed.

P240A: Geochemical exploration in complex lateritic environments of the Yilgarn Craton, Western Australia (1991-1993). Leaders: Drs R.E. Smith and R.R. Anand.
The approach of viewing geochemical dispersion within a well-controlled and well-understood regolith-landform and bedrock framework at detailed and district scales continued. In this extension, focus was particularly on areas of transported cover and on more complex lateritic environments typified by the Kalgoorlie regional study. This was supported by 17 companies.

P241A: Gold and associated elements in the regolith - dispersion processes and implications for exploration. Leader: Dr. C.R.M. Butt.
The significance of gold mobilisation under present-day conditions, particularly the important relationship with pedogenic carbonate, was investigated further. In addition, attention was focussed on the recognition of primary lithologies from their weathered equivalents. This project was supported by 14 companies.

Although the confidentiality periods of the research reports have expired, the last in December 1994, they have not been made public until now. Publishing the reports through the CRC LEME Report Series is seen as an appropriate means of doing this. By making available the results of the research and the authors' interpretations, it is hoped that the reports will provide source data for future research and be useful for teaching. CRC LEME acknowledges the Australian Mineral Industries Research Association and CSIRO Division of Exploration and Mining for authorisation to publish these reports. It is intended that publication of the reports will be a substantial additional factor in transferring technology to aid the Australian Mineral Industry.

This report (CRC LEME Open File Report 35) is a Second impression (second printing) of CSIRO, Division of Exploration Geoscience Restricted Report 020R, first issued in 1989, which formed part of the CSIRO/AMIRA Project P240.

Copies of this publication can be obtained from:
The Publication Officer, c/- CRC LEME, CSIRO Exploration and Mining, PMB, Wembley, WA 6014, Australia. Information on other publications in this series may be obtained from the above or from http://leme.anu.edu.au/
Cataloguing-in-Publication:

Exploration geochemistry about the Mt Gibson Gold Deposits, Western Australia. Progress to 31st March 1989
ISBN 0 642 28206 4
1. Geochemistry 2. Laterite 3. Gold - Western Australia.
I. Anand, R.R. II. Title
CRC LEME Open File Report 35.
ISSN 1329-4768

ABSTRACT

A regolith, landform, and geochemical orientation study about the S, C, and N lateritic Au deposits at Mt. Gibson clarifies landscape evolution and geochemical dispersion in terms of the dynamics of formation, preservation, and dismantling of the undulating lateritic weathering mantle.

The relatively complex regolith and vegetation patterns are explained in terms of the distribution of (i) sub-areas of erosion of the lateritic mantle to the level of saprolite, (ii) sub-areas of essentially-complete lateritic mantle, and (iii) sub-areas characterized by depositional accumulation of detritus provided by the dismantling of the lateritic mantle upslope, commonly burying the essentially complete laterite weathering profile in the local foot slopes and lowlands.

The regolith units were mapped over the central 3-km by 5-km area, the regolith stratigraphy established, and units of the upper regolith were characterized in field profiles petrographically, mineralogically, and chemically. An idealized regolith/landform facies model has been erected for use in predictions in appropriate terrain, and for planning and integrating follow-up research.

Geochemical analyses of samples of the loose pisolitic, nodular laterite unit collected systematically both from surface and from pit walls, where the unit occurred sub-surface, document the characteristics of the lateritic Au deposits. These and earlier results of the orientation study show that the lateritic Au ore and the area peripheral to it is a multi-element, chalcophile, geochemical anomaly, measuring 1 to 1.5 km across and greater than 4 km in length, with a Au Ag Pb As Bi Sb W association.

Within the loose lateritic unit, and in the underlying duricrust, coincident highs of several of these elements in centres within the overall anomaly suggested a close genetic link with bedrock sources, now verified by occurrences of gold-bearing quartz-hematite veining in saprolitic bedrock revealed by exploration and mining.

Geochemical results of 37 samples of the underlying lateritic duricrust show similar strengths and associations of elements as seen for the unit consisting of loose lateritic pisoliths and nodules. Close comparisons of the geometry of the dispersion patterns of these two closely related regolith units await the result of current research on more extensive sampling of the duricrust.

---o0o---

CONTENTS

1.0 PROJECT LEADER'S PREFACE

R E Smith, 17 March 1989

1.1 GENERAL

The area containing the Mt. Gibson Au deposits was ideal, for reasons given below, for basing substantial research on geochemical dispersion in lateritic terrain that, together with studies at the Boddington, Lawlers, and Bottle Creek Au deposits, would form the initial foundations of the CSIRO/ AMIRA Laterite Geochemistry Project. These studies focus on important Au deposits in differing lateritic landform/regolith situations, covering a range of climatic types and geographic locations.

The district about the Mt. Gibson Au deposits represents, and perhaps typifies, the complex lateritic sand-plain terrain of the Perenjori/Ninghan region, where an essentially complete laterite profile is extensively preserved, much of it lying beneath variable thicknesses and types of surficial regolith units.

At the commencement of CSIRO sampling at Mt. Gibson in November 1986, the areas destined for mining were little disturbed. Subsequent sampling and research has continued as the open-pit mining progressed. Mining has thus provided continued opportunity for comprehensive geochemical, mineralogical, and petrological study of the regolith units. These factors have allowed assembly of a framework of reference or synthesis of regolith relationships for the mining areas and their immediate surroundings.

Bedrock outcrop is scarce in much of the low-relief parts of the Perenjori/Ninghan landscape. In such situations, typical of much of the Yilgarn Block, regolith units form the dominant sampling media, chiefly for geochemistry, in the initial stages of many exploration programmes. To be properly effective, geochemical methods of exploration must be planned, executed, and interpreted within a well-controlled and understood synthesis of regolith characteristics and stratigraphy placed in the context of landform situation (Smith and Anand, 1988), a theme emphasized in this study.

We intend the Mt. Gibson research study, made possible by the co-operation between mining, exploration and research, and through the substantial CSIRO/AMIRA funding, to be a type example providing guidance on the understanding of geochemical approaches to exploration in complex lateritic sand-plain environments.

1.2 OBJECTIVES OF THE MT. GIBSON ORIENTATION STUDY

The objectives are to carry out a laterite geochemical orientation study about the Au deposits at Mt. Gibson within a well-controlled and understood regolith/landform framework.

1.3 ATTRIBUTES OF THE MT. GIBSON AREA

Several attributes were recognized before the study commenced:-

- the area represents complex sand-plain terrain of the semi-arid Perenjori/Ninghan region;
- it contains important styles of concealed ore deposits;
- was little disturbed; and
- contained buried laterite profiles.

Additional attributes were recognized during the study:-

- the area shows the importance of regolith/landform dynamics;
- out of equilibrium soils (high pH) overlie laterites (low-pH), and are related to dynamics;
- the area allows a genetic understanding of a variety of lateritic materials.

1.4 COMPONENTS OF RESEARCH AT MT. GIBSON

Multi-disciplinary CSIRO research at Mt. Gibson has the following components:

- The regolith/landform framework
- Characterization of regolith units
- Dispersion patterns in laterite
- Generalized models of regolith evolution and geochemical dispersion
- Statistics of geochemical variation for the laterite units
- Drilling methods for laterite geochemistry
- The siting and bonding of elements
- Ground-water regimes related to landform position
- Dispersion processes
- Classification of laterites.

The Mt. Gibson research will be reported in several parts. Presented here are the first two: REGOLITH RELATIONSHIPS (Section 2 of this report) provides documentation and understanding of the regolith units without which the significance of other research would be severely limited; GEOCHEMICAL DISPERSION PATTERNS . . . (Section 3) commences geochemical documentation in what we view as the prime sample media for exploration in lateritic terrain.

---o0o---

2.0 REGOLITH RELATIONSHIPS

2.1 INTRODUCTION

The Mt. Gibson Gold Project, a joint venture between Forsayth (Gibson) Ltd and Reynolds Australia Mines Pty Ltd, is located (117° 45′ E 29° 45′ S) some 300 km northeast of Perth and some 200 km from the west coast (Fig. 1). The mine site is 100 km NE along the Great Northern Highway from Dalwallinu and then 10 km east via a formed gravel road.

The purpose of this section is to provide a fundamental understanding of the regolith units in the central 3-km by 5-km part of the Mt. Gibson Au mining area (Figs 2 and 3) as a pre-requisite to describing and understanding geochemical dispersion patterns in laterite and their use for exploration. The report relates the surface distribution of regolith units to their geomorphological setting. The mineralogy, geochemistry, and petrography of the regolith units are described, a synthesis is made through interpretation of profiles, longitudinal and cross sections of regolith stratigraphy, and a working facies model is presented. This generalized model should allow recognition and prediction of regolith relationships in similar situations elsewhere.

The initial stages of the CSIRO research were conducted in parallel with a laterite geochemical exploration programme, which included a phase of regolith appraisal, carried out by GEOCHEMEX Australia for the Mt. Gibson Gold Project. The reports of the GEOCHEMEX work (Birrell and Butler, 1987; Smith, 1987) were made available to us for reference by the management of the Mt. Gibson Gold Project under confidentiality.

A study involving petrography, mineralogy, and geochemistry from four traverses of rotary drill holes at Mt. Gibson had been carried out by Davy *et al.* (1988). However, only the abstract of this work and that content presented at the Second International Conference on Prospecting in Arid Terrain have been available to us.

Davy *et al.* (1988) reported that the weathering profile at Mt. Gibson comprises soil, laterite, mottled clay, saprolite, and bedrock, but these units were not mapped. On the other hand, Birrell and Butler (1987) characterized the regolith units, presented their compilation of regolith stratigraphy and mapped the surface distribution of the units over a 7 by 12-km area centred on the current Au mining areas. The thrust of the GEOCHEMEX work was to sample, for multi-element geochemistry, the residual laterite mantle at surface and also subsurface, using back-hoe pitting and drilling.

2.2 PHYSICAL SETTING AND REGIONAL SURFICIAL GEOLOGY

The area has a semi-arid to arid, hot Mediterranean climate with a 250-mm average annual rainfall, most of which falls during the cooler months of May to August. However, there is a significant component of summer rainfall from erratic thunderstorms.

The area is mantled by thicket communities (Beard, 1976) of various acacia species (particularly *Acacia resinomarginea*). Eucalypt woodlands, largely of salmon gum *(Eucalyptus salmonophloia)*, York gum *(Eucalyptus loxophleba)*,and mallee *(Eucalyptus oleosa)*, together with some native pine *(Callitris columellaris)* occur on the finer textured soils along valleys and in local erosional tracts. *Acacia resinomarginea* is prominent amongst the sand-plain communities in both upland and lowland situations.

The gently undulating terrain of this area is part of the Great Plateau (Jutson, 1950), a major physiographic feature in the western quarter of the continent. The landforms are in keeping with those described by Bettenay and Mulcahy (1972) for the upper parts of the major regional drainage systems. Here broad saline valleys characterized by long gentle slopes rise to gently undulating uplands forming valley divides.

Deep lateritic weathering profiles are widespread and there has been partial differential stripping. Outcrop of bedrock is only sporadic and detritus derived from partial erosion of the lateritic mantle is widely distributed. Reconnaissance scale (1:250,000) mapping of the Ninghan sheet by Lipple

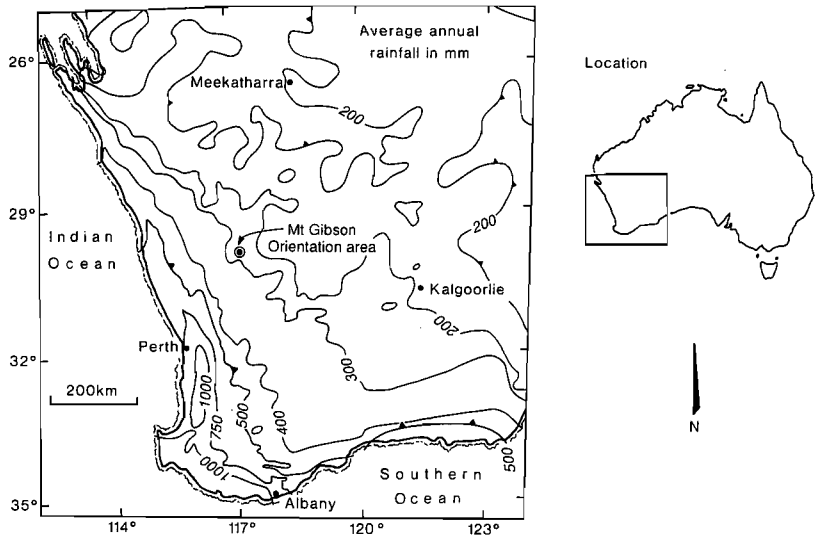

Fig. 1. Location of the Mt. Gibson orientation study area placed within the rainfall gradient for the south-west part of the continent.

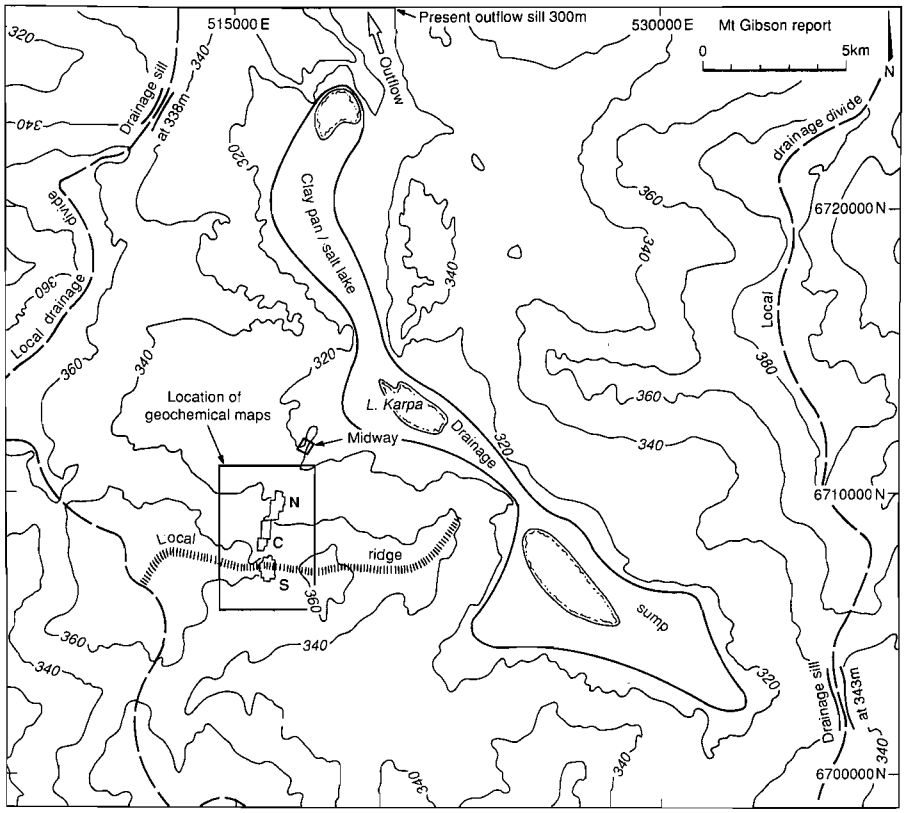

Fig. 2. Map showing the topographic setting of the Mt. Gibson gold mining area (the S, C, N, pits and Midway) and the surrounding district. The rectangle shows the area covered by this report.

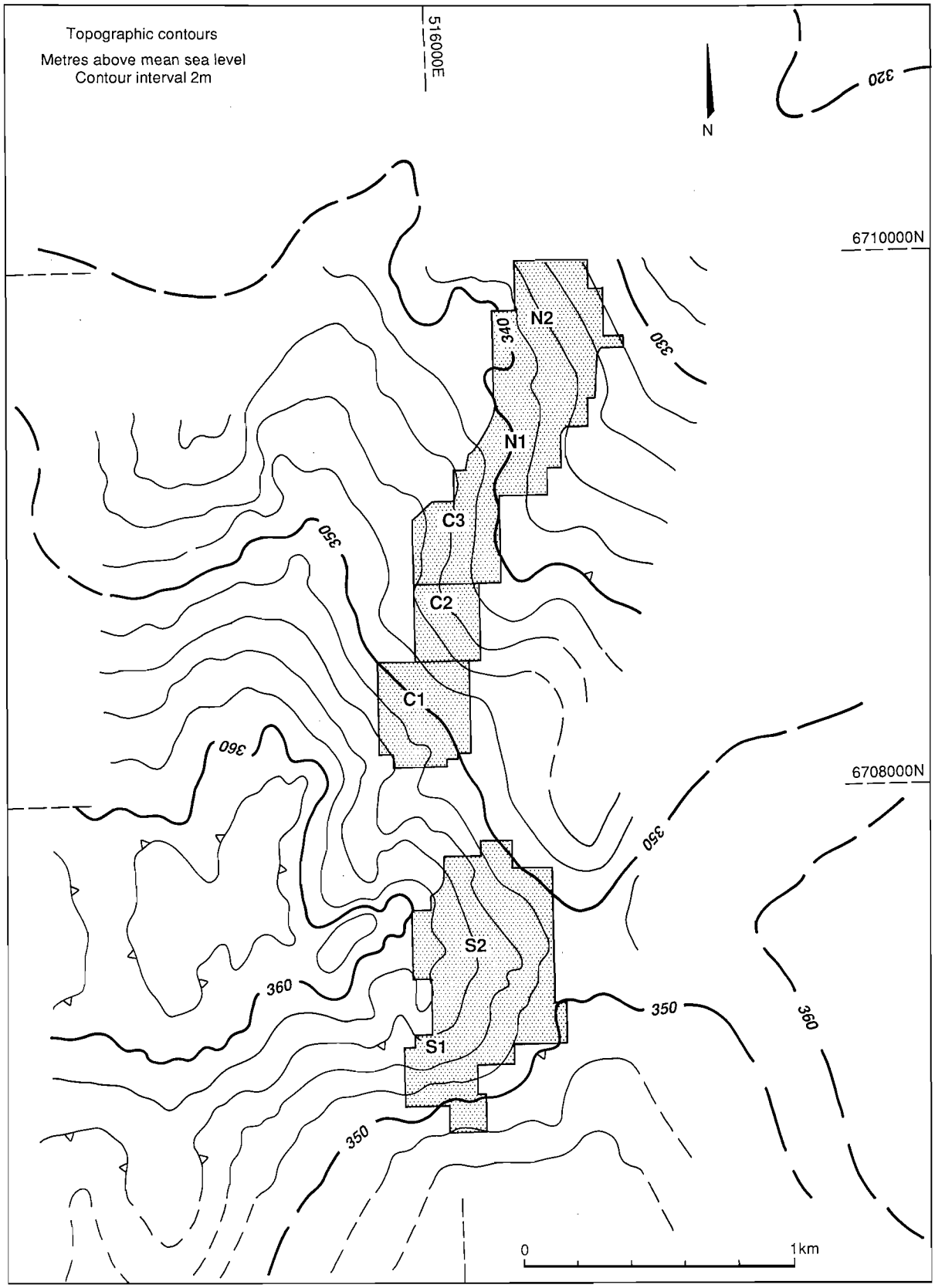

Fig. 3. Map showing topographic contours of the Mt. Gibson orientation area, detailed information is from Mt. Gibson mine plans.

et al. (1983) indicates a great extent of yellow sand-plain with some lateritic gravel units. Alluvial and colluvial deposits are common in gentle sloping valleys of active or infilled drainage channels. Calcrete is common in the lower reaches of the drainage basins (particularly in the courses of paleodrainages). Many of these general features occur in environs of the Mt. Gibson study area. However, generalizations of the previous workers were inadequate for the present study.

The Mt. Gibson area is at 330 to 360 m (Figs 2 and 3) above mean sea level on a broad divide between the extensive valley playas of Lakes Moore and Monger, both of which occur at levels of about 300 m. Much of the skyline has broadly convex local divides at 340 to 360 m flanked by long gentle slopes which grade at 1 in 50 (2%) on the upper slopes to 1 in 200 overall (0.5%), leading to the local Lake Karpa drainage sump at 310 m (Fig. 2). Emergent above the general plateau skyline are a few prominent crests and monadnocks flanked by steep irregular slopes. The most prominent are Mt. Gibson (the topographic feature, 480 m high, lying 18 km to the north and quite distinct from the Mt. Gibson Gold Project mining areas) and Mt. Singleton (620 m), which are related to some of the more resistant geological strata of the supracrustal fold belts.

The current pits at the Mt. Gibson mine, termed S1, S2, C1, C2, C3, N1, and N2 in sequence from south to north (Fig. 3), are arrayed along the upper flanks of a local ridge trending just east of north. Slight variations in this trend are associated with the heads of minor tributary valleys such as between the S2 and C1 mine pits and between the C1 and C3 pits. Broad shallow elongate depressions occur on the ridge crests just west of the S2, N1, and N2 main pits. The detailed topographic relationships in the vicinity of the mine pits will be discussed later.

Sporadic areas of outcrop and subcrop of fresh mafic lithologies and saprolite of a variety of types occur in zones of local erosion. Exposures of fresh granitoid rocks in terrain surrounding the project area often take the form of low domes, local pavements, and tors while kaolinized granitoid rocks are exposed in a few low breakaways.

2.3 GEOLOGICAL SETTING AND MINERALIZATION

Regional Geology

The study area forms part of the southern Murchison Province within the cratonic Archaean Yilgarn Block of Western Australia. Arcuate north to northwesterly-trending belts of thick synclinorial sequences of Archaean supracrustal rocks, comprising the Murchison Supergroup, are preserved within a gneissic terrain intruded by Archaean granitoids. Within the belts, the lithologic successions can be divided into associations of either mafic, volcanic, or sedimentary affiliation as recognized by Hallberg (1976) following Muhling and Low (1973). Four such lithologic associations were established by regional 1:250,000 scale mapping of the YALGOO, KIRKALOCKA, NINGHAN and PERENJORI sheets (Muhling and Low, 1977; Lipple *et al.*, 1983; Baxter *et al.*, 1983; and Baxter and Lipple, 1985). The sequence of these lithological associations is repeated from belt to belt with an apparent consistency of stratigraphic order. The four associations in order of decreasing age are listed below.

Lower mafic volcanic association (Murrouli Basalt, Golconda Formation and Gabanintha Formation (in part) in the Luke Creek Group) - comprises mainly tholeiitic metabasalts and dolerites with mafic and ultramafic intrusives. Pillow and vesicular textures are common. Banded iron formation and minor felsic (mainly dacitic) volcanics are present in cyclic alternation with the mafic flows. This association hosts the largest proportion of historical Au producers in the southern Murchison Province.

Lower sedimentary-volcanic association (mainly Windaning Formation in Luke Creek Group, also Gabanintha Formation in part) - comprises mainly fine-grained sediments with banded iron formation and volcaniclastic rocks. Minor felsic volcanics, constrained to local sub-aerial or sub-aqueous eruptive centres, are also present. The association is intruded by both mafic and ultramafic rocks. Lower units within this association host economic syngenetic base metal sulphide–gold/silver mineralization.

Upper mafic volcanic association (Singleton and Wadgingarra Basalts, Camberathumum Formation in Mount Farmer Group) - resembles the lower mafic volcanic association generally, but

differs in having a lower proportion of banded iron formation and a higher proportion of pyroclastic rocks and high-magnesium (komatiitic) basalts. Local dacitic to rhyodacitic volcanics are present.

Upper sedimentary association (Mougooderra Formation in Mount Farmer Group) - comprises mainly shale and siltstone with interbedded polymictic and oligomictic conglomerate with sandstone and minor banded iron formation towards the base of the sequence.

All four associations are most extensively developed in the Warriedar Fold Belt and its southerly prolongation into the Ninghan, Yandhanoo and Retaliation Fold Belts within which the Mt. Gibson Au deposits lie. Formal stratigraphic terms have only recently been applied (Watkins *et al.*, 1989) to the supracrustal units within the study area and many inconsistencies remain.

In the Warriedar Fold Belt, upwards of a 5-km thickness of supracrustal rocks, comprising the above associations, is preserved in synformal structures. Metamorphic grades within the belts are typically greenschist to amphibolite-transition facies. Contact metamorphic hornfels may be developed at the supracrustal-granitoid margins. Regional structures within the greenstone fold belts appear to have been controlled by the emplacement of the granitoid batholiths with folds being variably close or open with a heterogeneous structural fabric varying with rock type and proximity to the margins of the fold belts.

Geochronological data suggest that the volcanic component of the supracrustal belts in the southern Murchison Province formed at *c.* 3.0 Ga and was metamorphosed at *c.* 2.7 Ga. Browning *et al.* (1987) have shown that galenas contained in syngenetic volcanogenic base-metal mineralization at the Scuddles and Gossan Hill deposits in the Warriedar Fold Belt gave Pb model ages consistent with Sm-Nd, Pb-Pb, and U-Pb zircon ages for the greenstone belts. The majority of galenas associated with Au mineralization in the southern Murchison Province gave Pb model ages of *c.* 2.75 to 2.85 Ga, implying that epigenetic Au mineralization in the region was synchronous with regional metamorphism of the supracrustal belts, although Phillips (1985) has shown that, in some cases at least, peak metamorphism had outlasted the mineralizing event.

Mineral Deposits in the Region

Historically, mines in the YALGOO, KIRKALOCKA, NINGHAN and PERENJORI 1:250,000 sheets have produced in excess of 67 tonnes (to 1985) of Au, mainly from deposits in the Magnet Fold Belt, where the Hill 50 mine was the major producer. Most deposits are hosted by tholeiitic basalts or dolerites, although banded iron formations, ultramafic rocks, and granitoids also feature. Most deposits are viewed as epigenetic and many shears and mineralized vein systems are associated with CO_2, soda, and potash metasomatism, the mineralizing fluids conceivably being derived by progressive metamorphic dewatering of mafic and ultramafic sequences in the supracrustal pile (e.g., Browning *et al.*, 1987). Hallberg (1976) notes that on a gross scale, Au producers were virtually restricted to deposits within the two older supracrustal associations noted above and particularly within para-amphibolites, ultramafic schists, and banded iron formations grouped into the lower mafic volcanic association.

Within the Yalgoo-Singleton greenstone belt, significant resources of polymetallic base-metal mineralization of syngenetic volcanogenic association have been proven at Golden Grove; specifically at the Scuddles and Gossan Hill deposits. These deposits are sited in a unit of felsic, pyroclastic, and volcaniclastic rocks near the base of a pile of mixed volcano-sedimentary rocks, mafic volcanic rocks, and banded iron formation. Published *in situ* geological resources at Scuddles total 21 Mt @ 1.2% Cu, 0.6% Pb, 8.2% Zn, 67 g/t Ag, and 1.0 g/t Au (Ashley *et al.*, 1988), while the Gossan Hill deposit has a possible resource of 14 Mt @ 3.8% Cu with minor Ag values (*Mining Journal*, 1988). Detailed descriptions of the volcanogenic massive sulphide deposits at Gossan Hill and Scuddles have been given in a series of papers by Frater (1983a,b; 1985a,b) and Ashley *et al.* (1988), respectively.

Other metal commodities have been produced in significant quantity from the region. Mining of supergene-enriched banded iron formation at Koolanooka Hill resulted in the production of 6.7 Mt of iron ore. Molybdenum, Bi, Be, Ta, and Li have been produced from pegmatites and quartz veins in supracrustal metamorphic rocks, roofing granitoid intrusives (in the Noongal area), or emplaced in border-facies rocks associated with high-level granite intrusions at several localities throughout the

region. A resource of 1.6 Mt of 0.649% WO_3 (Baxter, 1978) has been established in a greisen sheet in a high-level leucogranite stock intruding rocks of the lower mafic volcanic association at Mulgine Hill in the Warriedar Fold Belt. In the vicinity of the Mt. Gibson mine, wolframite has been produced from quartz veins intruding sediments of the Mougooderra Formation in the Yandhanoo Fold Belt.

Mineralization and Mineral Deposits at Mt. Gibson

At Mt. Gibson, Au occurs finely dispersed through various units of the regolith profile (both residual and transported) overlying probable Windaning Formation equivalents, an essentially felsic volcanic and metasediment association with minor mafic units. It occurs particularly in loose lateritic pisoliths and nodules, in lateritic duricrust, to a lesser extent in hardpanized regolith (particularly lateritic debris), and at the Midway deposit reaches economic grades within saprolite and bedrock. Locally, some enrichments in Au values are related to the development of calcrete within the laterite profile.

Mining operations at the Mt. Gibson lateritic Au deposit commenced in November 1986, resulting in production of 2300 kg of Au to November 1987. The pits are located in Fig. 3.

At the Midway North prospect (Hornet zone), 4.5 km north of the Mt. Gibson mine plant, an *in situ* geological resource of 1.5 Mt @ 6.0 g/t Au, associated with Pb-Zn-Ag-Bi mineralization, has been reported from a plunging sequence of altered and sheared felsic and mafic volcanics with amphibolite (metabasalt) in the structural hangingwall and footwall of the orebodies (*Gold Gazette*, 1988). The geological setting appears similar to that hosting the auriferous quartz veins at the Mt. Gibson S, C, and N pit areas. Similar prospective volcanogenic/precious metal mineralization has been recognized in felsic volcanics in the Narndee complex (Marston, 1979).

Steeply-dipping hematite-quartz veins (1-10 cm thick) hosted by saprolitic ?tuffaceous metasediments were exposed in the S2, C1, C3, and N2 pits after partial stripping of the lateritic cover and were found to contain values up to 31 g/t Au. Although the size and frequency of known occurrences of these veins in the mine area appears to be inadequate to account for the Au content of the regolith, a number of small prospects (Tobias' Find, Orion, Mt. Gibson Well, Leake's Find) on the western fringe of the auriferous laterite, attest to a broader distribution of shear-controlled vein systems in the unmapped sub-surface.

The S, C, N, and Midway North deposits are sited within the Retaliation-Yandhanoo Fold Belt (Lipple *et al.*, 1983) comprising a basal sequence of mafic volcanic rocks with substantial epiclastic sedimentary and felsic volcanic components in the middle and upper parts of the sequence, all metamorphosed to low greenschist and low amphibolite facies.

Mapping and re-interpretation of the Mt. Gibson mine area (Watkins and Hickman, 1988a,b) identified the basal part of the Retaliation sequence as comprising tholeiitic basalts and derivative amphibolite and mafic schists, some high-Mg basalt overlain by volcaniclastic sediments, felsic lavas/tuffs, minor mafic volcanic rocks, and some banded iron formations. This sequence probably equates with the Gabanintha and Windaning Formations of Watkins and Hickman (1988b) and is separated, to the east, by a strike-slip fault from undifferentiated mafic volcanics. This supracrustal sequence forms a synformal enclave within gneissic Archaean granitoids.

At the Mt. Gibson mine, the primary Au mineralization appears to be developed in quartz veins along shears in a 400 to 500-m thick sequence of very poorly exposed interlayered volcaniclastic and epiclastic metasediments, felsic and mafic volcanic rocks, cherts and "quartz-eye" porphyries, and in the massive to weakly foliated amphibolite forming the structural footwall (Fig. 4). The enclosing granitoids are gneissic to pegmatoidal in character and outcrop to the east, south, and west of the mine site. Greenstones (amphibolites) are exposed as rubble on upland areas to the west (Tobias' Find and west of N1 pit) and to the east of the mine site.

The supracrustal sequence and the granitoids are intruded by ENE-trending dolerite dykes.

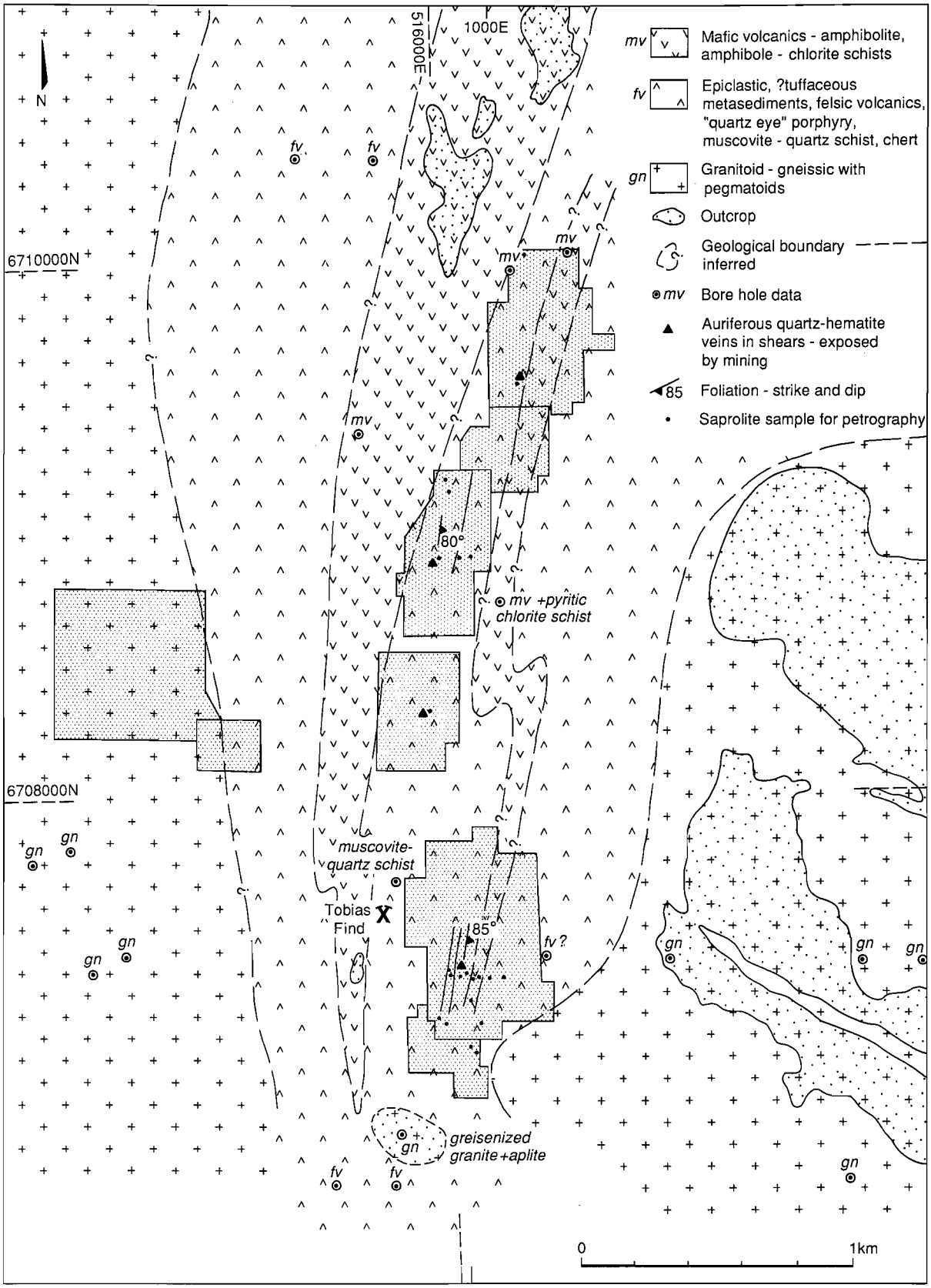

Fig. 4. Summary geological map of the Mt. Gibson orientation area based upon limited outcrop information.

2.4 SURFACE DISTRIBUTION OF REGOLITH UNITS

The regolith at the Mt. Gibson orientation area includes unconsolidated materials such as clays, sands, and various types of lateritic gravels overlying the more consolidated units which include red-brown hardpan, calcrete, and lateritic duricrust (Table 1). The regolith units are described below. The dominant features of the landscape of the study area, Fig. 5, are areas of red clay soils, most of which have a Eucalypt woodland (salmon gum, York gum) association contrasting with extensive areas of yellow sand plain having a dense tall shrubland (*Acacia resinomarginea*) association.

Granitic saprolite outcrops in the E and SE sections of the study area, whereas outcrops of Archaean supracrustal rocks are scarce, an example being the localized areas of amphibolite at Tobias Find. Four km NE of the study area, amphibolite and saprolitic meta-felsic volcanic rocks outcrop sporadically over distances of 1 to 2 km.

Units of friable red clays occupy a north-south zone (Fig. 5) surrounded by extensive yellow sands, with a narrow tract of yellow sand crossing the centre. The areas of red clay soils generally follow the broad crest of a sloping ridge (shown by the contours in Fig. 3) to the immediate west of the mine site. Two types of red clay soils occur: red clay overlying saprolite, and red clay overlying red-brown hardpan. These are referred to as RC1 and RC2 respectively in Fig. 5. The type RC1 is largely *in situ* whereas RC2 is transported from upland areas. The areas of red clays are flanked by areas of orange, slightly-sandy soils on the adjacent slopes.

Red clay soils range from acid to alkaline, the alkaline varieties being dominant, the variation typically being over distances of 100 m to 200 m. The alkaline red clays are calcareous and show a close association with weathered or sub-outcropping mafic rocks, patches of pedogenic calcrete related to mafic rocks, or else occur in a downslope position from mafic rock source areas, a theme which is investigated below.

Regolith relationships at Mt. Gibson are somewhat complex when it comes to linking regolith type, regolith stratigraphy, and topography to the dynamics of erosion and deposition. In order to clarify such relationships, it has been necessary to go through a series of descriptive and interpretative steps which we now follow.

2.5 REGOLITH STRATIGRAPHY

In the Mt. Gibson study area, exposures of the near surface regolith have been progressively provided by the open-pit mining operations. Until late 1988, emphasis has been on the mining of lateritic Au reserves, much of which occurred within 5 m of the original ground surface. The lateritic ore of the S, C, and N pits is part of an elongate geochemical, dispersion halo measuring some 1.5 to 2 km wide by 6 km along strike (Smith, 1987) with mining having been directed at those parts of the anomaly having Au values above 0.75 ppm (or higher depending upon contemporary economics). More recently, at the Midway deposit, mining of the saprolitic ore zone has commenced.

Opportunities to examine subsurface regolith relationships are also provided by spoil from numerous drill holes and from exploratory back-hoe pits, the latter usually stopping where hardpan or lateritic duricrust was encountered. Such information allowed Birrell and Butler (1987) to construct a series of 11 EW cross sections, each 5 km long, showing the upper regolith stratigraphy and to erect a generalized cross section of the regolith stratigraphy. Their study, which covered the S, C, and N pits and the adjacent areas along strike to the north and south, included mapping of surface regolith units within the central 7-km by 11-km area. The present study extended this approach and directed research at some of the enigmatic regolith relationships that the Birrell and Butler study had highlighted. It also drew from additional exposures created by more recent mining and from the report on regolith units in the S2 pit by Parker (1988).

The positions of exploration and mining grid lines and the designated mine pits, together with positions of observation points and key regolith profiles, are shown in Fig. 6.

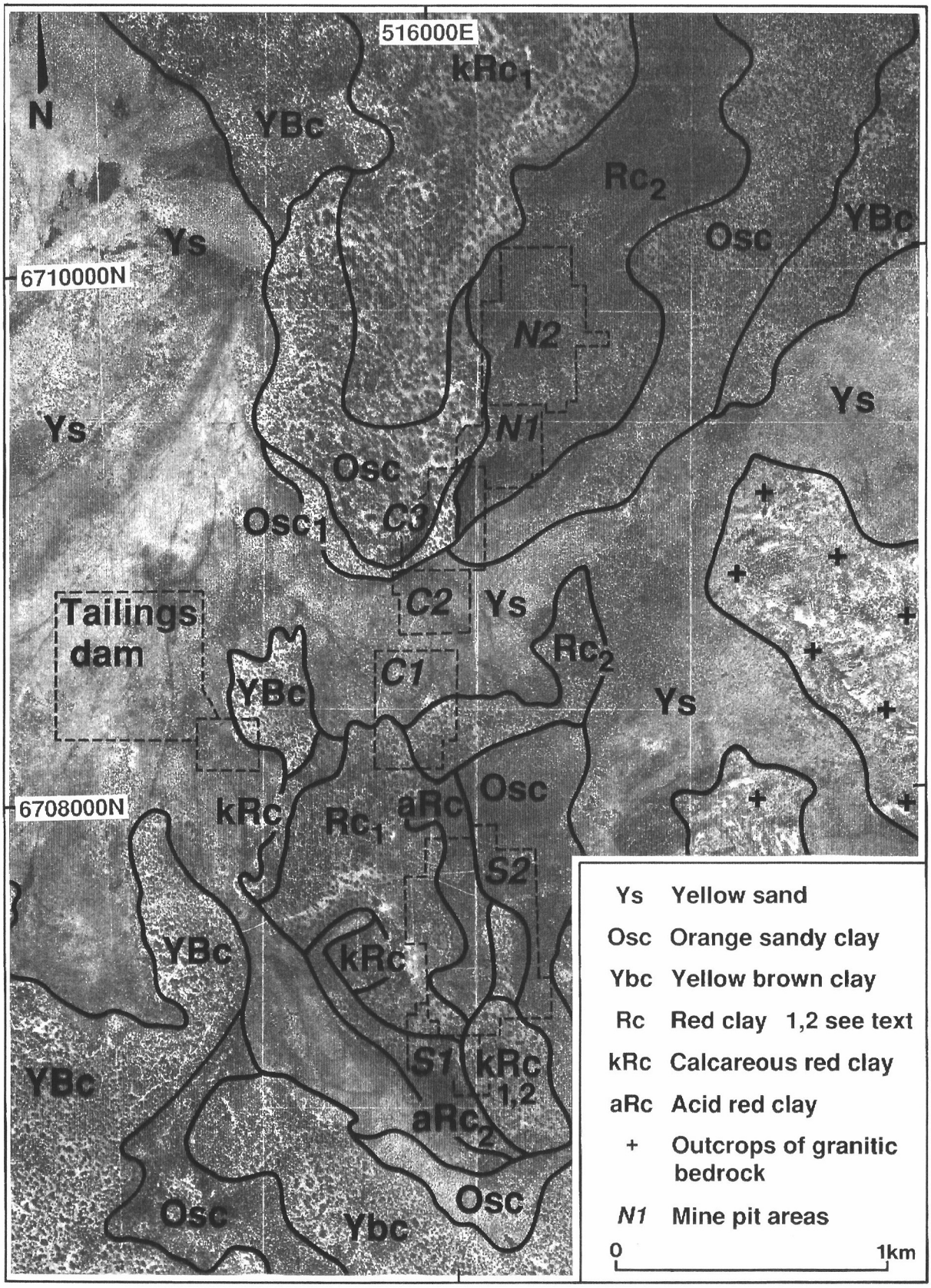

Fig. 5. Map showing the surface distribution of regolith units and vegetation patterns for the Mt. Gibson orientation area as an overlay to a black and white air photograph (Ninghan, run 11, 5239, Sept. 1980). DOLA Licence 548/98. WA 1929, Run 11, Frame 5239, Project 790020.

TABLE 1. Regolith facies units for the Mt. Gibson orientation area, arranged stratigraphically and showing typical thicknesses.

		Sub-area type					
		Areas eroded to saprolite	Depositional areas, transport to about 1 km	Depositional areas, transport about 1-3 km	Areas with residual duricrust		
VEGETATION BROAD REGOLITH UNITS		Eucalypt woodland, some tall scrub	Tall scrub	Tall scrub, sporadic Eucalypt woodlands	Tall scrub	Scrub and heath	
SOILS		Red clay soils Red plastic clays 1-5 m, grades into saprolite	Gravelly red clay soils 0.3 m to 1 m - calcareous red clay soil k RC2 - Acid red clay soil a RC2	Red sandy clay soils + 1 m (Hardpan can be present at 1-5 m)	Gravelly orange sandy clay loams 1-2 m, 0.2-1.5 m Gravelly orange clay	Gravelly yellow sands 1-1.5 m	Yellow clayey sands 1-3 m
ALLUVIUM		(minor)	(see hardpan)	White sandy clay (0-15 m)	-	-	-
HARDPAN (developed in colluvium/alluvium)		(minor)	Red-brown hardpan 1-3 m: Silty hardpan / Gravelly hardpan	Hardpan can be present at 1-5 m	-	-	-
CALCRETE		*Pedogenic calcrete* (thickness unknown)	Nodular calcrete 0-0.5 m Calcrete pods, layers 0-1 m Laminated calcrete 0-1 m	?	-	-	-
FERRUGINOUS ZONE	Loose lateritic residuum	-	(Generally missing)	(Can be buried)	Loose lateritic pisoliths, nodules 0.5-3 m		1-2 m
	Lateritic duricrust	-	Pisolitic, nodular duricrust (1-4 m) Vermiform duricrust Massive duricrust (0-2 m)	(Can be buried)	Massive/nodular duricrust (poorly indurated) (1-3 m) Silicified duricrust	Pisolitic, nodular duricrust 0-2 m	Packed nodular duricrust 2-4 m
MOTTLED ZONE		-	Mottled zone : Hardened mottled, matrix (1-5 m)				
SANDY CLAY OR ARENOSE ZONE		Terminology - not yet developed					15-50 m
SAPROLITE		Saprolitic: metasediments, quartz muscovite schist, quartz porphyry, metabasics, etc.					
BEDROCK		Various categories as above etc.					

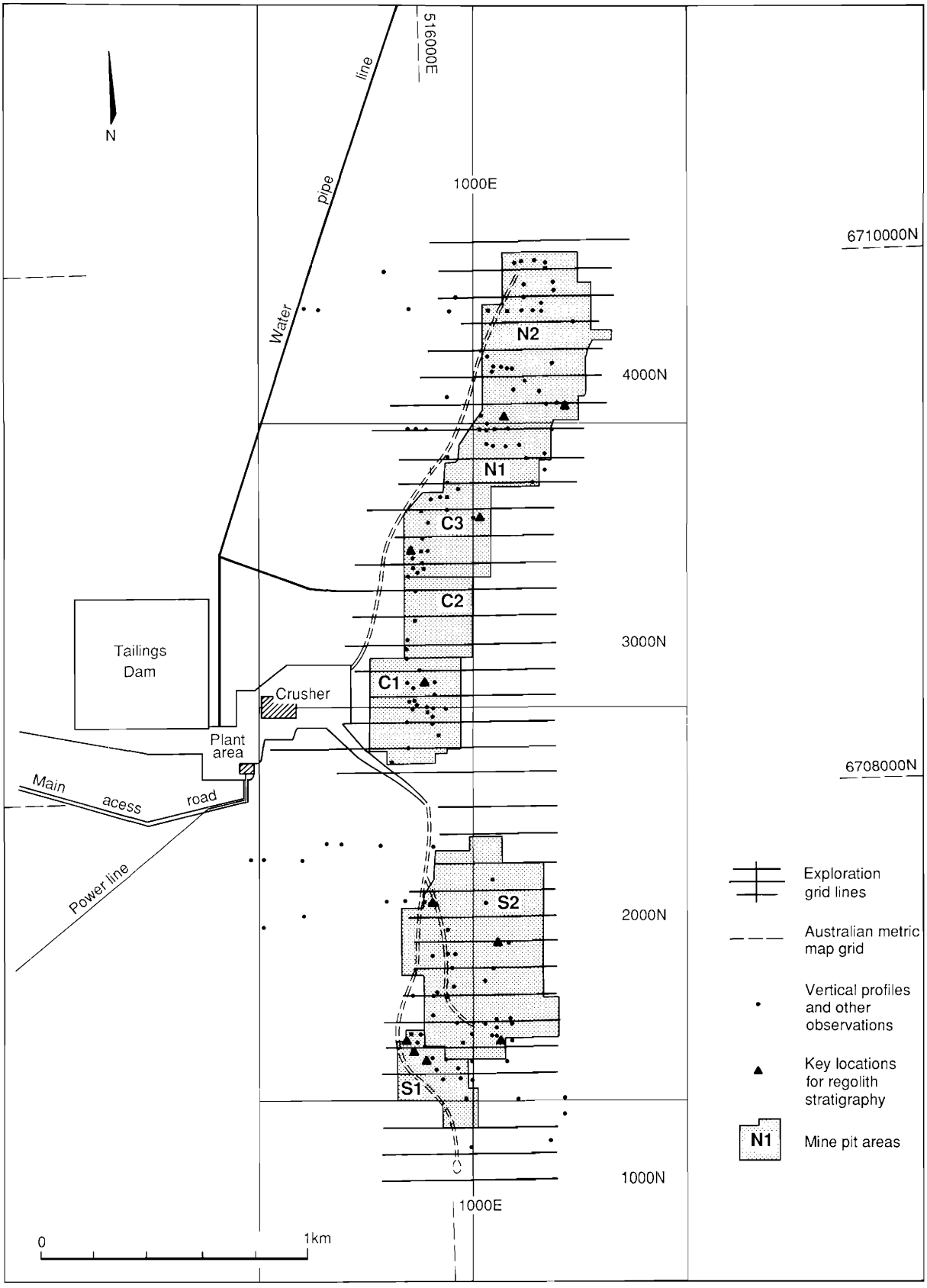

Fig. 6. Map of the Mt. Gibson orientation area showing the positions of the mine grid, open cut mining area, specific observation points, and other features. The Midway mining area of the Mt. Gibson Gold Project lies 2 km along strike to the NNE of the N2 pit.

Figure 7 shows an E-W cross section through the N2 pit at line 3800N. The local upland area to the west is characterized by red clay soils overlying saprolite with sporadic fresh suboutcrop of amphibolite. In the western part of this cross section, lateritic pisoliths, nodules, or lateritic duricrust have largely been removed by erosion. Close to the N2 pit and within its western edge, mottled zone and nodular duricrust beneath hardpan have been exposed by mining. The local upland area is thus interpreted to be a partly stripped laterite profile.

The central part of Fig. 7 shows the characteristic red clay soil of the N1 and N2 pits (RC2 of Fig. 5) underlain by nodular sandy and gravelly colluvium/alluvium which is now hardpan (Fig. 8A). The colluvium/alluvium was derived by erosion of a laterite profile interpreted to have once covered the adjacent upland area. Wispy carbonate cementation along bedding and parting planes is common in the hardpan unit and, at the base of the hardpan, calcrete reaches 1 m in thickness. The hardpan unit generally lies upon one or more of the lateritic units, namely loose lateritic pisoliths/nodules, nodular duricrust, or, in places, the lateritic mottled zone. The base of this colluvial/alluvial hardpan is thus interpreted as a local unconformity in the detailed regolith stratigraphy.

Red friable clay soils merge laterally, downslope, with orange sandy clay soils. Hardpan and carbonates were rarely seen as a substrate to the orange sandy clays. Rather the typical substrate is poorly indurated nodular, massive, or mottled duricrust which occurs at a depth of 1 to 1.5 m, as is shown in Fig. 8B.

Extensive yellow clayey sands, shown at the eastern edge of Fig. 5, dominate the sand plain at Mt. Gibson and the surrounding region. The yellow clayey sands typically overlie coarse lateritic nodules which in turn may overlie nodular pisolitic duricrust.

Units of the regolith stratigraphy used in this report are given in Table 1. Typical vertical profiles through the regolith stratigraphy are described in Appendix 1. Descriptions of various regolith units are given below. Described material may be located by means of the mine grid coordinates in Fig. 6.

2.6 DESCRIPTIONS OF THE REGOLITH UNITS

Soils

The soils forming the upper part of the regolith at Mt. Gibson are generally very friable and have a matrix grain size ranging from clay to clayey sands; typically they show little profile development. Excluding the RC1 areas of Fig. 5, the upper 30 cm of soil generally contains small amounts of lateritic gravels, the amount of which commonly increases markedly with depth becoming heavy gravels. Three main soil groups, based on colour, namely red, orange, and yellow, are recognized and described below. Most of the area now mined was overlain by red and orange soils, but there were notable pockets of yellow clayey sands.

Red clay soils (RC2; 2.5 YR 4/8 to 4/6; 10 R 4/6 moist, using notation of the Munsell soil colour charts), overlying red-brown hardpan are friable light clays commonly containing significant amounts of gravel-sized material (in the 2 to 15-mm class) and reach 1 m in thickness. The gravel fraction consists of ironstone nodules (ferruginous pellets, red to black lateritic nodules, pisoliths) and lithorelics (Fig. 9A). Both magnetic and non-magnetic ferruginous pellets and lateritic nodules are present. In the red clays, lateritic nodules have thin (< 0.5 mm) or no concretionary coatings. They may have a smooth shiny surface. The sand-sized fraction, typically 15-30% by volume, is largely quartz with small amounts of fine ferruginous pellets, pisoliths, nodules, and fragments of feldspars. The clay fraction (about 40-60 vol %) is kaolinite, hematite, and goethite.

Friable calcite is the dominant carbonate, and generally occurs at a depth of 30 cm in the soil unit, Fig. 10A, coinciding with pH values in excess of 8.0. However, zones of hard carbonate nodules and pisoliths are also widely distributed within friable red clay units. The hard carbonates are dominantly calcite, with minor amounts of dolomite.

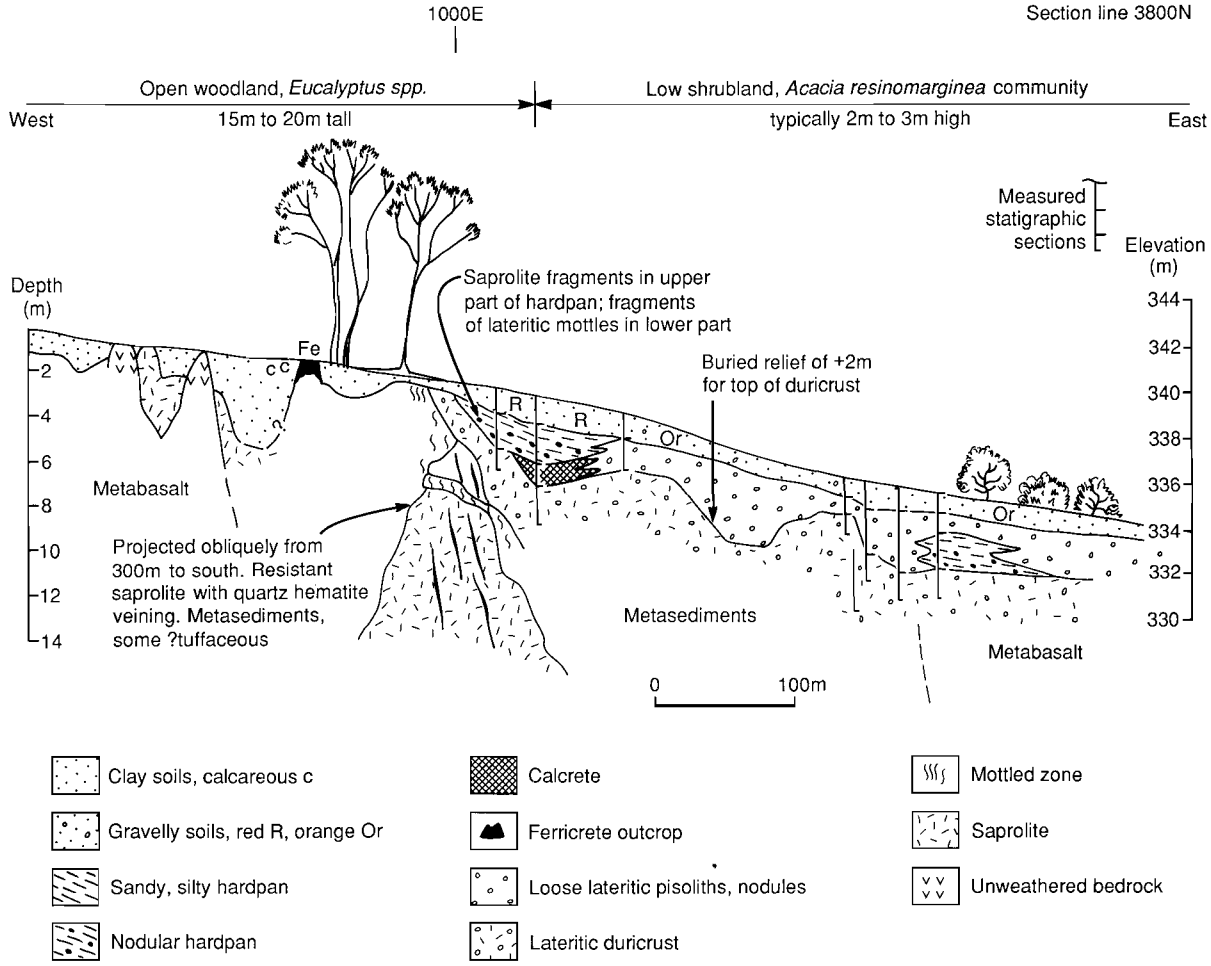

Fig. 7. Cross-section through the N1 pit (Line 3800N) showing upper regolith and vegetation relationships.

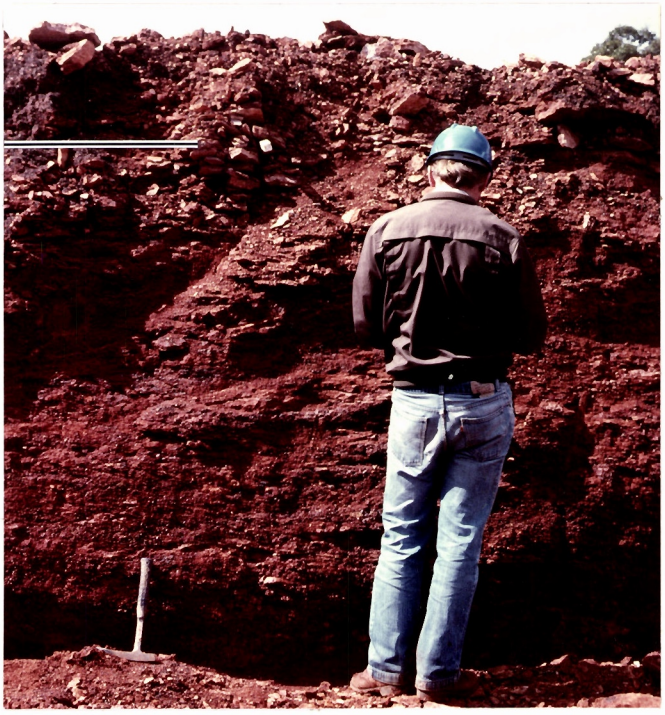

Fig. 8A. Mine pit exposure of a hardpan unit developed in colluvium/alluvium, location 2650 N, 880 E, C1 pit.

Fig. 8B. Vertical profile showing the transitions between orange sandy clay soil, loose pisolitic nodular laterite, and poorly-indurated nodular duricrust, location 2050 N, 1050 E, S2 pit.

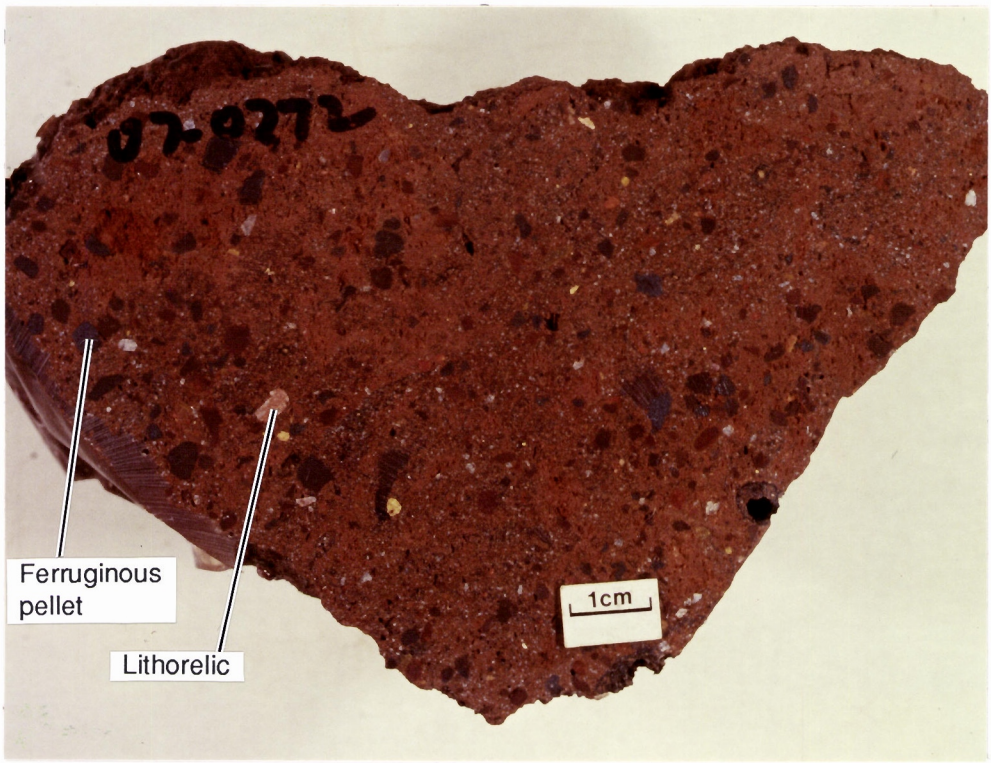

Fig. 9A. Slice through an epoxy resin impregnated red clay soil showing ferruginous pellets and lithorelics in a clayey matrix, location 2050 N, 845 E, S2 pit.

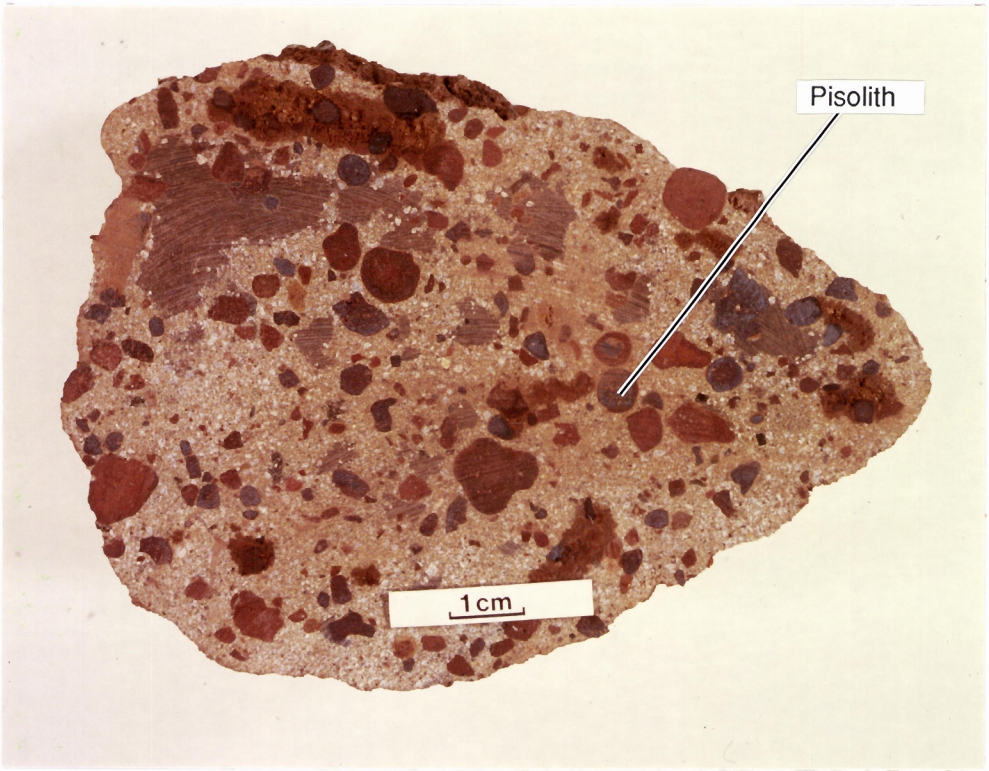

Fig. 9B. Slice through an epoxy resin impregnated orange sandy clay soil showing lateritic pisoliths and nodules set in a sandy clay matrix, location 2050 N, 1050 E, S2 pit.

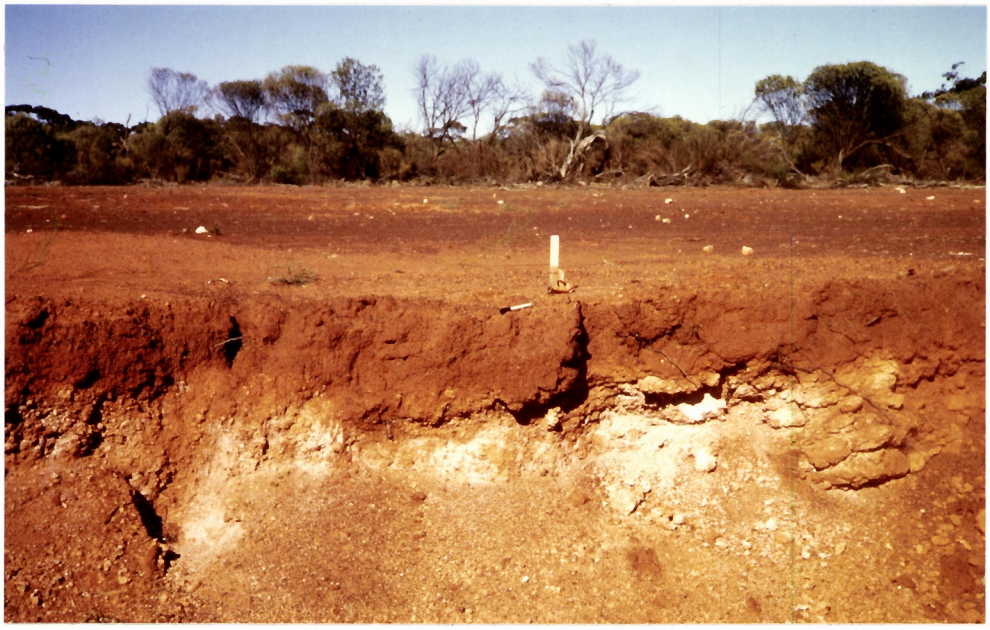

Fig. 10A.Mine pit exposure showing red clay soil overlying a powdery carbonate unit, location 1800 N, 900 E, S2 pit.

Fig. 10B. Friable red clay over red plastic clay. The friable red clay contains much carbonate that is uniformly distributed. The carbonate extends into the plastic clay as well-defined coarse pockets. Location 1530 N, 1100 E, S2 pit.

Red clay soils overlying saprolite (RC1; 10 R 3/6 moist) commonly contain only a minor gravel fraction. Lateritic pisoliths and nodules are typically absent, the gravel fraction being dominated by ferruginous black pellets and lithorelics. The pellets commonly reach 20 mm in diameter, are mostly hematite- and goethite-rich and are interpreted to have formed *in situ* during post-lateritic weathering.

Red plastic clays (10 R 4/6 moist) form a substrate to some of the friable red clays (Fig. 10B) which have carbonate throughout the profile. Plastic clays are less sandy and have higher moisture contents than the friable red clays (RC1 and RC2). These plastic clays commonly occur at depths of about 50 cm and merge with pale-coloured saprolite at depths of 3 to 5 m. Such clays occur in areas of erosion of the laterite profile such as the minor concavities topographically below subdued breakaways.

Orange sandy clay soils (5 YR 6/8 to 5 YR 4/6 moist) are also very friable, but are slightly more sandy than the red clays. In the Mt. Gibson study area, these orange sandy clay soils typically contain a dominant (25-50 vol %) gravel component of 2 to 25-mm sized lateritic nodules and pisoliths (Fig. 9B) and are up to 1.5 m thick. These nodules and pisoliths typically have yellowish brown concretionary coatings. In contrast with red clays, iron-rich pellets and black coated nodules are rare. These soils are mildly acid (pH 4.5 to 6.0), and carbonates are absent. Mining exposures show that red brown hardpans rarely occur under these soils. Instead, loose lateritic nodules and massive to nodular lateritic duricrust are the typical substrates.

Yellow clayey sands (10 YR 7/8 moist) are loose, brownish yellow, non-calcareous sands with a minor (< 10 volume %) admixture of clay. The pH ranges from 5.5 to 6.0. Many of the yellow sands outside the mine area, particularly on long gentle slopes associated with granitic terrain, have considerable amounts of coarse lateritic nodules within 20 cm of the surface and this nodular horizon may overlie nodular, pisolitic duricrust similar to that of the orange sandy clay areas. However, within the mine area, there are areas of yellow sands containing very small amounts (5%) of lateritic nodules overlying red-brown, friable clayey sands with moderate amounts of (10-15%) of lateritic nodules. These are well exposed in the north wall of pit C1. Here a layer of loose pisoliths underlies red clayey sands which in turn overlies the fine (~1 m thick), medium (~1 m thick) and coarse (~1.5 m thick) layers of packed nodular pisolitic duricrust. Pisoliths and nodules in the packed duricrust (with a little sandy matrix) underlying the yellow/red sands appear well sorted (Fig. 11B) and there is a sharp boundary between the soils and the underlying lateritic pisoliths/nodules. Yellow sands within the mine area may be aeolian in origin.

Red brown hardpan (gravelly, silty colluvium/alluvium)

Hardpan is commonly formed beneath the red friable clays at depths of 30 cm to 100 cm and is brittle, partly silicified, red to dark red, or red- brown in colour (2.5 YR 4/6-4/8 or 5/6-5/8, moist). The hardpan is developed within layers of nodular gravelly and sandy colluvium/alluvium which reach 2.5 to 3 m in thickness. The gravel-sized materials consist of variable amounts of lateritic nodules, pisoliths, hardened mottles, and rock fragments, which are most abundant in the lower and middle parts of the unit. The nodular gravel occurs as lensoid beds which typically reach 5 to 10 cm in thickness. The nodules and pisoliths are black to red, black ones generally being magnetic, and vary in diameter from 2 to 20 mm. Other nodules, pisoliths, and hardened mottles may have yellow-red concretionary skins. Small grains of quartz (< 1 mm) are present in the hardpan matrix as well as within some of the nodules. The interiors of most pisoliths and nodules are composed of varied amounts of hematite, maghemite, goethite, and kaolinite. Most pisoliths and nodules have thin concentric skins of this varying mineralogy. For some, concretionary skins reach 5 mm in thickness. Silty-sand units, typically 1 to 3 cm thick, occur throughout the hardpan units, and can dominate the top 50 cm of the hardpan where nodular lenses are rare. Examples of silty and nodular hardpans are shown in Fig. 12A and B.

In the study area, calcium carbonate and white, finely-granular opaline silica are commonly concentrated along and adjacent to partings within hardpan. Calcrete pods and sheets may also occur within the hardpan units. A number of different fabric elements can be seen within the hardpan in thin sections. The hardpans show zones of strongly-oriented clay around quartz grains and lateritic nodules

Fig. 11A. Vertical profile showing the transition of yellow clayey sand to loose lateritic pisoliths in a sandy clay matrix.

Fig. 11B. The substrate to the profile in Fig. 11A showing a sharp textural change from pisolitic to nodular duricrust, location 2825 N, 725 E, C1 pit.

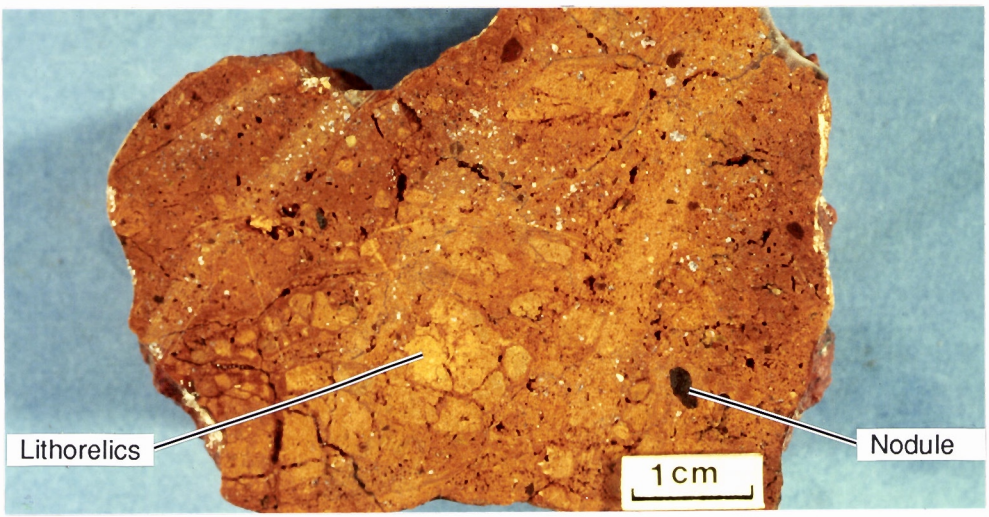

Fig. 12A. Slice through a silty hardpan showing lithorelics and sporadic lateritic nodules in a silty matrix, location 2795 N, 850 E.

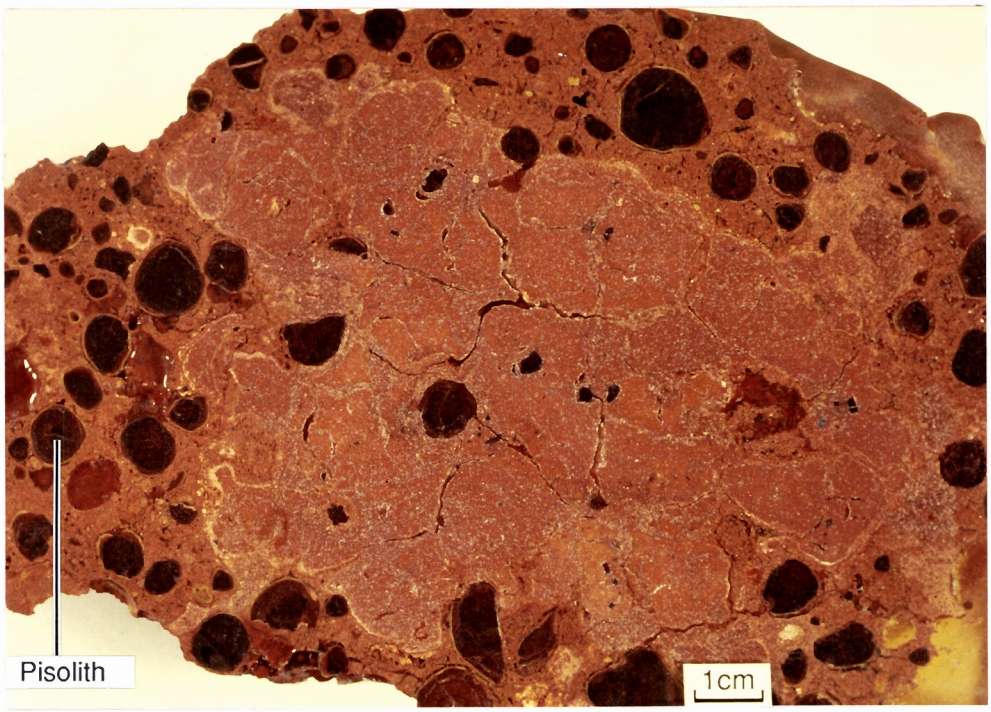

Fig. 12B. Slice through an epoxy resin impregnated hardpan developed in colluvium, containing abundant gravelly lateritic pisoliths. The siliceous and calcareous patch may have grown by replacement (presently under investigation), location 2650 N, 850 E.

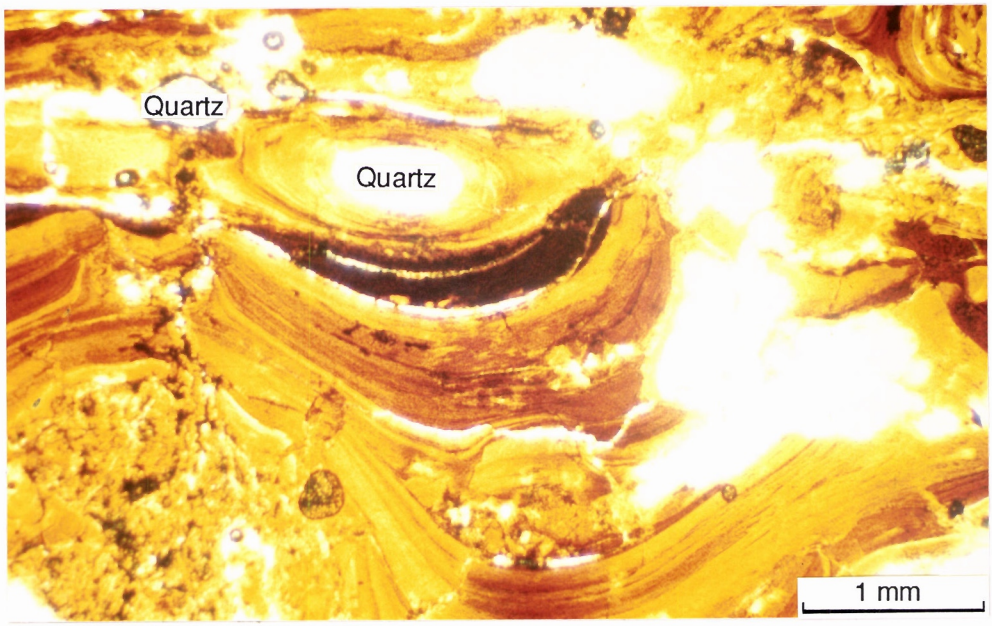

Fig. 12C. Polished thin-section through matrix of a silty hardpan showing oriented bands of kaolinitic clay, goethite, and amorphous silica around quartz grains, location 2745 N, 850 E.

with isotropic material containing amorphous silica and zones of carbonates filling fissures (Fig. 12C). Accumulations of black Mn oxides are characteristic and can occur on subhorizontal partings and on vertical hardpan fracture-surfaces. The formation of Mn oxides was probably influenced by retarded drainage, due to the impermeability of the hardpan.

Calcrete and carbonates

Carbonate segregations are present in a number of forms including:

- Powdery carbonates
- Nodular calcrete
- Calcrete pods
- Calcrete sheets (in hardpan)
- Laminated calcrete.

Powdery carbonates and nodular calcrete commonly occur under friable red clays. Powdery carbonate is loose, finely-divided carbonate and lacks any nodular development. Nodular calcrete is composed of coarsely-platy, cream to pinkish nodules (Fig. 13A), varying from 1 to 5 cm in diameter, set in a loose calcareous clayey matrix. Lateritic pisoliths and nodules less than 15 mm in diameter are commonly included in coarse calcrete nodules as well as in the calcareous clayey matrix. Calcrete pods (Fig. 13B) and calcrete sheets occur beneath or within hardpan units as indurated horizons. They appear to show partial or complete replacement of regolith materials. Fig. 13B shows a partial calcrete replacement of nodular laterite; appreciable amounts of lateritic nodules are still present in a matrix of calcite and dolomite. In contrast, laminar calcrete (Fig. 13C) shows complete replacement of the earlier lateritic duricrust.

Laterites

The main categories of laterite recognized in this study are the loose pisolitic, nodular laterite, and the underlying duricrust (a consolidated unit) of which three varieties are described, namely nodular pisolitic duricrust, massive duricrust, and vermiform duricrust.

Loose lateritic pisoliths/nodules

Loose or weakly cemented lateritic pisoliths/nodules in a yellow to red sandy clay matrix form a widespread unit that can outcrop, or more commonly lies beneath soil, hardpan, or calcrete units. This unit generally merges at depth with lateritic duricrust. In the situations examined, the pisolitic/nodular laterite reaches 2 m in thickness. Loose nodular laterite is prevalent throughout the northern and eastern sections of the S2, C3, and N pits. Nodules and pisoliths may sometimes be present in equal amounts, however nodules are generally dominant. Matrix up to 20-30 volume % may be present, and consists of kaolinite, goethite, hematite, and quartz.

Nodules are yellow to red, subrounded to irregular in shape with a size range of 5 to 50 mm and they consist of multi-coloured cores with thin coatings. Of the various size categories, 10-15-mm nodules are the most common. The largest nodules generally have the most complex multi-coloured cores. Nodules are indurated by hematite, goethite and, for some, maghemite, and may contain residual quartz grains and lithorelics (Fig. 14A). Compound nodules are also present. Nodules with black nuclei are generally magnetic because of the presence of maghemite. However, non-magnetic nodules are more abundant and account for about 60% of the total gravel fraction. Magnetic nodules generally have much higher Fe (as oxides) and lower Si and Al (as kaolinite) contents compared with non-magnetic nodules.

The loose lateritic pisoliths mainly occur in the western section of the S1, northern section of the C1, and southern part of the C3 pits. Individual pisoliths are round, 10-50 mm in diameter and contain black to red hematite nuclei (Fig. 14B). The surfaces of these pisoliths are coated with a greenish, pale yellow, and, for some, a light red material which is mainly a mixture of goethite, hematite, gibbsite, and kaolinite. The coatings around hematitic nuclei are generally 2-15 mm in thickness, consisting of light and

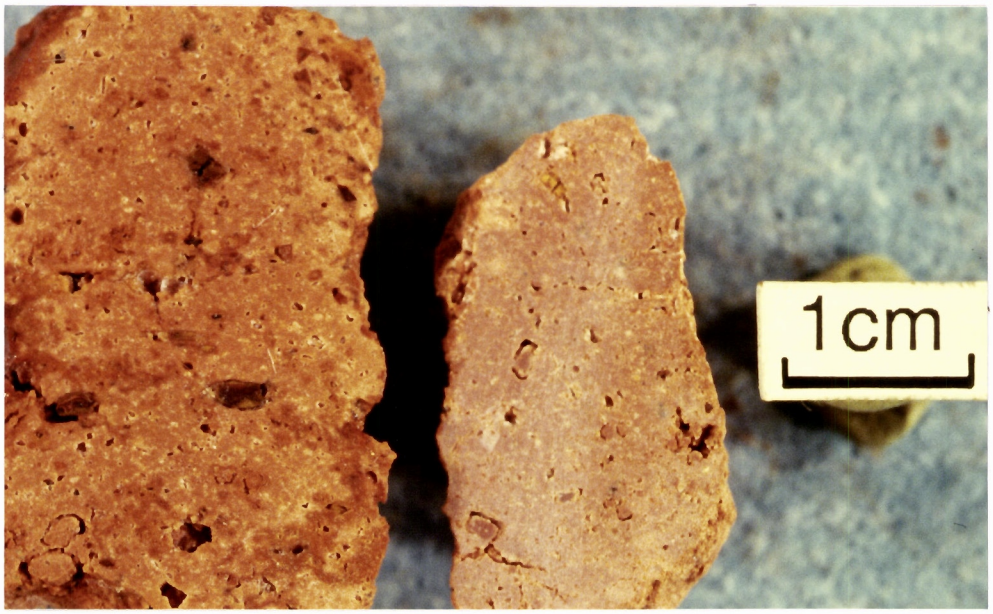

Fig. 13A. Slice through two nodular calcretes separated from their calcareous clay matrix, individual calcrete nodules probably are replacements of lateritic nodules by carbonate, location 1900 N, 1100 E.

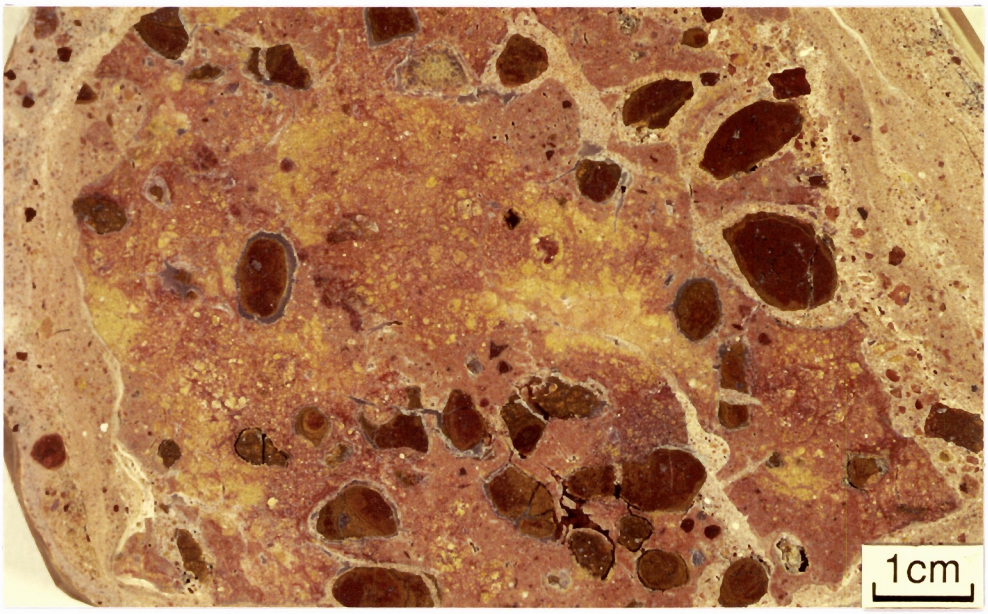

Fig. 13B. Slice through a calcrete pod showing partial replacement of laterite nodules by carbonate, with a carbonate-rich clay matrix, S1 pit.

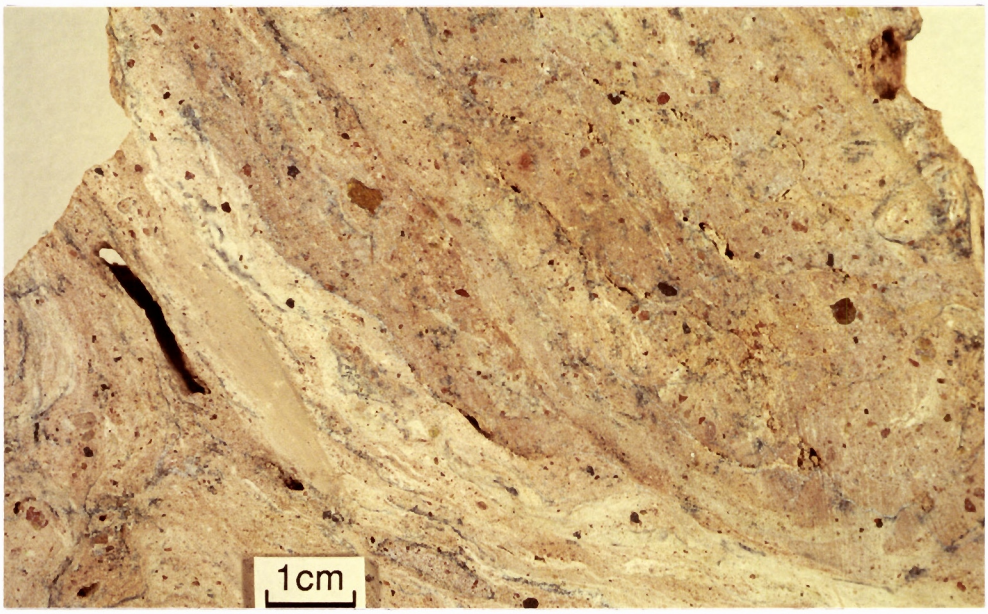

Fig. 13C. Slice through laminar calcrete showing complete replacement of lateritic regolith by carbonates, N1 pit.

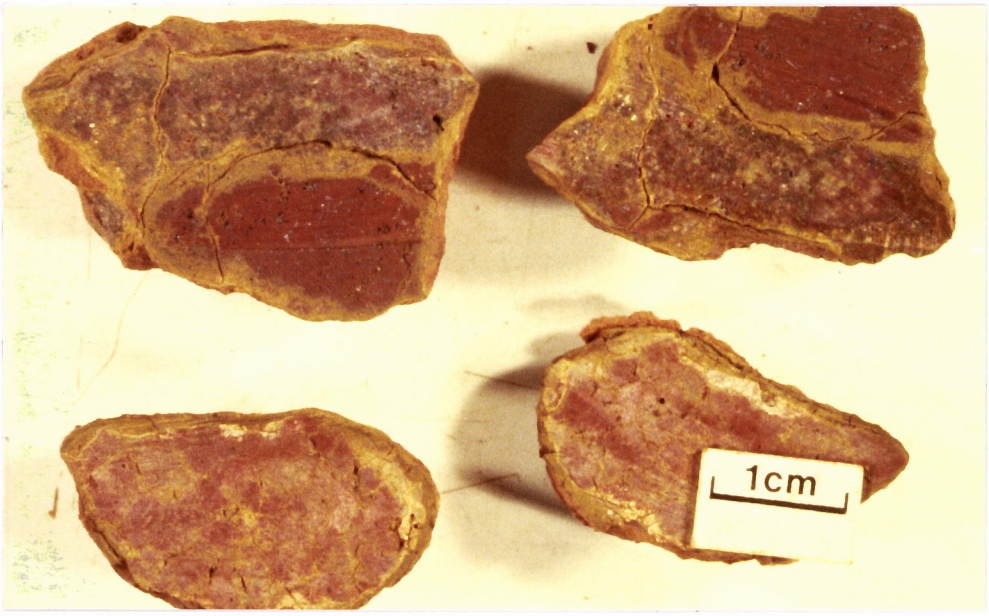

Fig. 14A. Slice through two lateritic nodules (top one is a compound nodule) from the unit consisting of lateritic pisoliths and nodules, location 2745 N, 850 E.

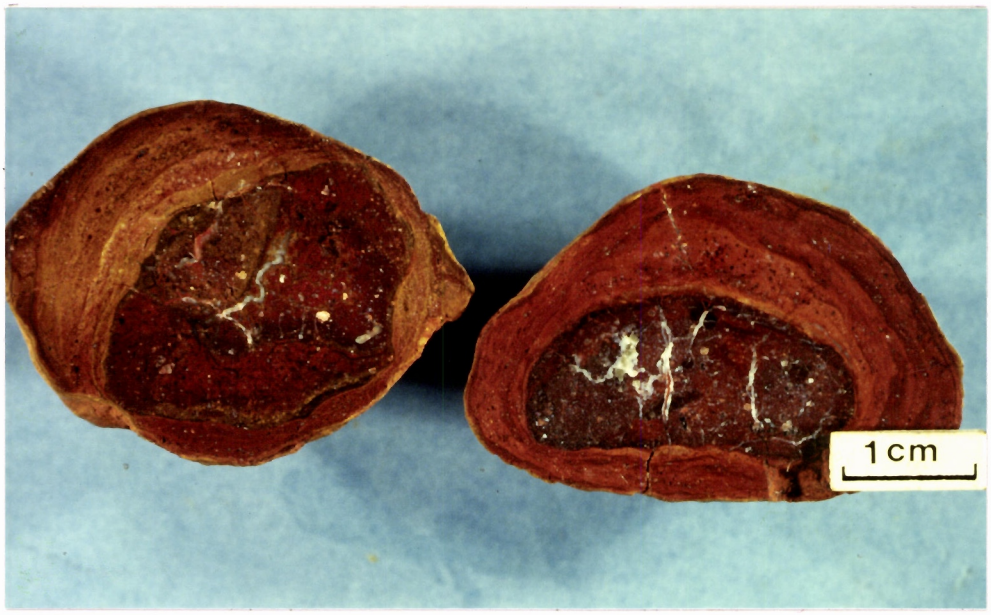

Fig. 14B. Slice through two lateritic pisoliths from the loose pisolitic unit showing concentric banding of light yellow and red materials around the silicified nuclei, location 1525 N, 740 E.

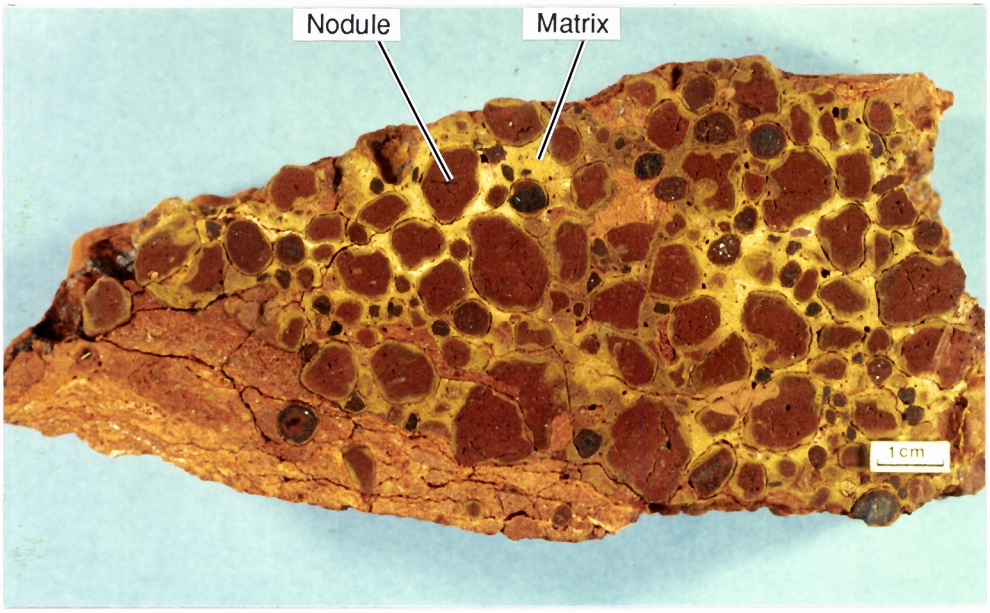

Fig. 14C. Slice through hardpanized nodular duricrust showing nodules set in a sandy clay matrix, location 3890 N, 1355 E.

dark red banded zones. Pisoliths can also be partly replaced or surrounded by authigenic calcium carbonate and silica. Such pisoliths are relatively weak and their skins can be readily removed by hand. Lateritic pisoliths and nodules, except for their shape, are essentially the same. Pisoliths, by definition, are spherical or sub-spherical, whereas nodules are less regular in shape with rounded edges.

Nodules and pisoliths underlying orange sandy clay soils are different from those underlying red clays in respect to the thickness of skins and sphericity. This may be due to differences in weathering status or to differences in substrate lithologies.

Lateritic duricrust

Lateritic duricrust is widespread throughout the mine area, generally occurring beneath the loose pisolitic unit. It is typically 1-4 m thick where exposed in pit faces. Introduction of silica cement has modified some duricrusts, resulting in a coarsely laminated appearance, referred to as "hardpanized duricrust". Evidence of penetration of duricrust by tree roots is seen in the vertical pipe-like structures typically filled with loose pisoliths and nodules.

The duricrusts are generally dark brown (7.5 YR 3/4 dry), dark red (7.5 YR 3/8 dry) to brownish yellow (10 YR 6/8 dry). They comprise merged intergrowths of ferruginous concretions forming a continuous skeletal mass with a varied internal structure. Structures in duricrust range from those in which iron oxides form discrete segregations (nodules, pisoliths), those in which iron minerals occur as a continuous cementing skeleton (vermiform) to those that have a uniform, massive texture. Assessment of these structures in the duricrusts is based on the exposure of the upper part of duricrust in the floors of the mine pits, a situation which does not generally provide the opportunity to examine fully the range of structures in the duricrust. However, where the duricrust was fully exposed (e.g., western sections of S2 and C3 pits) nodular duricrust overlies massive duricrust which grades downwards into a mottled zone, nodular structures decreasing with depth.

Nodular pisolitic duricrusts are the most common types of duricrust in the study area. They are coherent weathering crusts composed of accumulations of ferruginous nodules cemented by iron oxides and clays (Fig. 14C). Pisoliths are also present in the nodular duricrust type. Ellipsoidal to irregular voids (1-5 mm across) also occur in the nodular duricrust and are generally less than 10% of each hand specimen. However, voids do not impart a characteristic cellular or vermiform fabric, voids may have earthy infill of kaolinite and goethite. A sandy clay matrix (30-60 vol. %) is yellowish brown (10 YR 5/8, dry) to dark red (7.5 R 3/4 dry) and is predominantly kaolinite, goethite, and quartz. The matrix may be uniformally coloured or segregated and may contain rounded to angular quartz grains (1-2 mm). Nodules make up about 40-60% of hand specimens and are dark reddish brown (2.5 YR 3/4 dry) to black (2.5 YR 3/0 dry). Both magnetic and non-magnetic nodules are present. They are sub-rounded to irregular in shape and vary from 2 mm to 20 mm in size, the 5-10 mm size being the most common. Large nodules are observed enclosing smaller ones. Nodules may have thin pale yellow goethitic/kaolinitic coatings and can contain quartz grains in the nuclei. More than one type of nodule occurs in some duricrusts which may differ in colour, presence or absence of quartz, concretionary coatings or lithorelics, and in relative proportions of goethite, hematite, and maghemite. Some nodules are porous while others are massive. Porous nodules show the development of etch pits in the nuclei which suggests the dissolution of iron oxides and kaolinite. Pisoliths contain nuclei of hematite and kaolinite surrounded by fine concentric rings with varying proportions of kaolinite, goethite, hematite, and quartz. Transformation of goethite to hematite is observed along cracks in many nodules/pisoliths.

The crystal sizes of goethite, hematite, and maghemite measured from line broadening of XRD reflections are small (<1000 Å). The mean crystallite dimension (MCD) derived from the 110 reflection of hematite was greater than that for the 104 reflection, which indicates a platy morphology (Campbell and Schwertmann, 1984). The MCD (110) indicates the width of hemtatite crystals perpendicular to the *c*-axis, whereas MCD (104) is an approximate measure of thickness along the *c*-axis (Schwertmann and Kampf, 1985). The mean crystallite dimension of goethite (300-400 Å) is smaller than hematite (600-800 Å) which would present greater surface area for adsorption of metal cations, a topic to be investigated later.

Massive duricrusts are less common than nodular duricrusts, but were observed in the western section of the S2 and C3 pits. By definition, structures such as pisoliths and nodules are not present in significant quantities in massive duricrust. However some transitional varieties show the development of incipient nodules and the matrix may be uniformly coloured or mottled (Fig. 15A). The sandy clay matrix is porous (mostly small pores, <1 mm), relatively soft, and is kaolinitic. Mottles are generally well defined and multi-coloured (yellow to red) and may be goethite or hematite rich. Incipient nodules are greenish to light red in colour and consist mostly of goethite and kaolinite. Nodules have more or less diffuse outer rims and are only slightly indurated. In the upper part of massive duricrust, the nodules become more indurated and their boundaries with the matrix become sharper.

Vermiform duricrust. Cellular and vermiform structures are dominant in some samples imparting a characteristic fabric to the duricrust (Fig. 15B). Nodules and pisoliths are not often present in the vermiform duricrust. Tubular voids reach 50 mm in length and usually have an earthy, light red coloured infill of goethite, kaolinite, and quartz. Some tubules are filled with hematite and kaolinite; most are filled with goethite and kaolinite. The infilling is weakly indurated and can be easily removed for analysis. The red to reddish-brown matrix is mainly kaolinite, goethite, and hematite. Angular to rounded quartz grains may also be present in the matrix. Tubular structures which characterize these vermiform duricrusts appear to be dissolution features.

The micromorphological structures of lateritic duricrusts were examined to identify features which may assist understanding the genesis of lateritization as well as post-lateritization processes, a phase of the research which continues. In polished thin sections, the central parts of the nodules show the preservation of pseudomorphs of goethite, hematite and, for some, kaolinite after muscovite (Fig. 15C) typical of *in situ* weathering as described by several authors (e.g. Bisdom *et al.*, 1982; Muller, 1985). In contrast, the clayey matrices are characterized by the absence of original structures of primary minerals.

Mottled zone

The mottled zone of the weathering profile at Mt. Gibson is only sporadically visible, due to the limited depth of mining at this stage, as well as the general lack of natural exposures. Occurrences were noted in blast holes in the S2 and C3 pits where the mottled zone occurs beneath lateritic duricrust. Typically, the mottled zone is a 2-3 m thick clayey horizon which ranges in colour from pinkish white to purple with a very coarse mottled texture in the 10 cm to 20 cm range. The mottling is due to local accumulations of Fe oxides. In some examples, pisolitic and nodular structures are present in the mottles. In the S2, C1, C3, and N2 pits auriferous quartz-hematite veins embedded in north-south striking shear zones occur in sporadic exposures of the mottled zone continuing downwards into saprolite.

Saprolite

Sporadic exposures of saprolite have resulted from mining activities in the S, C, and N pits. In some cases, saprolite is overlain by a thin (< 1 m) mottled zone (e.g., C3 pit) and in others a nodular duricrust lies directly on the saprolite with a sharp contact (e.g., south end of S2 pit). Drilling suggests that saprolite can reach 50 m in thickness, but the thickness is known to vary with different bedrock lithologies. Immediately to the north at Midway, for example, relatively fresh mafic rocks are known to occur at depths of 15 to 20 m whereas sheared felsic volcanics can be weathered to 50 m.

Unweathered bedrock is not yet exposed in the S, C, or N pits.

Examination of a suite of 56 thin sections of saprolite samples from the mine pits, used in the compilation of the geological maps, Fig. 4, indicates a variety of rock types. A 200 to 500-m wide sequence of north-south striking and steeply east-dipping metasediments (siltstones, mudstones, rare cherts), mafic volcanics, and quartz-muscovite schists is sited between thick sequences of fine to medium-grained amphibolite (metabasalt) in both the structural hanging wall and footwall of this sequence. Thick (to 20-m) units of sheared "quartz-eye" porphyry, with little apparent strike continuity, occur within the sequences. One is well exposed in a blast hole in the S2 pit. It is not clear whether the porphyries are intrusive or extrusive. Pyritic chlorite schist/amphibolite has been noted in pulps from air core holes collared near the base of the hanging wall amphibolite sequence to the east of the C1/C3 pits.

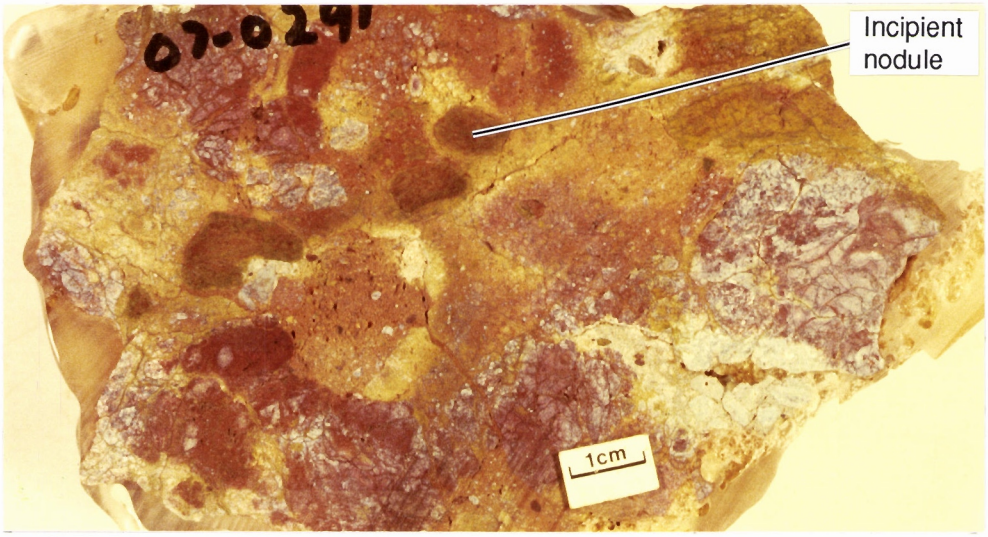

Fig. 15A. Slice through a massive duricrust showing incipient nodules and mottles in a multi-coloured sandy clay matrix, location 3350 N, 785 E.

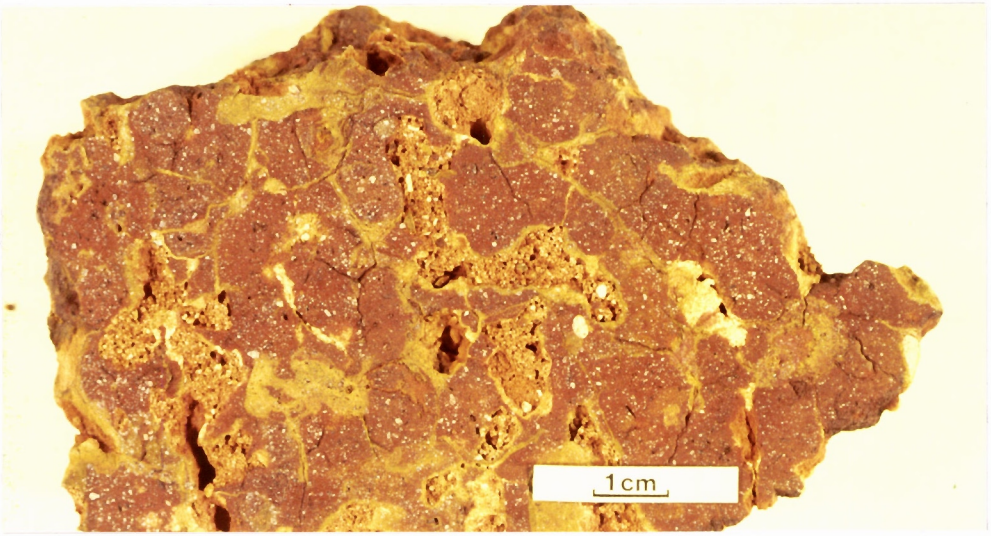

Fig. 15B. Slice through a vermiform duricrust showing vermiform voids in a sandy clay matrix, location 4450 N, 1170 E.

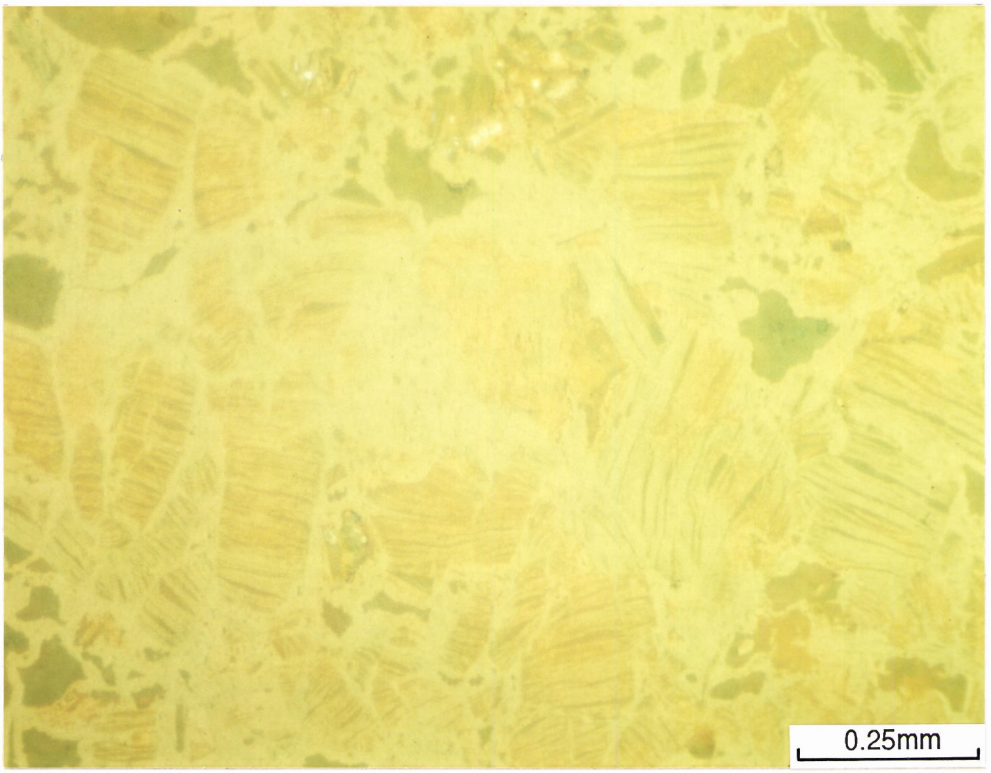

Fig. 15C. Polished thin-section of part of a nodule in nodular duricrust showing pseudomorphs of secondary minerals (goethite, hematite, kaolinite) after muscovite, location 1800 N, 915 E.

It is possible that felsic tuffs and aphanitic extrusives form part of the lower mine sequence; however, the fine-grained texture, dynamic metamorphic recrystallisation, and metasomatic alteration make it difficult to assign original lithologic types.

Chlorite-group minerals and calcite are widely developed in the saprolite separates, particularly in the metasediments, and suggest that widespread CO_2-Mg metasomatism of the mine sequence rocks has occurred. There is also extensive iron-oxyhyroxide infusion into the saprolites, resulting in the colloform crystallization of hematite, goethite, Fe-chlorite, and probably other Fe-oxyhydroxide species around primary mineral grains, particularly quartz.

Four shear-hosted auriferous hematite-quartz veins occur in the S2, C1, C3, and N2 pits. The host rocks in the S2 and C3 pits are saprolitic "quartz-eye" porphyry and probable tuffaceous metasediments. The host rock in the other cases is indeterminate.

Goethite pods

Goethite pods occur sporadically within the lateritic duricrust in all the mine pits and are common to units that are under both the red clays and the orange sandy clay. The pods, however, are most common in soils and duricrusts in upper and mid slope positions in pit S1. The pods are dark brown to black, have irregular cavities (vesicular-textured) and have a dominant goethite mineralogy. They occur as boulders up to 100 cm in diameter or small nodules (~40 mm in diameter) in the duricrust. Where goethite pods are adjacent to red hematite-rich patches, goethite appears to have replaced hematite. This replacement seems to have commenced around the outer rims of hematite nodules and progresses inwards (Fig. 16). The origin of these goethite pods is a topic of current research.

2.7 BULK CHEMISTRY AND MINERALOGY OF REGOLITH UNITS

Bulk Chemistry

The chemical compositions of bulk samples (typically of about 1 kg) of the main regolith units have been plotted on ternary Al_2O_3-Fe_2O_3-SiO_2 diagrams, the fields being shown in Fig. 17. The apices of the triangular diagrams, which correspond to 100% of the relevant oxides, can also represent, respectively gibbsite, iron oxides, and quartz. Kaolinite occupies an intermediate position between gibbsite and quartz. A relatively simple mineralogy results from the intensity and thoroughness of lateritic weathering. In such cases, chemical composition provides a general indication of mineralogical composition.

Figure 17A shows the overlap in the compositions of the various regolith units, with hardpans and soils having a broad range of compositions from silica-rich varieties to iron-rich types. Samples of saprolite and mottled zone are silica rich, and contain more alumina relative to soils. Laterites (lateritic duricrust, loose pisoliths/nodules) on the other hand, are characterized by comparatively high concentrations of Fe, with about equal concentrations of silica and alumina. Goethite pods are extremely Fe rich.

The chemical compositions of bulk samples of the various sub-units of the regolith types have also been plotted (Figs 17B to E). Soils occupy a broad field of chemical compositions which mainly arises from variations in SiO_2. Red/yellow sands are high in silica due to their high content of detrital quartz, whereas red clays and orange sandy clay soils are more Fe rich.

The broad chemical composition-field of the hardpans encompasses the two fabric types described earlier. Silty hardpan tends to be enriched in silica due to a high content of detrital quartz, clay, and amorphous silica. On the other hand, nodular hardpan is enriched in Fe due to the high detrital content of lateritic nodules and pisoliths, which themselves are rich in Fe. However, nodular hardpan shows a large variation in SiO_2, due to varying degrees of both detrital quartz and silicification ("hardpanization").

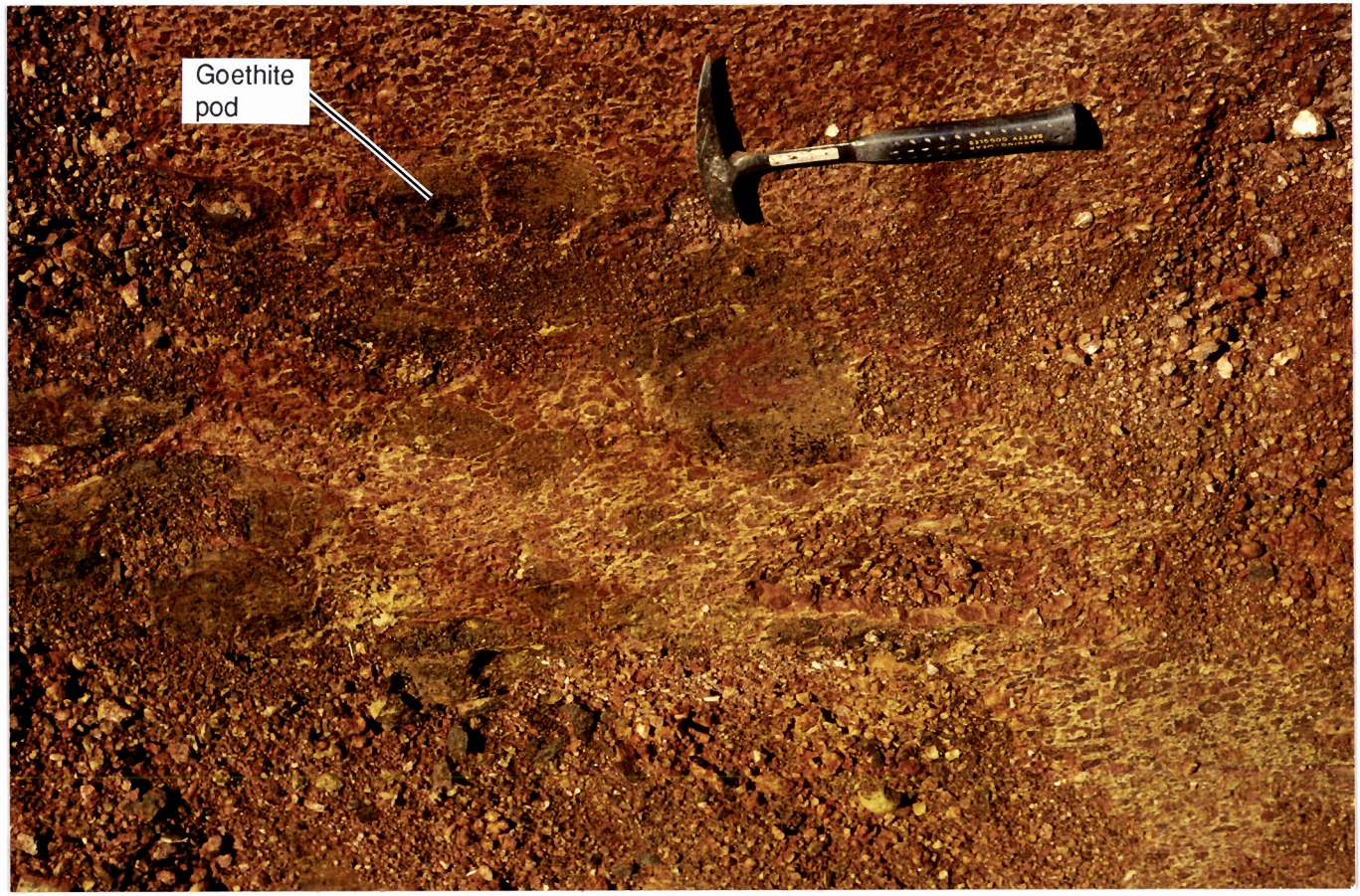

Fig. 16. Goethite pods in a brown nodular duricrust showing the interpreted replacement of hematite by goethite around the outer rims of nodules. Isolated goethite pods are also present, location S1 pit.

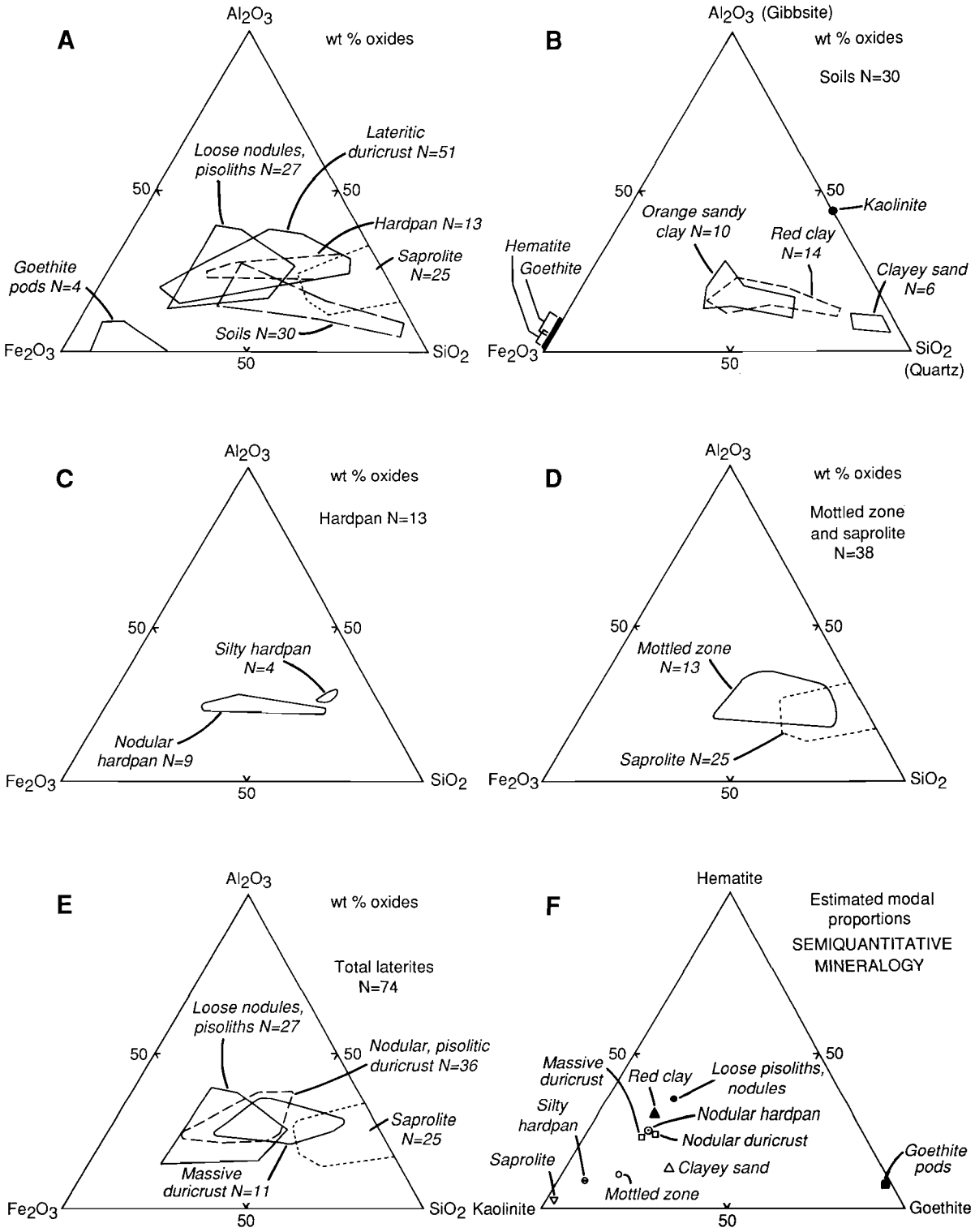

Fig. 17 A to E. Triangular diagrams showing compositional fields for the main regolith units in the Mt. Gibson orientation area, in terms of the dominant oxides. A: shows the distribution of all the compositional fields studied. F: The estimated modal proportions of the mineralogy of selected samples are shown, based upon interpretation of X-ray diffraction and whole rock chemical composition.

The compositional fields of saprolite and mottled-zone samples lie close to each other. As expected, there is a tendency for a higher concentration of Fe in the mottled zones relative to saprolite, due to the presence of ferruginous nodules and mottles.

Among the lateritic ironstone categories, nodular duricrusts have a wide compositional range, evidently reflecting variations in the chemical composition of both the constituent pisoliths/nodules and the matrix, which contains clays. Loose pisoliths/nodules have a relatively restricted compositional range.

Goethite pods have a much smaller range of composition than the nodular duricrust and loose nodules/pisoliths. Goethite pods are consistently higher in Fe_2O_3 and lower in $SiO_2$and Al_2O_3.

Mineralogy

Semiquantitative abundances of minerals were estimated using a combination of X-ray diffraction and chemical analysis of bulk samples. The relative proportions of constituent minerals were estimated from peak intensities of selected characteristic lines on X-ray diffraction traces of bulk samples. This approach provides a reconnaissance assessment of relative mineral abundance. Results obtained are plotted on a triangular diagram in terms of normalized values for hematite, goethite and kaolinite, Fig. 17F.

In the soil group, differences in the relative proportions of goethite, hematite, and kaolinite, easily separate clayey sands from red clay. There is also a clear demarcation between hematite-rich nodular hardpan and hematite-poor silty hardpan. Mottled-zone materials contain both clays and iron oxides. In contrast, the saprolite samples studied to date have a low content of iron-oxide minerals.

Mineralogical data also allow distinctions to be made between various types of laterites. Duricrusts (massive and nodular) have significantly lower hematite contents than the loose nodules/pisoliths. The differences in the abundances of hematite and kaolinite between duricrust and isolated loose nodules/pisoliths are controlled by the composition of matrix, in particular, by variable amounts of goethite and hematite.

Detrital quartz is the other major mineral present in all the regolith types. Relict feldspars showing various degrees of weathering/alteration were detected only in red clays and in hardpan, taken as an indication of less mature weathering of their source materials. Maghemite was detected in magnetic lateritic gravels present in soils, loose nodules/pisoliths, nodular hardpan and some samples of duricrust. The calcrete samples studied at Mt. Gibson are composed mainly of calcite and dolomite, with some kaolinite, goethite, and hematite. The hardpan samples also contain small amounts of calcite and dolomite. Muscovite (up to 20%) was found in saprolite. Gibbsite occurred rarely in calcrete, hardpan, and laterite samples.

2.8 REGOLITH/LANDFORM DYNAMICS

Much of the Perenjori/Ninghan region is characterized on air photos and photomosaics by complex regolith/landform/vegetation patterns. The combination of areas of sand plain, many being part of a lateritic peneplain, subdued breakaways and their associated pediplains, and local areas of colluvium and alluvium result in a variability, particularly across distances of 2 to 5 km. These patterns are particularly visible on the 1:50,000 mosaics (2338 I and III) which cover the district about Mt. Gibson. The dominant characteristics are those of a lateritic peneplain presently undergoing dismantling.

An area of red clay soils within the central part of Fig. 5 was selected for clarification of the processes which have resulted in the relatively intricate patterns we now see. Topographic contours for this part of the area, Fig. 18A, show the ridge immediately W of the S pits, and the NE sloping flanks. Contours in the lower left part of this diagram show a gentle erosional catchment which is one of several presently active about the lateritic ridge.

Inspection of this catchment, coupled with interpretation of topographic contours, reveals that there has been erosion to some 5 m below the original laterite surface. Red clay soils occur on saprolite of felsic, metapelitic, and basic lithogies, with some areas of subcrop of amphibolite. Patches of pedogenic calcrete are conspicuous, some being closely associated with subcrop of mafic lithologies. Outcrops of laterite are absent from the catchment area which is thus now starved of lateritic debris. The only present contribution of lateritic debris comes from positions b and c at the drainage divide in Fig. 18B, this contribution being minor in comparison with erosion of the soils and saprolite.

The downslope bulge shown by the contours in Fig. 18A, reaches 3 m above the surroundings, and suggested deposition. This is confirmed by mining activity in the C1 pit which has exposed the upper regolith stratigraphy over 4 hectares about position a. The regolith stratigraphy here shows a surface unit consisting of 0.5 m of red clay, overlying 3 m of a sandy, silty, gravelly colluvial/alluvial unit, which is now cemented forming a hardpan, in turn resting on nodular lateritic duricrust. The lower two-thirds of the colluvial/alluvial unit consists of lenses and sheets typically 2 to 10 cm thick containing abundant lateritic nodules and pisoliths. These gravelly lenses are interbedded with sandy and silty layers 1 to 3 cm in thickness which are relatively devoid of pisoliths and nodules. The top 30 to 50 cm of this colluvialalluvial unit is a laminated silty sandy hardpan within which pisoliths and nodules are rare or absent, but sporadic saprolite fragments and amphibolite lithorelics occur.

The above observations, together with other field relationships, lead to the conclusion that within this detail area is an erosion/deposition couple. The dismantled nodular lateritic duricrust from the gentle erosional catchment has been deposited as gravelly colluvium/alluvium. Once the catchment was essentially stripped of its duricrust, and thus relatively starved of lateritic debris as we see it today, erosion of soil and saprolite led to the silty sandy upper part of the colluvial/alluvial unit.

In this case, the depositional sequence (gravelly colluvium/alluvium of lateritic debris, then silty debris with saprolite and bedrock fragments) shows a general reversal of units of the former upland laterite profile. However, one cannot always expect such idealized simplicity.

Interpretation was extended to cover the main area of this study, using further interpretation of air photos, topographic contours, and vertical profiles through the upper regolith units. The resulting map of the regolith dynamics is shown in Fig. 19. Regolith/landform relationships for the Mt. Gibson area are thus seen in terms of the residual laterite profile, and the dynamics involved in its dismantling, namely by erosion coupled with deposition and burial.

Once the mantle of duricrust is locally removed (Fig. 20A), erosion has access to the relatively soft upper clay zone and, in turn, to saprolite. Where dismantling of duricrust commenced at a ridge crest, transportational direction can change noticeably as erosion cuts deeper into the saprolite. In the N1 and N2 pit areas, for example, slope directions (both present and palaeoslopes) imply W to E transportation of pisoliths, nodules, and mottled zone debris of the hardpanized colluvium. Their provenance is interpreted as lateritic duricrust that formerly overlay the now-eroded area adjacent to the W. Present-day erosion of this part of the area, now cutting into saprolite, has a different transportational direction, namely NNE towards the low-lying areas about Midway.

Occasional breaches in the subdued eastern catchment border at the W edge of the N pits, Fig. 19, have resulted in depositional splays superimposed upon the earlier easterly deposition in the N1 and N2 pits, sometimes causing erosion of underlying units.

Deposition of the colluvial/alluvial units can bury duricrust, as at the N1, N2, and the SE part of the C1 pits. Alternatively, depositional units can lie upon partly eroded profiles as in parts of the S2 pit.

Regolith and landform evolution at Mt. Gibson can be related to the general change to a drier climate for much of Australia, a change which has taken place since the mid-Tertiary, the first arid period believed to have been late Miocene, with cycles of aridity continuing to the present (Barlow, 1981). Deep lateritic weathering ceased and vegetation changed, resulting in slope instability. Erosion

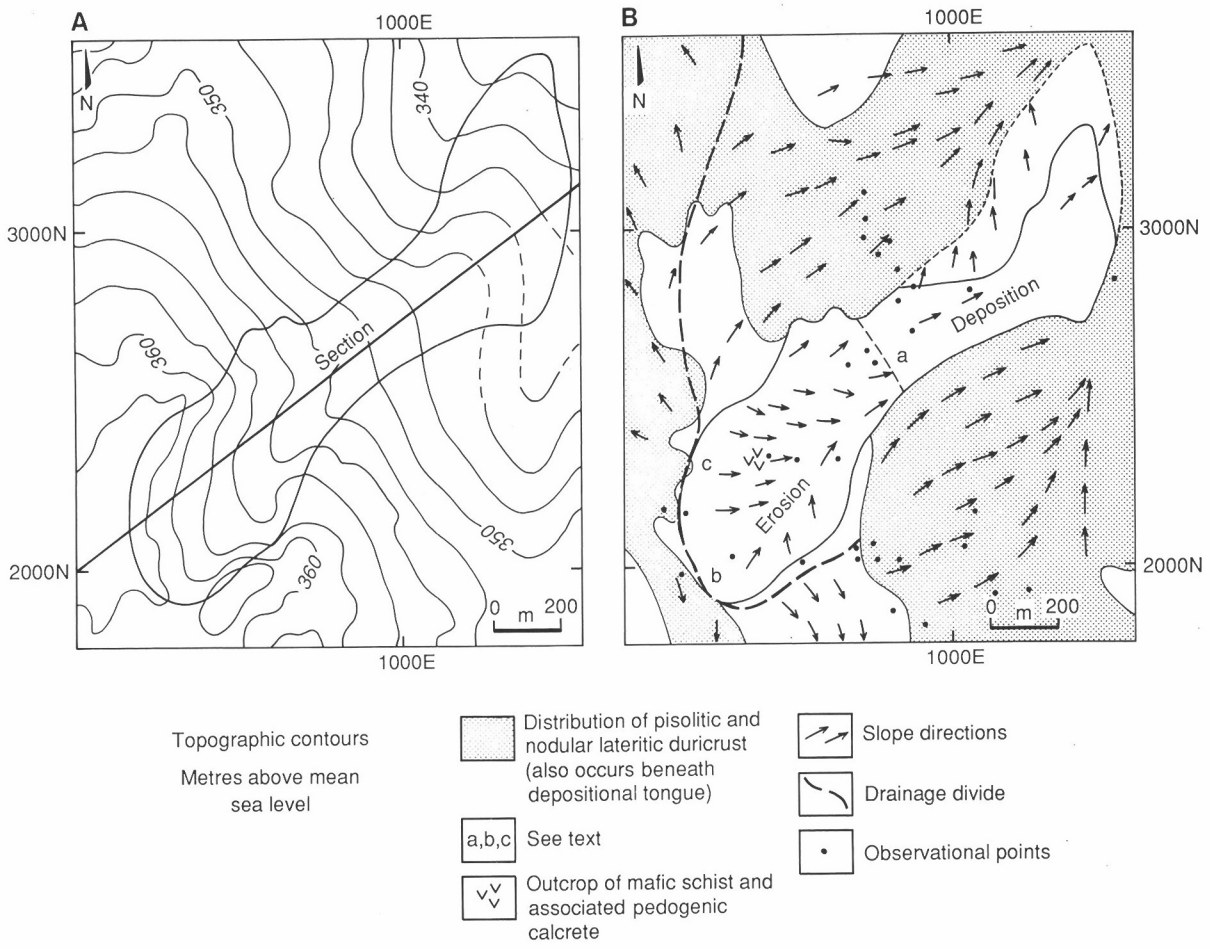

Fig. 18. Detail parts of the Mt. Gibson orientation area. A, topography; B, interpretation of the erosional depositional dynamics.

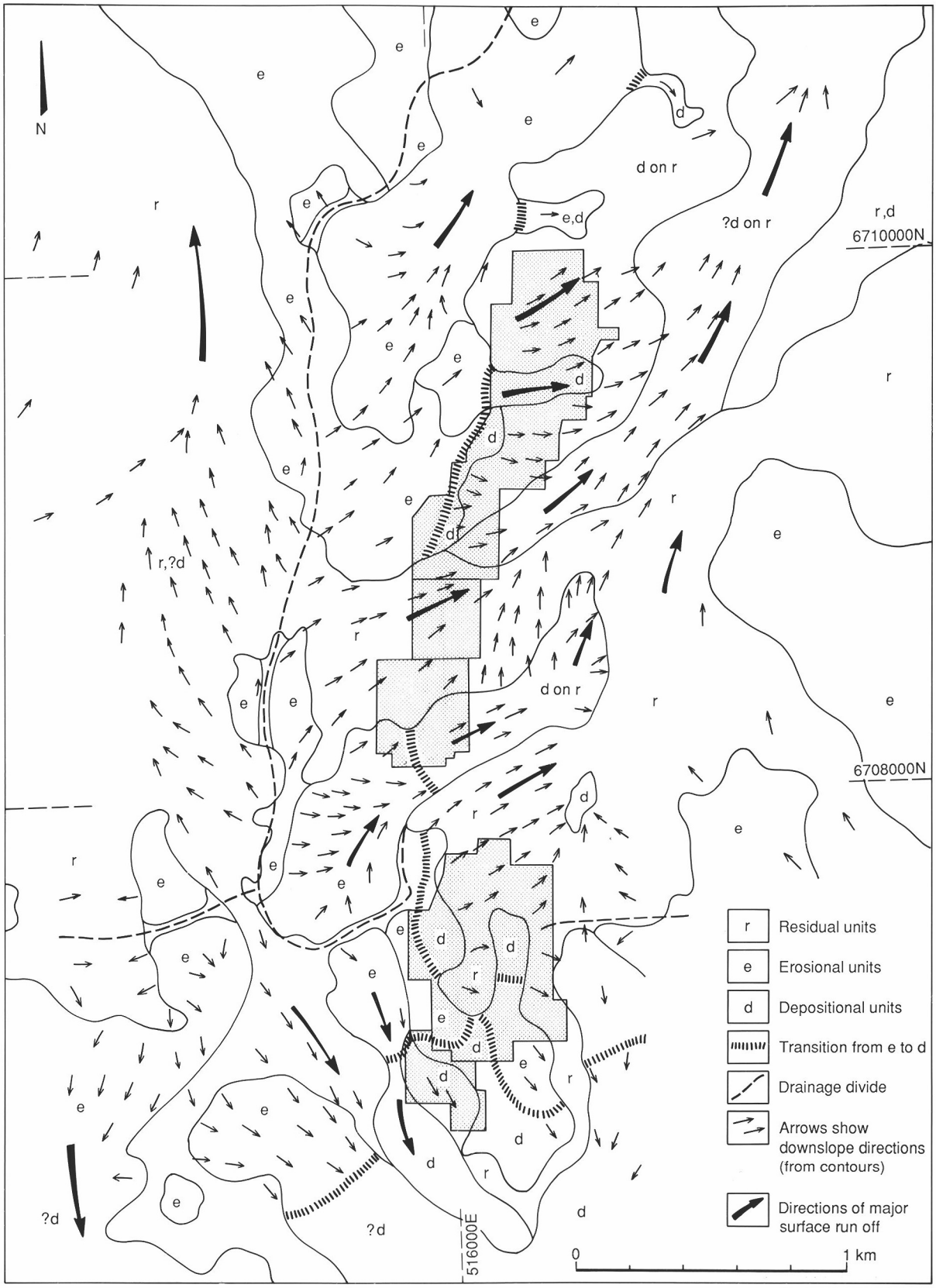

Fig. 19. Map of the Mt. Gibson orientation area showing a synthesis of regolith/landform dynamics.

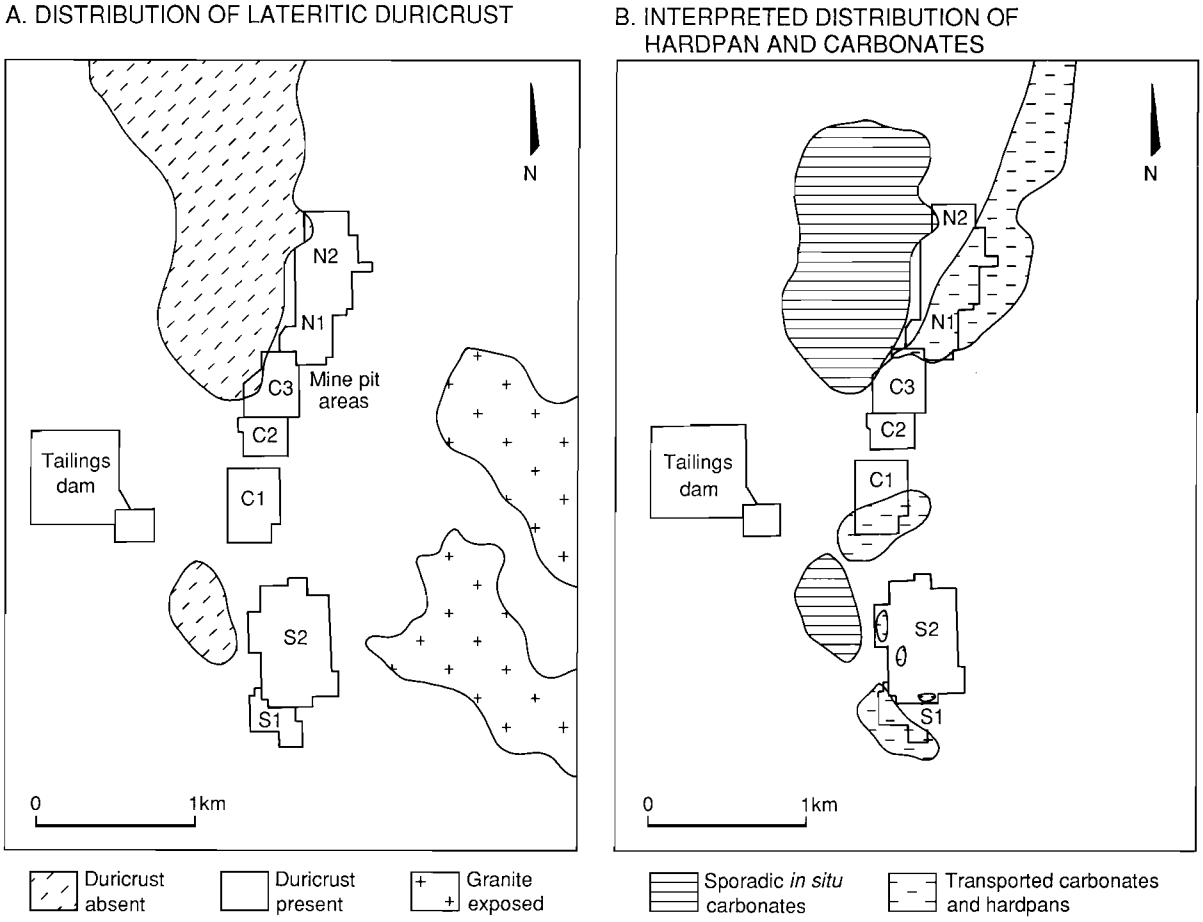

Fig. 20. Thematic summary maps of the Mt. Gibson orientation area. A, showing the interpreted surface and subsurface distribution of lateritic duricrust versus its removal. B, the identified source areas of carbonate, for comparison with mostly subsurface areas of transported and reprecipitated carbonates coinciding with hardpan.

and profile truncation have taken place via pedimentation and headward stream erosion - processes which are still continuing. In these arid areas of low relief, pedimentation occurs by scarp retreat and removal of debris by sheet wash, the end result being an undulating etch plain. In the Mt. Gibson area debris removal is incomplete.

2.9 AUTHIGENESIS AND FORMATION OF HARDPANS AND CALCRETE

The introduction of cementing materials is one of the most recognized modifications to a laterite profile occurring in response to the climate change. Silica and carbonate cements are common features of the regolith in semi-arid regions, and the products can form both near-surface and outcropping units widely distributed over the landscape (Mabbutt, 1980; Butt, 1985).

Formation of hardpan

Bettenay and Churchward (1974) suggested that hardpan is developed in colluvium and alluvium on surfaces either carved out of, or enveloping the lower parts of the laterite mantled landscape. This silicified colluvium/alluvium was given the name of 'Wiluna hardpan' (Bettenay and Churchward, 1974). They showed that cementation is due to the deposition of clay and silica, with silica forming the main cementing agent. The process of cementation was thought to result from sporadic periods of waterlogging and subsequent long periods of desiccation.

At Mt. Gibson, hardpan is developed within nodular, gravelly, and sandy colluvium/alluvium which typically contains an abundance of lateritic pisoliths, nodules, and pebbles of hardened ferruginous mottles. Micromorphologically, hardpan shows zones of strongly oriented clay around amorphous silica and zones of carbonates filling fissures. Weathering of silicate minerals is the primary source of silica for the process of hardpanization. Microscopic evidence indicates a complex development of cementation resulting in hardpan development. This appears to be related to alternating authigenic deposition of silica, clay, and carbonate phases. These findings contrast with some previous views that amorphous silica cementation is dominantly responsible for the distinctive properties of hardpan. Although amorphous silica undoubtedly occurs within the hardpan investigated, it is by no means the only cementing agent.

Wiluna hardpan was originally defined as silicified colluvium, namely mechanically transported overburden that has subsequently been partially cemented by chemically precipitated silica (Bettenay and Churchward, 1974). Hardpan is now known to incorporate residual parts of the laterite profile, and pass downwards from colluvium into brecciated saprolite, with the individual saprolite blocks retaining their original orientation even though surrounded by the silica cement. For example, at Mt. Gibson some of the lateritic duricrust and loose pisoliths/nodules are silicified (hardpanized) and as a result the duricrusts can acquire a laminated appearance. The term hardpan may need to be redefined based upon the presence of the characteristically porous matrix typically red-brown in colour, cemented by silica, clay, and/or Fe oxides that can effect a variety of transported and in situ materials.

Formation of calcrete

The distribution of transported carbonates at the Mt. Gibson area closely coincides with the distribution of hardpan (Fig. 20B). This may indicate that hardpanization and the formation of calcrete may be associated with each other. At Mt. Gibson, calcium carbonate and white, granular silica are concentrated along and adjacent to partings within hardpan. The presence of carbonates infilling the sub-horizontal fissures, penetrating the hardpan as well as forming on hardpan surfaces, indicates that the precipitation of carbonate postdates the deposition of matrix and nodules. Calcrete pods and sheets also occur within and beneath the hardpan. Suitable sources for these calcium carbonate precipitations were recognized in the adjacent upland areas. They include carbonate in red clay soils, pedogenic calcrete, and the weathering of mafic rocks.

The origin of carbonates in the downslope areas may have involved lateral transportation and redeposition of weathered fragments of calcrete which are then dissolved and precipitated at the top of profile. Probably the most common form of calcrete is authigenic calcite precipitated from laterally moving groundwater. The introduced carbonates probably develop initially as a void filling and act as a

chemical diluent. An initial period of diffuse accumulation is followed by the development of carbonate cutans, soft nodules, veins, etc.. It is concluded that fluctuating high solubilities of carbonate minerals in the groundwaters have resulted in segregation and the development of secondary structures, the growth of which may displace existing material. An abundance of growth of authigenic carbonate results in disruptions, brecciation, and displacement of existing material, as illustrated in Fig. 21. Back scattered electron (BSE) images of a lateritic nodule show the nodule to consist of alternate layers of low and high atomic number elements. Scanning X-ray images of Fe, Ca, Mg, Al, Si confirm that the light tones in the BSE image correspond to Fe oxides and clays and dark tones to carbonates. Iron is present as goethite, hematite and maghemite; Ca as calcite and dolomite; Mg as dolomite, Al and Si as kaolinite. The distribution of Ca and Mg in these images shows that calcite and dolomite precipitated from groundwaters have formed coatings around nuclei and have also infiltrated the Fe oxide species. Evidence suggests that this process, taken to completion, would eventually result in replacement of the pre-existing lateritic nodules and pisoliths.

2.10 FACIES RELATIONSHIPS AND A GENERALIZED REGOLITH/LANDFORM FACIES MODEL

Application of facies concepts and facies modelling, techniques widely used in stratigraphic basin analysis, particularly in petroleum exploration, offers promise for the systematic study of regolith materials in geochemical exploration of deeply weathered terrain. Principles of facies analysis as presented by Walker (1984) are being developed and applied in the Mt. Gibson study and will be applied in other orientation studies.

The aim of this section, following the approach of Walker, is to construct a generalized regolith/landform model that:

- provides a useful summary of relationships at Mt. Gibson;
- acts as a norm for comparisons with other orientation areas;
- acts as a framework and guide for future observations at Mt. Gibson;
- acts as a predictor in new situations:
  - locally within the study area at Mt. Gibson,
  - elsewhere in the Mt. Gibson region,
  - in other districts of similar terrain type;
- acts as an integrated basis for interpretation of:
  - the weathering and depositional environments,
  - the siting and bonding of elements,
  - the groundwater regimes,
  - dispersion processes.

The various facies of regolith materials used so far in this Mt. Gibson study are listed in Table 1, referred to earlier. Each facies is a lithological or sedimentological unit recognizable in the field, each being distinguished by its characteristic lithology, weathering or sedimentary structures, and organic characteristics. These facies are shown in relation to one another in Figs 22 and 23, in which arrows show the genetic links, italic type emphasizes processes, and roman type emphasizes products.

(a) Relationships for duricrust formation and dismantling

In Fig. 22, materials with which we are dealing are listed together with *weathering, erosional*, and *depositional* processes. A scheme of categorized arrows provides an indication of our level of understanding of the genetic processes.

Part of Fig. 22 represents the main period of lateritic weathering whereby bedrock is converted to the thick, deeply-weathered, lateritic mantle. The alkali and alkaline-earth elements are removed from the system in solution, Fe accumulates in the upper part of the profile by solution, transport, and precipitation in the form of oxides and oxyhydroxides as a result of ferrolysis, then by residual accumulation, while Si accumulates residually due to the relative insolubility of SiO_2. The ground surface is thus progressively, though not uniformly, reduced in altitude by this chemical weathering as the first

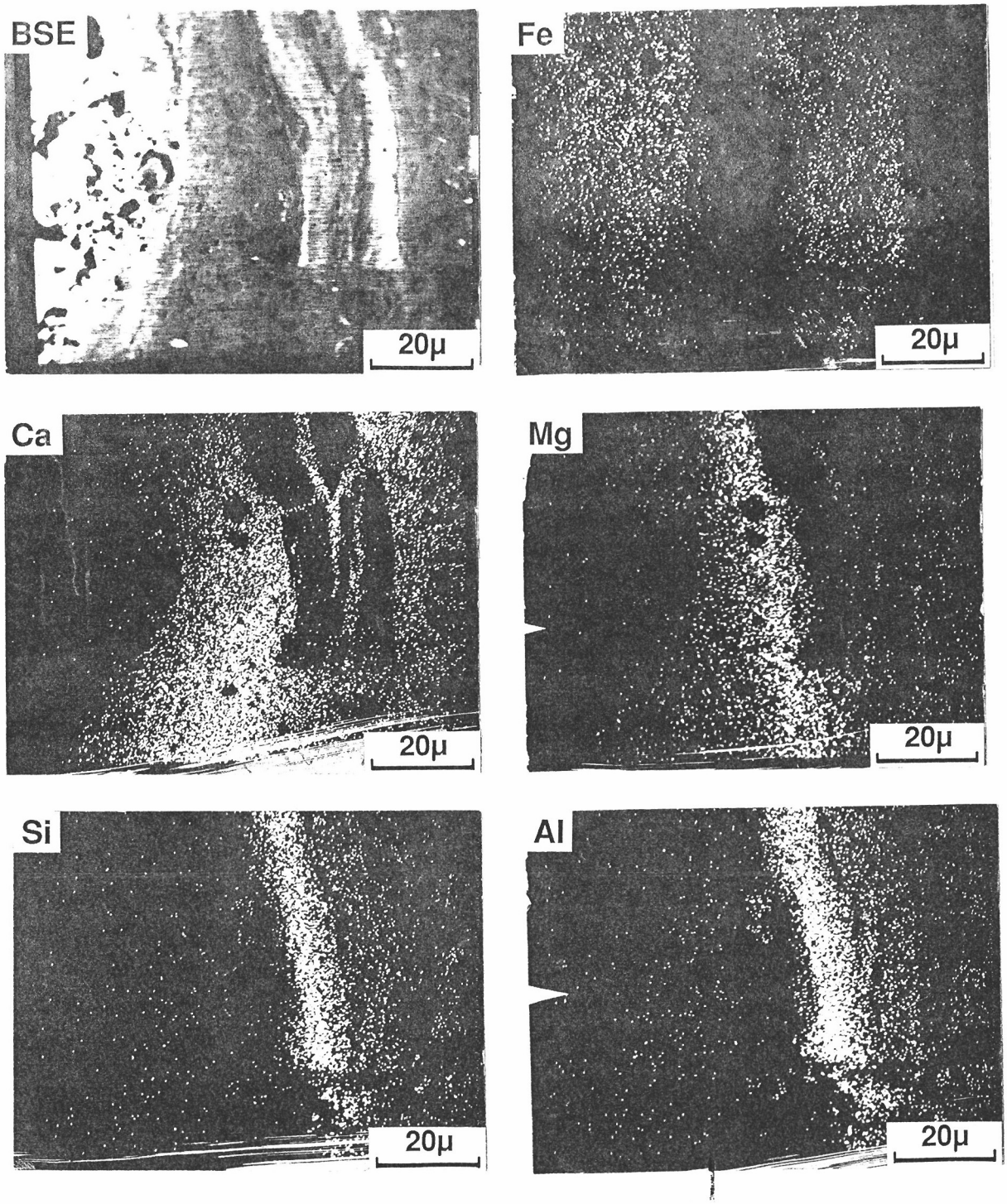

Fig. 21. Electron microprobe back scattered electron image showing the contrasts in average atomic number in a lateritic nodule from a calcrete unit, see text. X-ray images showing the distribution of Fe, Ca, Mg, Si, and Al in the same lateritic nodule, location 3530N, 855E.

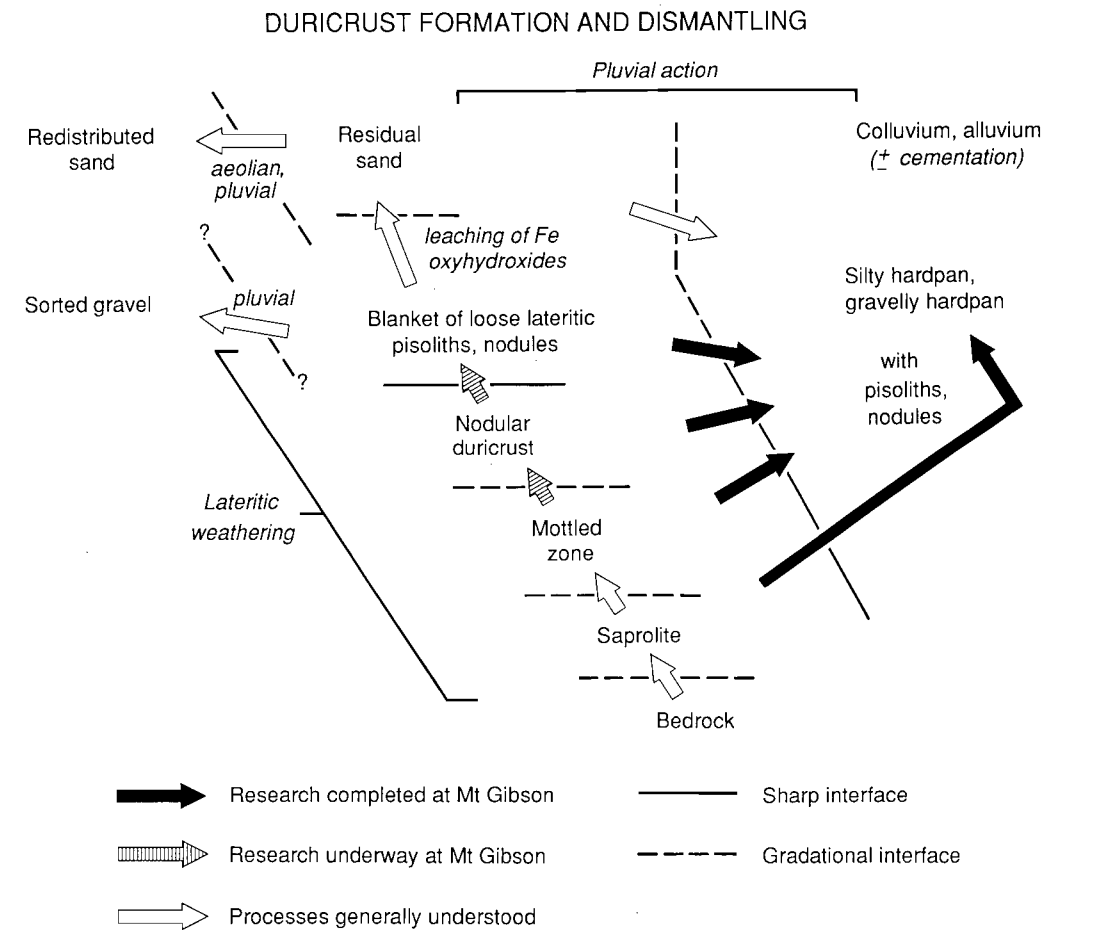

Fig. 22. Schematic facies relationship diagram for the formation of the lateritic weathering mantle and its subsequent dismantling

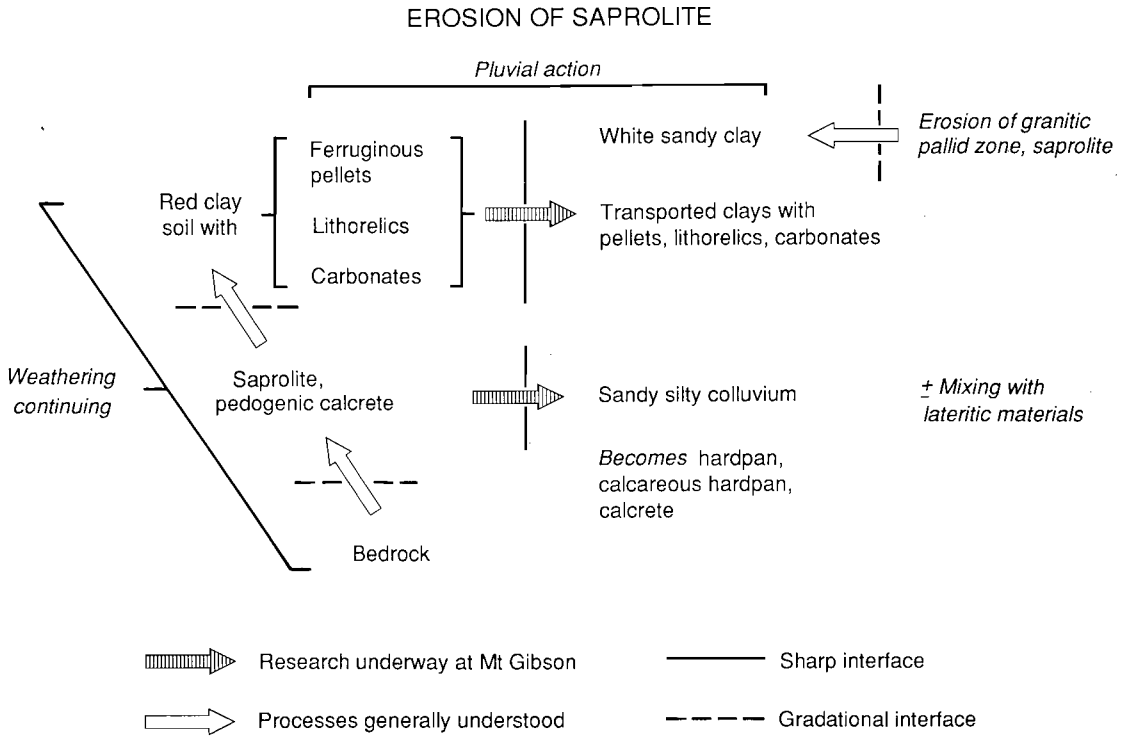

Fig. 23. Schematic facies relationship diagram for the period of erosion of saprolite coupled with post-lateritic weathering.

stage of an etch process. A most important part of this stage is the dispersion of the ore-associated elements from mineral deposits in the bedrock, discussed later, and the formation and preservation of associated geochemical haloes.

In formation of the lateritic weathering profile, each successor originates essentially *in situ*, at times with shuffling and disaggregation, from a preceding one. It is possible in some cases to recognize in each stage relics of former facies. The earliest formed lateritic facies may preserve structures and textures from the parent rock. As weathering progresses, clays are broken down and the concentration of residual Fe in spots, blotches, and streaks leads to the generation of mottles, forming a mottled clay zone, where the major difference between mottles and the surrounding matrix is the Fe content. The Fe concentrations or mottles increase in size upwards. With further mobilization and concentration, the Fe oxides become re-organized into secondary structures such as nodules. In the upper part of the mottled zone and lower part of the massive duricrust, the nodules have more or less diffuse outer rims and are partly indurated (soft, incipient nodules). In the upper parts of massive duricrusts, the nodules become more indurated and their boundaries with the matrix become distinct. Nodules become increasingly abundant towards the top of the nodular duricrust. As sphericity of nodules increases by dissolution of irregularly-shaped edges, some nodules develop into rounded pisoliths. Following this evolutionary trend, pisoliths are relatively more abundant in the upper portion of the nodular duricrust. Pisoliths/nodules may be banded or unbanded. Banded pisoliths may form by centripetal concentrations of Al- and Fe-rich coatings around various nuclei.

Some nodules in the duricrust show the pseudomorphic preservation of original rock textures by goethite, hematite, and kaolinite. In contrast, the clayey matrices are characterized by the absence of original structures of primary minerals. Because of their inherited structure, evidence suggests that some nodules represent an earlier stage of weathering than the surrounding matrices.

Vermiform structures occur in the duricrust where tubular channels are filled with kaolinte and goethite. The dominance of goethite suggests that the Fe oxides impregnated former kaolinite-rich soil materials. Based upon examination of a relatively limited number of samples, it is suggested that this vermiform fabric may represent a degradation of the duricrust through dissolution of the original matrix material and subsequent infilling by Fe oxides and clays. No evidence was seen to suggest that ants or termites are responsible for the formation of the tubules as has been suggested by some authors, nor were any seen to have colonized the clay filled channels and developed extensive galleries.

In the upper part of some pits, the duricrust was crumbly and forming an essentially *in situ* pebbly horizon composed of coarse and fine lateritic gravel. The duricrust matrix is breaking down by dissolution, which allows separation of nodules and pisoliths, producing a highly porous horizon of nodules and pisoliths dispersed in a sandy clay matrix. Fine cracks are seen in duricrust which split pisolith/nodules into fragments essentially without displacement. These are dissolution cracks. Further dissolution of Fe oxides and oxyhydroxides produces a residual quartz-rich sand which can be subjected to various fluvial and aeolian processes.

Also shown schematically (Fig. 22) is the dismantling of the upper parts of the laterite profile (mottled zone, duricrust, and loose lateritic pisoliths and nodules) by pluvial processes. Dismantling leads to the deposition of colluvial/alluvial units rich in lateritic debris, with subsequent cementation resulting in hardpan.

(b) Relationships for Partly-Stripped Areas

Figure 23 depicts the effects of post-lateritic weathering upon areas where stripping has removed the ferruginous and mottled zones.

Weathering of saprolite and bedrock exposed in erosional areas continues. Red clay soils are characteristic, particularly in areas of amphibolite and are typically associated with open Eucalypt woodlands. Ferruginous pellets and carbonate nodules are formed *in situ* in red clay soils and lithorelics are also common. The parent materials upon which weathering is acting can be relatively labile where

mafic bedrock is near the surface and pedogenic carbonates can be locally abundant. Pedogenic calcrete forms by the relative accumulation of carbonates due to the alteration of host materials in saprolite resulting from the selective removal of non-carbonate fractions.

In areas where soil is developed on saprolite, rainfall more easily initiates overgound sheet wash because of the relative impermeability of the clay-rich soils. This sheet wash causes shallow erosion more easily than in areas characterized by a sandy, gravelly duricrust. In the latter, near-surface and subsurface permeability allows a higher throughflow of groundwater.

Pluvial action thus leads to deposition of clay-rich colluvial/alluvial units on top of laterite. Subsequently, soil formation results in episodes of clay illuviation and silicification, forming hardpan. Where there is a carbonate source upslope, deposition can lead to carbonate-bearing colluvium with high pH overlying the low pH laterite profile (an out of equilibrium situation) as well as extensive carbonate cementation.

Stripping of granitic saprolite can lead to burial of the laterite profile and the related lateritic colluvial/alluvial units by a characteristic white sandy clay, such as that in the lowlands near Midway (Fig. 2). Continued weathering superimposes ferruginous mottling upon this sediment and this must be distinguished from the mottled clay zone of the original laterite profile which, in such a case, may occur some tens of metres deeper in the profile.

(c) Generalized Regolith/Landform Model

The generalized regolith/landform model derived from the Mt. Gibson study is shown in Fig. 24. The essential ingredients are a residual lateritic weathering profile that undulates over the landscape, and, as discussed above, erosion partly dismantling the duricrust, cutting into saprolite, the resulting debris being deposited locally as aprons, in deltaic splays, or more distally in alluvial valley fill. Essentially complete laterite profiles can be extensively preserved beneath this valley fill.

Transportation of carbonate bearing colluvium over distances of 300 m has led to calcareous soils (pH 8-9) overlying the laterite profile adjacent to upland areas undergoing erosion and containing mafic bedrock types.

The impact of high pH carbonate-bearing soils overlying the low pH laterite profile on groundwater and laterite geochemical cycles (including that for Au) is presently being researched.

Where the weathering profile is buried beneath alluvium, the complete profile will not be preserved everywhere because many of the district and regional scale trunk drainages, now choked with sediments, would once have been active erosional areas.

2.11 DISCUSSION

Lateritic horizons, red-brown hardpan, calcrete, and soils are conspicuous elements of both the landscape and the regolith stratigraphic column in the Mt. Gibson mine area. The landforms and regolith of the complex lateritic sandplain of the Perenjori/Ninghan region, typified by the Mt. Gibson area, can be related to a complex physiographic history, including deep weathering and processes of erosion and deposition. Stripping of the weathered profiles to varying degrees, is an important process, giving several different apparent land surfaces related to a single older weathering profile. Stripping is clearly expressed on crests. In contrast, the deeply-weathered materials in footslopes are little affected by erosion. Materials from erosional areas have been moved from crests into upper and midslope areas with the consequent burial of the residual laterite profile. Both the hardpan and calcrete are clearly much younger than the weathered surface and develop in detritus resulting from the erosional modification of the old surface. The influx of silica and carbonates is a relatively recent addition to the landscape and was not involved in the creation of the original deep weathering profiles in which they are now found.

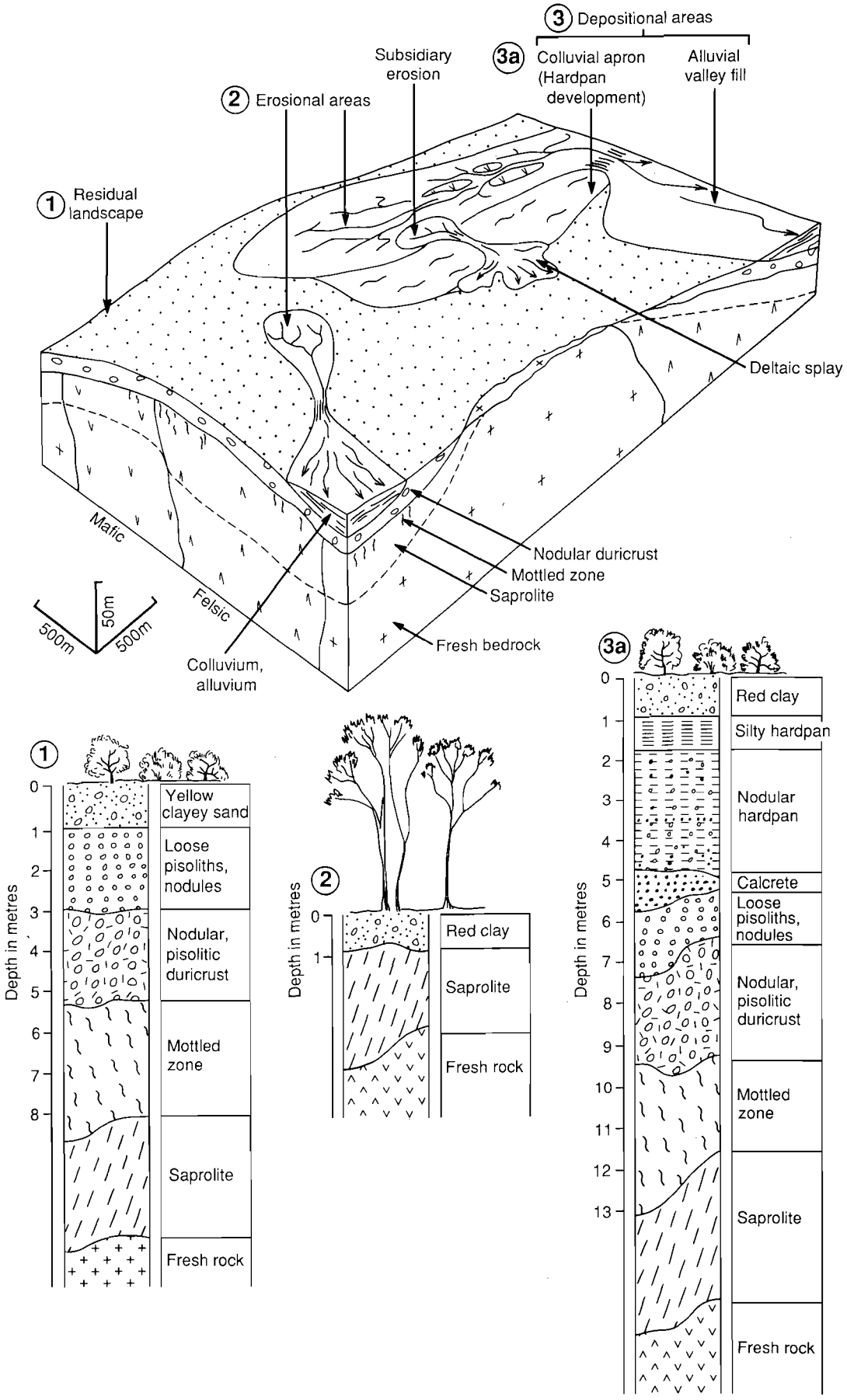

Fig. 24. Generalized regolith/landform facies model based upon the Mt. Gibson orientation area.

Recently, Ollier *et al.* (1988) suggested that the ferricretes (laterites) in the Kalgoorlie region, Western Australia, form in sediments that unconformably overlie either bedrock or saprolite. Iron solutions pass through the relatively porous and permeable sediments and cement them. Laterite, in the landscape we have studied, represents various stages in the development or dissection of the ideal laterite profile. The combination of field observations and laboratory data suggest that laterites at the Mt. Gibson area are largely *in situ* and formed by the process of lateritization. Nodules and pisoliths in lateritic duricrust show the preservation of pseudomorphs of clay minerals and Fe oxides after primary minerals typical of *in situ* weathering as described by several authors (e.g., Bisdom *et al.* 1982). However, some element of transportation may have been involved in the formation of laterites in the northern section of pit C1. Nodules and pisoliths in packed duricrust (with little sandy matrix) underlying yellow/red sands appear to be well sorted and there is a sharp boundary between the soils and the underlying lateritic pisoliths/nodules. Packed duricrust is probably developed from the partial destruction of primary lateritic duricrust or the denudation of lateritic soils, followed by the transportation of the fragments of original duricrust, their subsequent deposition and later recementation by secondary enrichment with Fe minerals (Pullan, 1967; McFarlane, 1976). The possibility of forming packed duricrust *in situ* may not be completely ruled out. Breakdown of duricrust accompanied by dissolution of matrix can also produce packed duricrust. However, an unusual depth of laterite (4-5 m) for the area and the sorting of gravels favour the first hypothesis.

---o0o---

3.0 GEOCHEMICAL DISPERSION IN LOOSE PISOLITIC AND NODULAR LATERITE

3.1 INTRODUCTION

Orientation sampling over the area, including the S, C, and N pits at Mt. Gibson by the CSIRO Laterite Geochemistry Group, was commenced in November 1986, prior to the beginning of mining operations. This sampling focussed initially upon the regolith unit consisting of loose lateritic pisoliths and nodules. During 1987 further orientation sampling was carried out by GEOCHEMEX Australia under contract to the Mt. Gibson Gold Project as part of a geochemical survey which extended over a 7-km by 11-km area. That survey was coupled with their regolith/landform appraisal, mentioned earlier, over the same area.

The combined orientation results of these two studies showed that the Mt. Gibson lateritic Au deposits at the S, C, and N pit areas were part of a chalcophile multi-element geochemical anomaly, having an overall Au, Ag, Pb, As, Bi, Sb, W, and Ge association (Sb, Pb, and W being zonally stronger in the northern part of the anomaly). The geochemical anomaly had a consistent NS elongate geometry and measured 7 km in length and 1 km to 1.5 km in width. Until recently, no obvious suitable source or sources of the anomaly were agreed upon, but were presumed to be Archaen greenstones (Davy *et al.*, 1988). These authors, however, reported a basemetal sulphide association (pyrite, sphalerite, galena, rare chalcopyrite), with a maximum for Au values of 0.6 ppm at Mt. Gibson Well, 4 km to the N of this study area.

The coincidence within the lateritic geochemical anomaly of eight chalcophile elements, including Au, forming three geochemical centres (at the S, C and N pits) suggested close genetic links to bedrock sources. The simplest explanation was that the pisolitic laterite was essentially *in situ* (Smith, 1987). The multi-element chalcophile suite of elements in the laterite geochemical halo suggested a polymetallic sulphide system in bedrock as the most likely source. More recent mining activity has in fact exposed some bedrock sources of Au and chalcophile elements by way of quartz-hematite veining, which show a direct relationship to some of the strongest parts of the geochemical anomaly, discussed later.

A phase of detailed research into the geochemical dispersion patterns and processes by the CSIRO Laterite Geochemistry Group commenced in December 1987 under AMIRA funding. The aims included the filling in of orientation sampling so as to provide a continuous network of control samples which would form a geochemical reference group. Another aim was to systematically sample other units of the laterite profile as mining provided further exposure of the regolith stratigraphy. To date, the loose pisolitic nodular laterite unit has been extensively sampled, the main topic of the geochemical patterns in this report, as well as the underlying nodular to massive lateritic duricrust, the geochemistry of which is nearing completion.

3.2 SAMPLING PARAMETERS

The geochemical patterns presented in this report are based upon a total of 109 sample sites of loose pisolitic nodular laterite giving an average density of 18 samples per square kilometre. Sixty-seven of these samples represent an approximate triangular grid pattern of 200 m by 300 m. Additional data is provided by 42 samples taken at specific sites.

Data on 22 GEOCHEMEX samples from within the orientation area are kindly made available by the management of the Mt. Gibson Gold Project for inclusion in the research. The GEOCHEMEX samples received non-metallic sample preparation to CSIRO specifications at AMDEL, followed by the same analytical methods, both data sets thus being compatible.

Samples, upon which the geochemical patterns presented in Figs 25 to 35 are based, were collected from the regolith unit consisting of loose lateritic pisoliths and nodules, an essentially residual unit directly overlying lateritic duricrust.

A 1-kg sample was taken at each site for crushing and analysis with a duplicate 1 kg for future reference and for follow-up research. Field sheets record whether samples were taken from the natural ground surface, the surface after stripping of the top soil, or from exploratory or mining pit faces, noting also whether the material comprising a sample was taken over a radius of 5 to 10 m on the ground surface (in order to suppress any unforseen local variation) or sub-horizontally for 5 m along the unit. Samples of specific units within vertical profiles generally consisted of a 1-kg grab sample.

The lateritic pisoliths and nodules were generally in the size range 0.5 cm to 2.0 cm and were either collected using a non-metallic sieve or were hand-picked from the sub-ordinate amount of fine sandy or silty matrix. Separate studies have generated analytical information on the matrix for comparative purposes. This will be reported at a later date. The pisoliths and nodules were ultrasonically washed so as to avoid the possibility of contamination of their surfaces from adhering mine dust. Generally this is unlikely because at many sample sites fresh surfaces were exposed by hand in pit walls before sampling.

3.3 SAMPLE PREPARATION

Samples were crushed and ground using non-metallic methods described by Smith (1987). Oversize material from the bulk sample was reduced to minus 8 mm by crushing between zirconia plates in an automated hydraulic press with the undersize then being processed through an epoxy-resin lined disc grinder with alumina plates and reduced to minus c. 1 mm. Final milling was done in an agate mill. Cleaning of the equipment was performed by a combination of air- and sand-blasting and by the passage of quartz blanks.

Eighty-seven of the 109 samples received their full crushing and grinding at CSIRO. The twenty-two GEOCHEMEX samples were prepared to the same non-metallic crushing and grinding specifications at AMDEL in Adelaide.

3.4 CHEMICAL ANALYTICAL METHODS

A combination of analytical methods were used as shown in Table 2. These include major and minor elements by ICP (Si, Al, Fe, Ti, Cr, V after alkali fusion, others after $HCl/HClO_4/HF$ digestion), some minor and trace elements by AAS after HF digestion, many trace elements determined by XRF on pressed powder discs, some using extended counting times to lower detection limits, and Au on a 30-g pulp using aqua regia digestion and graphite furnace AAS. The CSIRO samples were analysed for in excess of 30 elements, some being verified by additional methods. The GEOCHEMEX samples were analysed for the 15 most useful elements shown by the CSIRO sampling. Table 2 shows the elements analysed, the methods, and the lower limits of detection.

3.5 GEOCHEMICAL ASSOCIATION OF THE LIKELY SOURCE MINERALIZATION

The available information, presently sketchy, on the geological setting of the orientation area was presented above (Section 2.3 and Fig. 4).

Little geochemical information has been compiled on likely bedrock sources at this stage. Table 3 lists the ranges of some elements of interest in three samples of quartz-hematite veins in saprolite exposed in the mining pits, coinciding with strong parts of the laterite geochemical anomaly. These few samples clearly show a Au As Sb Bi ± (Cu Pb Ge Se) association.

A similar structural setting, lithological and geochemical associations, also exists at the Hornet pit in the Midway North area, 4 km north of the Mt. Gibson plant site. There, a strong Au-As-Bi association is developed with Bi sulphosalts being recorded from the zone of primary sulphides (Simon Coxhell, pers. comm., Feb. 1989).

TABLE 2. Chemical analytical methods used showing lower limits of detection.

Element		Method	Lower Limit of Detection ppm except where shown wt%	
SiO_2		ICP	0.1	%
Al_2O_3		ICP	0.02	%
Fe_2O_3		ICP	0.01	%
MgO		ICP	0.01	%
CaO		ICP	0.01	%
Na_2O		ICP	0.01	%
K_2O		ICP	0.06/0.01	%
TiO_2		ICP	0.003	%
Mn		ICP	15	
Cr	Gx	ICP & XRF	10	
V		ICP & XRF	10	
Cu	Gx	XRF & AAS	10	
Pb	Gx	ICP, AAS & XRF	5	
Zn	Gx	XRF AAS	5	
Ni	Gx	XRF & AAS	10	
Co	Gx	XRF & AAS	5	
As	Gx	XRF	2	
Sb	Gx	XRF*	2	
Bi	Gx	XRF*	2/5/1	
Cd		XRF	1	
In		XRF	1	
Mo	Gx	XRF*	2	
Ag	Gx	AAS	0.1	
Sn	Gx	XRF*	3/1	
Ge	Gx	XRF*	2/1	
W	Gx	XRF*	5	
Zr		ICP	4	
Nb		XRF	3	
Se		XRF*	2/3/2	
Au		Graphite furnace AAS Aq reg.	0.001	
B		YET to be analysed		

ICP = Inductively coupled plasma optical spectroscopy, Si, Al, Fe, Ti, Cr, V after an alkali fusion, others after HCl/HClO4/HF digestion.
AAS = Atomic absorption spectrophotometry, after HCl/HClO4/HF digestion.
XRF = X-ray fluorescence.
XRF* = X-ray fluorescence using extended counting times.
GX = Elements analysed in the GEOCHEMEX orientation survey.

TABLE 3. Ranges in values for three samples of mineralized hematite-quartz veins in saprolite, S2, C1 and N2 pits.

Element	Min. Value	Max. Value
Wt Percent		
SiO_2	55.40	76.15
Al_2O_3	4.63	7.16
Fe_2O_3	17.16	32.46
MgO	0.030	0.048
CaO	0.017	0.022
Na_2O	0.022	0.057
K_2O	0.017	0.105
TiO_2	0.202	0.272
Values below in ppm		
Mn	24	100
Cr	58	657
V	621	1170
Cu	24	464
Pb	71	159
Zn	6	41
Ni	<5	47
Co	<5	<5
As	11	2800
Sb	1	43
Bi	6	340
Mo	<1	<1
Ag	0.5	1.0
Sn	1	11
Ga	2	11
Ge	<2	5
W	1	12
Nb	<3	5
Zr	<4	48
Se	<2	11
Be	<1	<1
Au	0.6	31.0

Analyses by ANALABS (Perth)

3.6 RESULTS

Analytical data for samples from the regolith unit consisting of loose lateritic pisoliths and nodules are plotted in Figs 25 to 35, showing both the analytical values and hand interpreted contours. Analytical data on individual samples are given in Appendix III.

Au

The geochemical pattern for Au (Fig. 25) shows marked consistency over the 1-km width of the anomaly for a strike length in excess of 4 km, the anomaly continuing to the north. A threshold between 30 and 50 ppb would be appropriate in reconaissance for such an anomaly. This is in keeping with experience elsewhere in the Yilgarn Block, as shown by percentiles inset in the figure.

The N to NNE trend of the anomaly parallels both the regional magnetic trend and the strike of the underlying sheared metasediment-metavolcanic sequence. Four discrete bull's-eye anomalies are superimposed on the broad pattern, each sited over a known epigenetic auriferous quartz-hematite vein or vein swarm in sheared saprolitic tuffaceous sediment or "quartz-eye" porphyry. The three foci based on the C1, C3 and N2 veins are concentric while that over the S2 pit is skewed, showing some downslope dispersion over about 400 m to the SE.

Gold shows a more widespread and homogeneous dispersion pattern in this regolith unit than any of the chalcophile elements. The closest associations with Au are shown by Ag, Pb, As, Bi, Sb, and W, which are now discussed.

Ag

The dispersion pattern of Ag (Fig. 26) maintains the strike continuity of the Au pattern but not the width. There is a rapid drop-off to values below the detection limit of 0.1 ppm and the vein-related bull's-eye anomalies are not as pronounced as with Au. The anomalies are skewed in relation to bedrock mineralization and show a pattern extending downslope some 800 metres to the south of the S2 pit and also to the NE of the veins in the C1, C3, and N2 pits.

Some of the highest values of Ag are not obviously related in detail to any of the recognized vein locations. Silver values exceeding 1 ppm, as we see here, are very rare in the Yilgarn Block, Ag tending to be strongly leached during lateritic weathering.

Pb

Lead is similar to Au in the strike continuity and breadth of its dispersion pattern (Fig. 27) although the anomalies are rather subdued with peak maxima at 100 to 135 ppm Pb. There are bull's-eye anomalies centred on the S2, C1, and N2 veins as well as highs in the S1 and northern N2 pit areas which do not relate to exposed veins. The more gentle E gradient to the geochemical pattern is compatible with a 400 to 500-m dispersion downslope, somewhat similar to that shown by Ag.

As

The As pattern is extensive both within Fig. 28 and along strike to the N, but it is generally weak relative to patterns commonly seen in the Yilgarn Block. Recognition of this As anomaly thus depends upon it being located in a district with low background As levels. The same holds for the usefulness of the As anomalies at Golden Grove (Smith and Perdrix, 1983).

The As pattern is centred some 200 m E of the recognized quartz-hematite veins. This is compatible with the downslope directions. However, more bedrock knowledge is required, as well as research, in order to reach conclusions on dispersion distances and mechanisms.

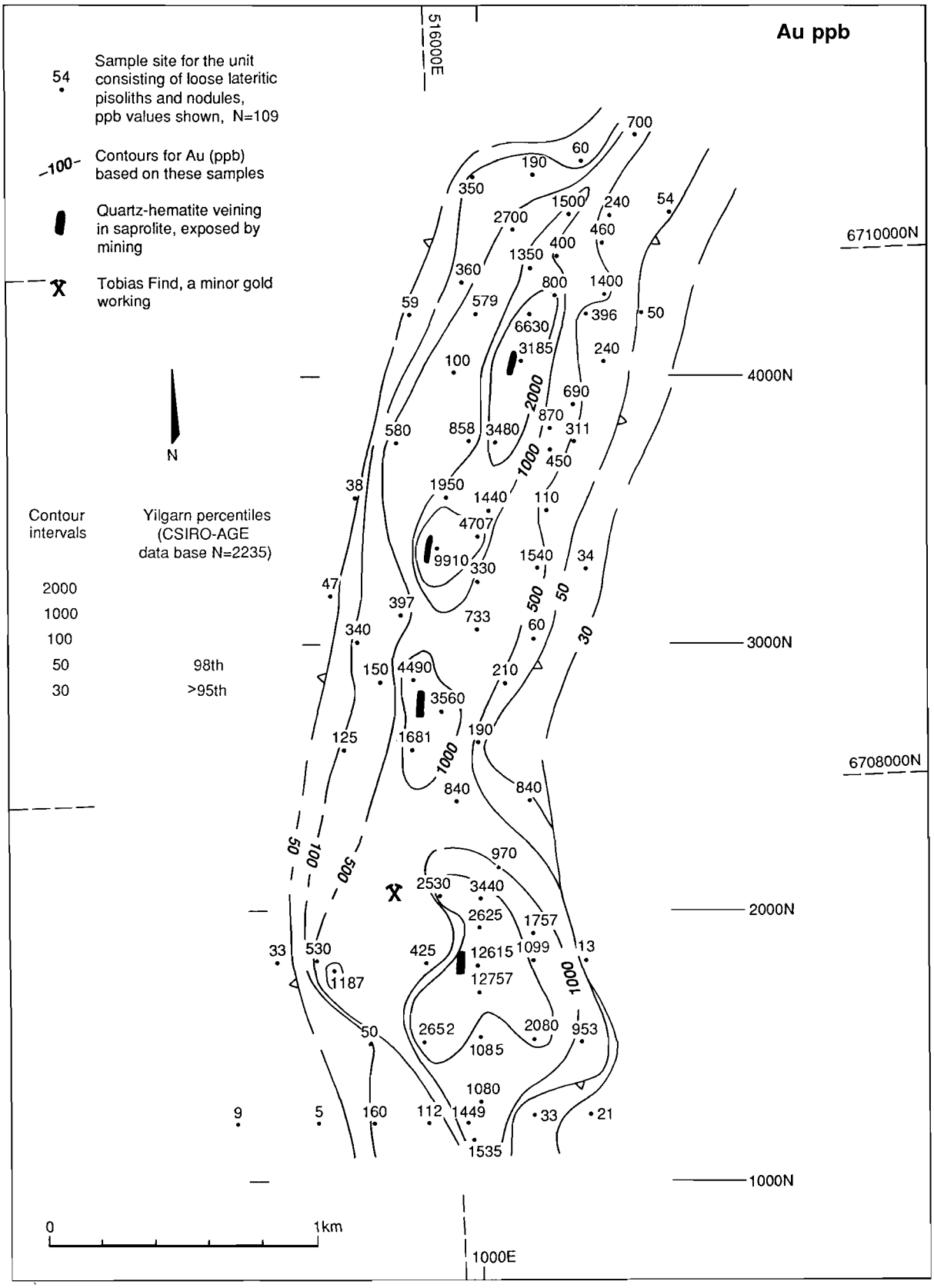

Fig. 25. Plan of the Mt. Gibson orientation area showing the distribution of Au in the regolith unit consisting of loose lateritic pisoliths and nodules.

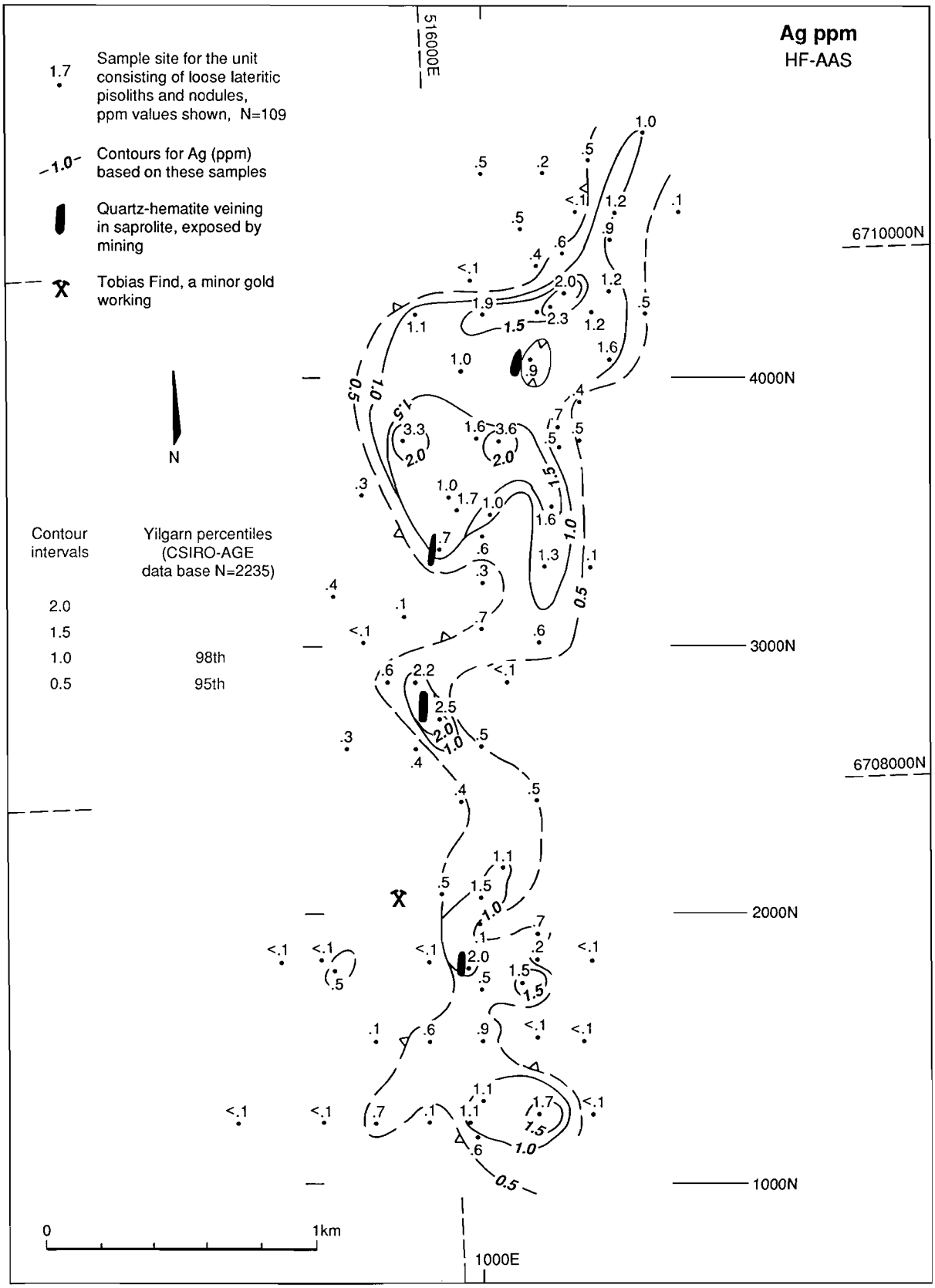

Fig. 26. Plan of the Mt. Gibson orientation area showing the distribution of Ag in the regolith unit consisting of loose lateritic pisoliths and nodules.

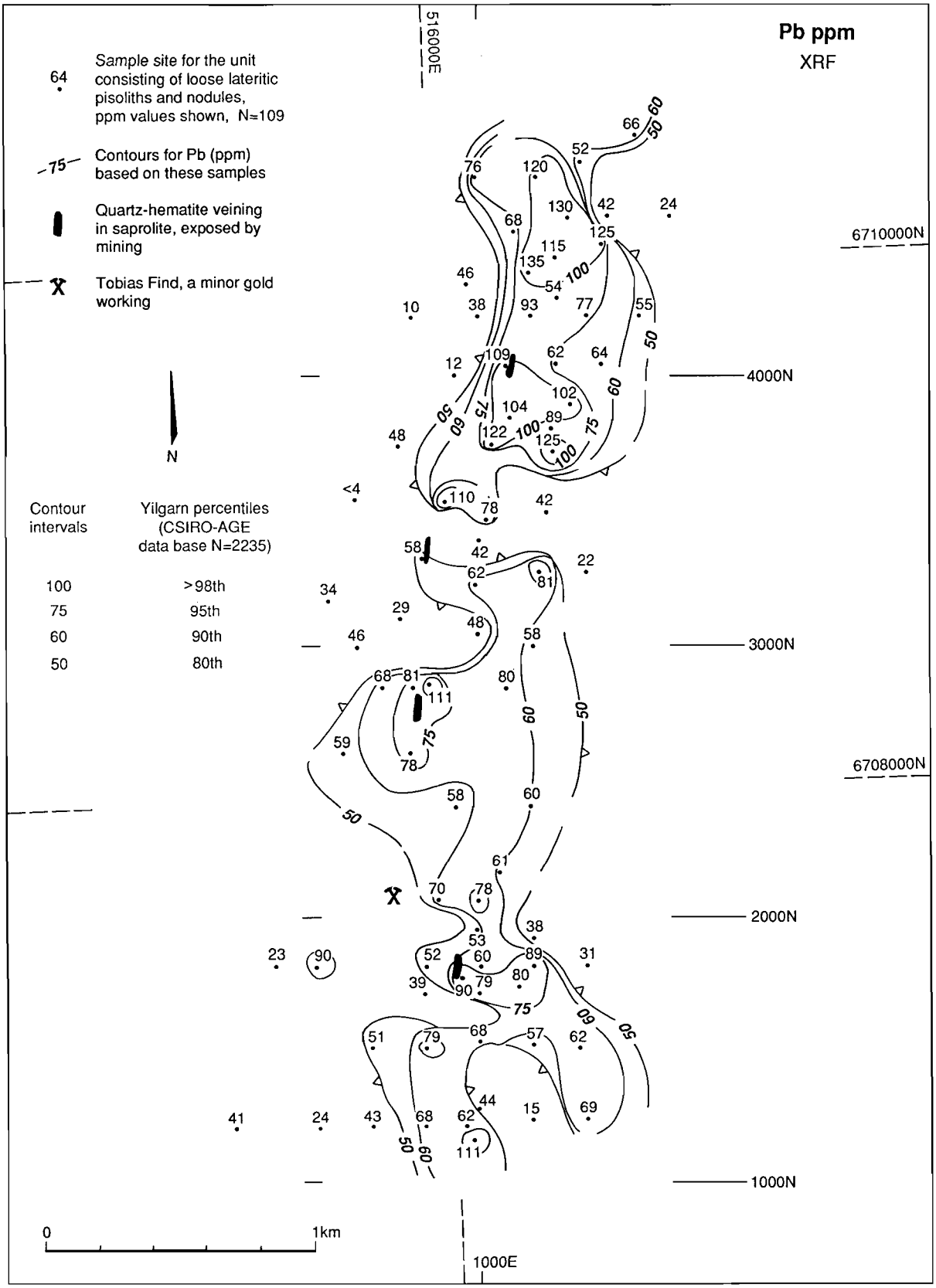

Fig. 27. Plan of the Mt. Gibson orientation area showing the distribution of Pb in the regolith unit consisting of loose lateritic pisoliths and nodules.

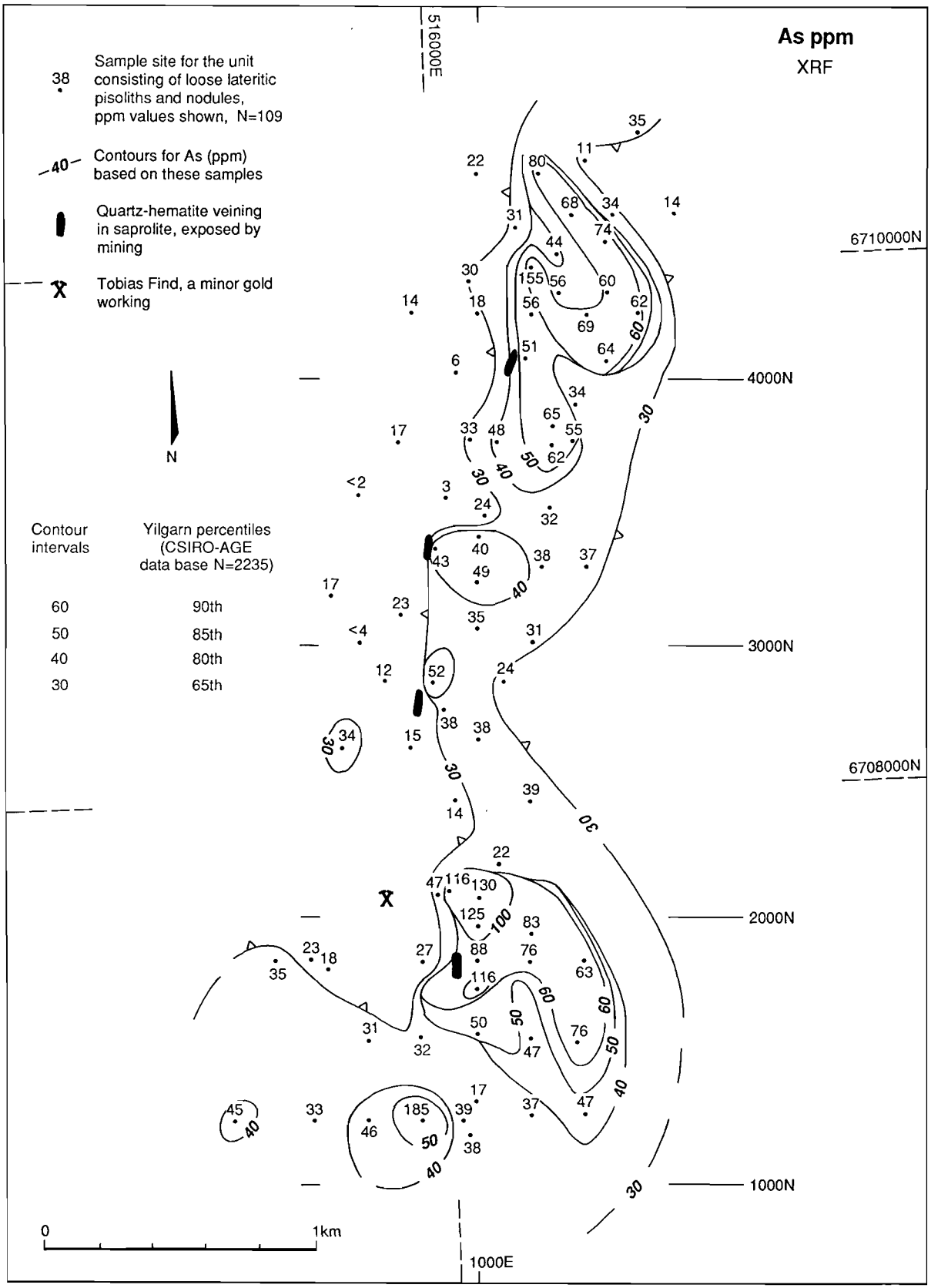

Fig. 28. Plan of the Mt. Gibson orientation area showing the distribution of As in the regolith unit consisting of loose lateritic pisoliths and nodules.

Bi

Bismuth has developed a dispersion pattern (Fig. 29) closely resembling that of As in strike extent, breadth, and in the extent of downslope dispersion, particularly to the S and to the E of the mineralized veins. It differs from As, in that skewed bull's-eye anomalies are developed around each of the mineralized veins and that there are other sporadic highs in this broad pattern with no obvious relationship to known bedrock mineralization.

The Bi anomaly is open at both ends. Some research will be directed at testing analytical methods for Bi which have the potential to lower its detection limits.

Sb

The Sb pattern (Fig. 30) lacks the continuity of Au, Ag, Pb, and As although the pattern shows a close relationship with three of the quartz-hematite vein occurrences. The most marked feature is that Sb is widespread in the northern part of this figure.

W

Tungsten is not uniformly distributed within the overall multi-element anomaly, being most widespread in the northern part, Fig. 31. The W pattern measures 1 km wide and more than 2 km long with values that are very unusual for the Yilgarn Block. Tungsten also shows a close local relationship to the quartz-hematite veins.

Other Elements of Interest

The pattern for Ge (not illustrated) in this regolith unit is characterized by isolated anomalous values between 3 and 8 ppm, the most significant suggesting a zone 800 m long coinciding with the Pb, Sb, W zone. Though weak, such levels are rare in the Yilgarn Block (the 98th percentile is 2 ppm). Because Ge is a well-known associate of some sulphide ore types, the results suggest that further analytical research could be rewarding.

Copper shows a localized pattern with anomalies reaching 100 to 300 ppm particularly in the S2 pit area, where traces of malachite were observed within saprolite exposed by mining operations.

Zinc values only reach 25 ppm and do not appear to be particularly useful in defining patterns related to mineralization.

Cr

The pattern for Cr is shown in Fig. 32 because of its possible use in interpreting bedrock lithologies, being associated with mafic and ultra-mafic lithologies as well as with some Archaean metasedimentary rocks.

Geochemical Indices

Figure 33 shows the geochemical pattern using a chalcophile geochemical index CHI-6*X (see formula in the diagram). This index brings together several chosen elements and has been useful in both gossan and laterite geochemistry in previous studies. The main parts of the geochemical anomaly at Mt. Gibson are defined using levels that are anomalous for the Yilgarn Block. It should be noted that Au is deliberately omitted from this version of the index so as to show the pattern for comparisons with situations where Au depletion can be expected.

The index NUMCHI-MGa (Fig. 34) simply sums the number of chosen elements that exceed the selected threshold levels for each (see figure), reporting values for each sample site as a score between 0 and the maximum possible score of 7, there being seven elements chosen for the index. This

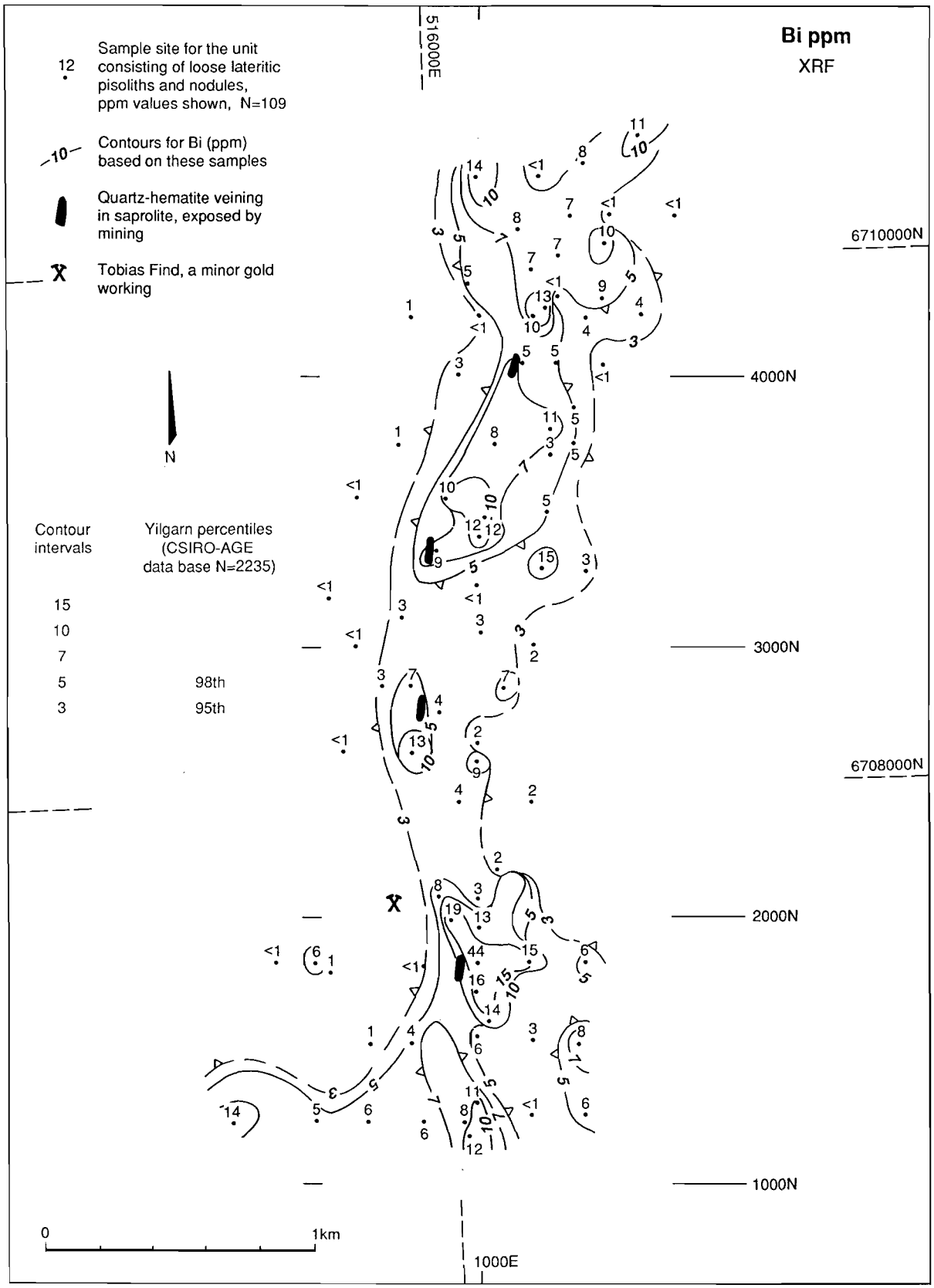

Fig. 29. Plan of the Mt. Gibson orientation area showing the distribution of Bi in the regolith unit consisting of loose lateritic pisoliths and nodules.

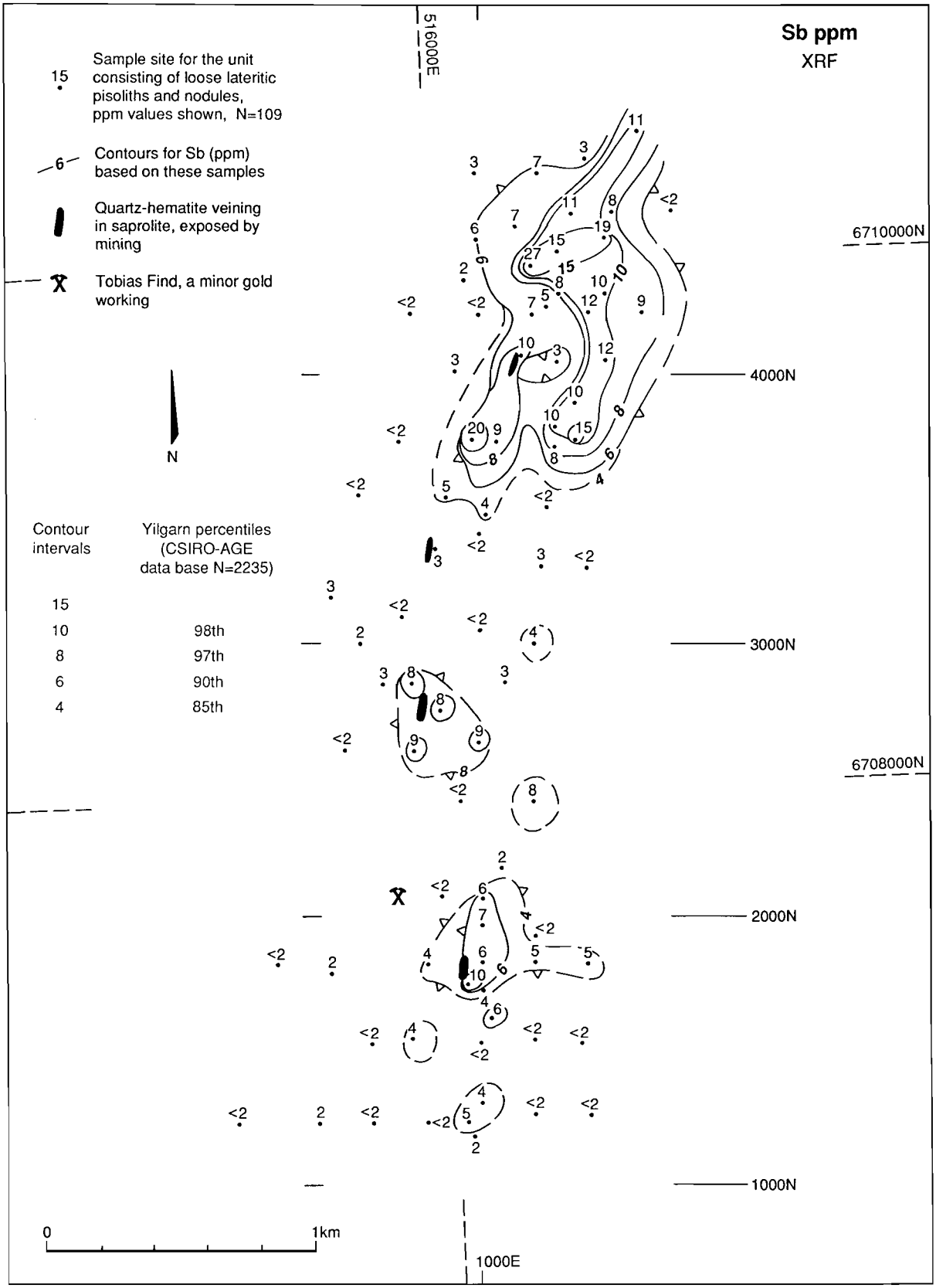

Fig. 30. Plan of the Mt. Gibson orientation area showing the distribution of Sb in the regolith unit consisting of loose lateritic pisoliths and nodules.

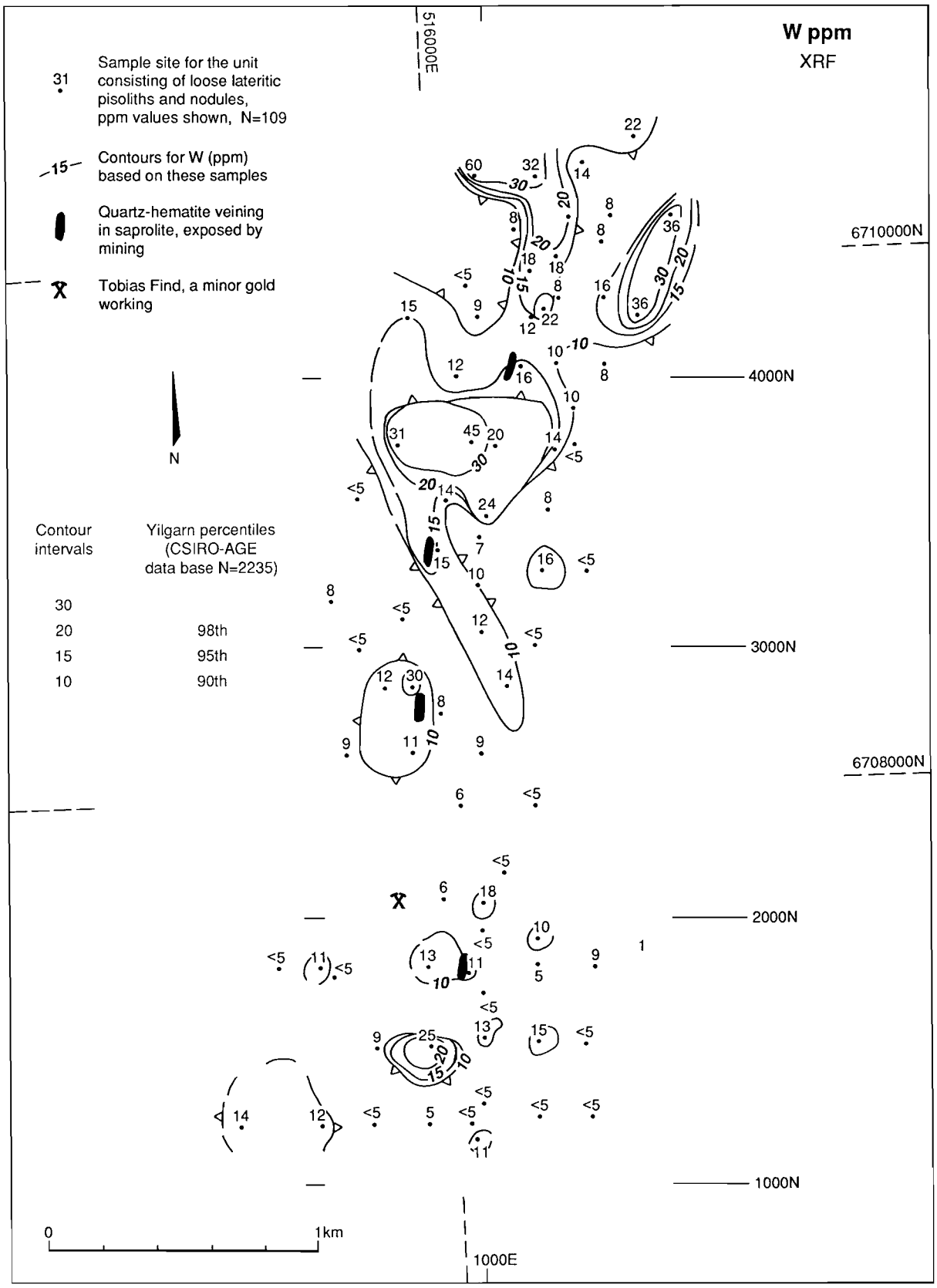

Fig. 31. Plan of the Mt. Gibson orientation area showing the distribution of W in the regolith unit consisting of loose lateritic pisoliths and nodules.

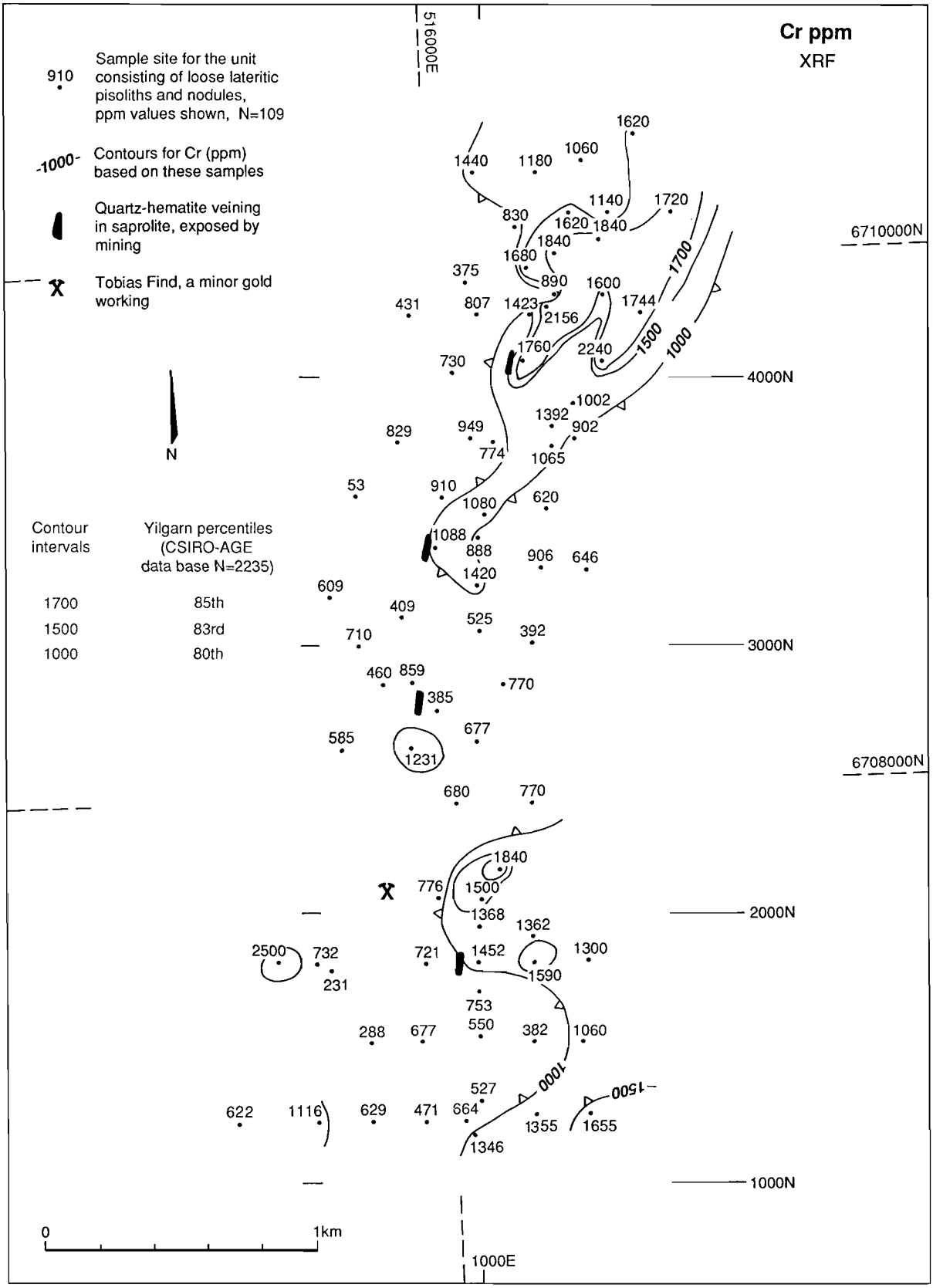

Fig. 32. Plan of the Mt. Gibson orientation area showing the distribution of Cr in the regolith unit consisting of loose lateritic pisoliths and nodules.

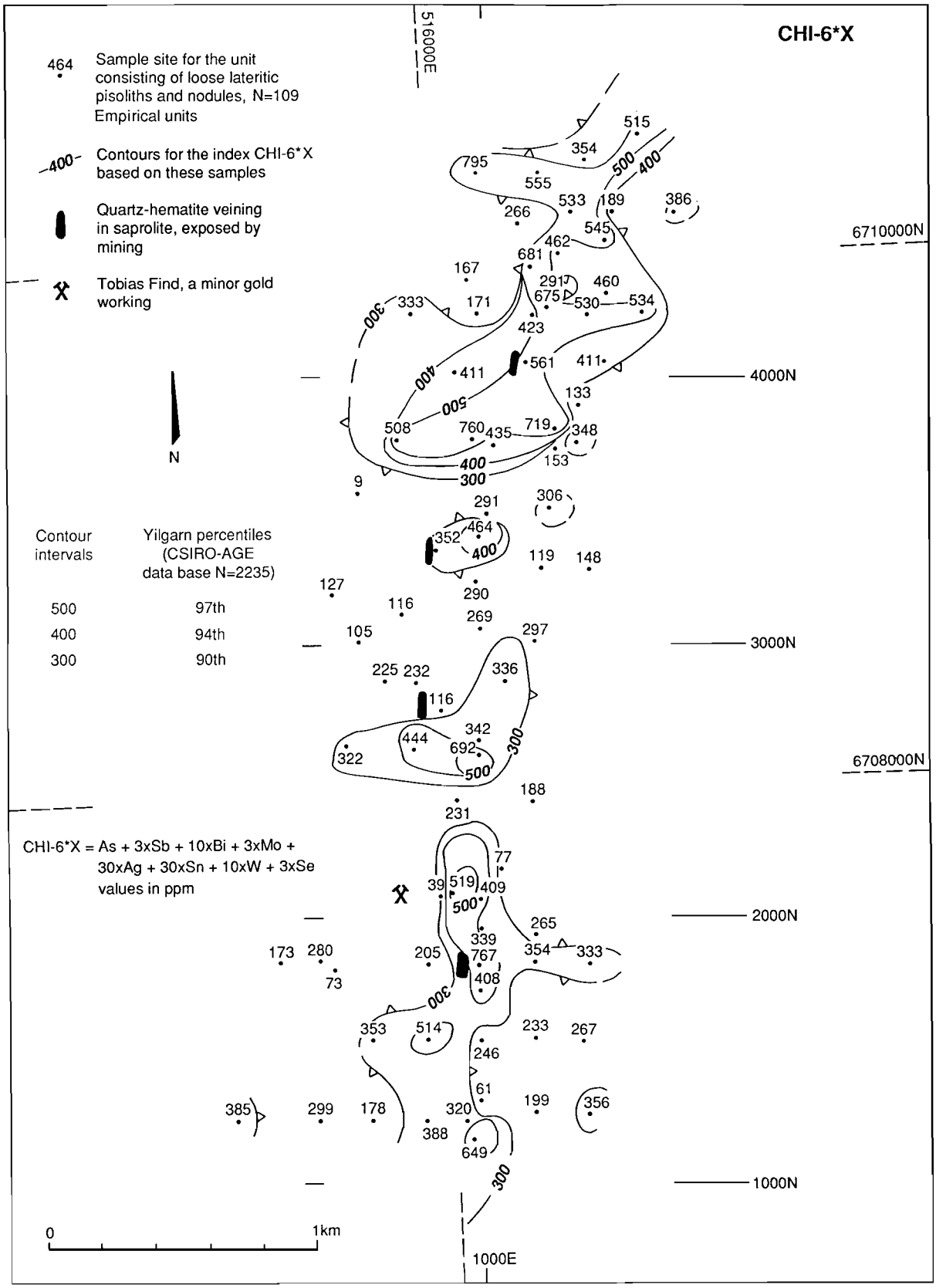

Fig. 33. Plan of the Mt. Gibson orientation area showing values for the chalcophile index CHI-6*X in the unit consisting of loose lateritic pisoliths and nodules.

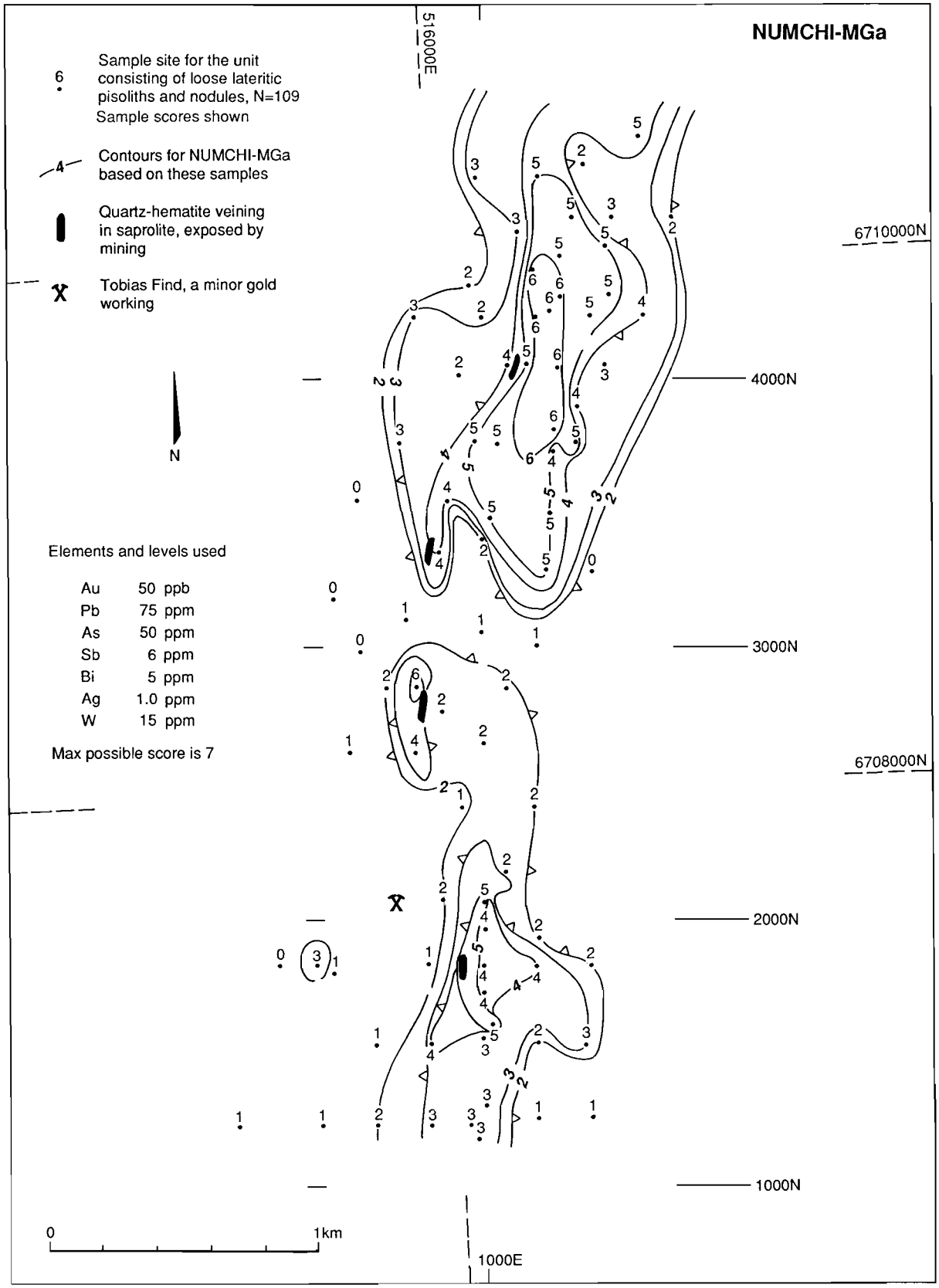

Fig. 34. Plan of the Mt. Gibson orientation area showing scores for a customized proximity index, using geochemical data of the unit consisting of loose lateritic pisoliths and nodules. Note that Au and Ag are used.

index is designed as a proximity indicator, based on the reasoning that as an ore system is approached the number of anomalous elements typically increases, the bedrock pattern of increase being shown by the secondary dispersion patterns within laterite.

Up to six elements co-exist at anomalous levels in lateritic pisoliths and nodules in the C1 and N2 pit areas and five in the S2 pit area.

The NUMCHI-MGb index (Fig. 35) was designed as a proximity index in situations where either Au or Ag may have been depleted in the regolith and are dropped from the index. It has a maximum possible value of 5.

Thus Fig. 35 presents the anomalous geochemical pattern that could be expected for a situation where groundwater conditions would have led to downward mobility of the Au and Ag, i.e., in areas where surface depletion and supergene enrichment of Au and Ag might be expected. It is significant that this pattern, based upon Pb, As, Sb, Bi, and W, still forms a useful-sized anomaly. The contoured NUMCHI-MGb values tightly define the mineralized vein systems in the saprolite bedrock.

3.7 DISCUSSION

The geochemical results presented in Figs 19 to 35 show a continuous multi-element halo within the loose pisolitic/nodular laterite unit that forms a drape across the landscape. The unit and its contained geochemical anomalies partly outcrops but much of it is also buried beneath some metres of younger sediments derived by dismantling of the laterite profile in the immediately adjacent upland areas.

Where the lateritic blanket is buried, cementation of the overlying colluvium/alluvium commonly results in the formation of hardpan. In such situations, an adequate form of drilling that can penetrate hardpan and allow recognition of the regolith untis is needed. When carefully carried out this can allow geochemical haloes in subsurface laterite to be recognized, delineated, and used to define bedrock target zones.

Results of the geochemical orientation research to date coupled with the idealized regolith/landform model (Fig. 24 and Section 2.10) allow the following generalizations to be made.

The size and consistency of the geochemical halo in laterite shows that most efficient exploration for Au and polymetallic sulphide deposits can be carried out where the lateritic duricrust is preserved. This refers to situation 1 (Fig. 24) with the essentially complete lateritic duricrust at or near surface, and situation 3, where it is buried. However, in situation 3, hardpan is commonly formed within the upper several metres of depositional units. Typically, this requires drilling rather than pitting by backhoe to provide samples of the buried duricrust.

In situation 2, different sample media (e.g., saprolite or soil) have to be employed because the lateritic duricrust is removed. Truncation of the profile, however, may be advantageous to exploration if saprolite and bedrock are exposed, allowing conventional mapping, or occur at shallow depth within reach by a backhoe. In such areas, saprolite is the parent material of recent residual soils and the chemical composition of soils would generally reflect saprolite.

In drilling designed to detect buried laterite geochemical haloes, it is important to distinguish between colluvial/alluvial units containing an abundance of lateritic pisoliths and nodules from *in situ* lateritic duricrust. It is also important to recognize whether the profile at depth is essentially complete or is stripped. Ferruginous pellets that have developed from saprolite in post-lateritic soils, typical of situation 2, must be distinguished from genuine lateritic pisoliths. The origins are different and they have different geochemical characteristics. Furthermore, as a result of erosional/depositional dynamics, the present location of ferruginous pellets can be out of sequence. For example, in some buried situations, they may occur on top of the full laterite profile, (as at the south part of Midway).

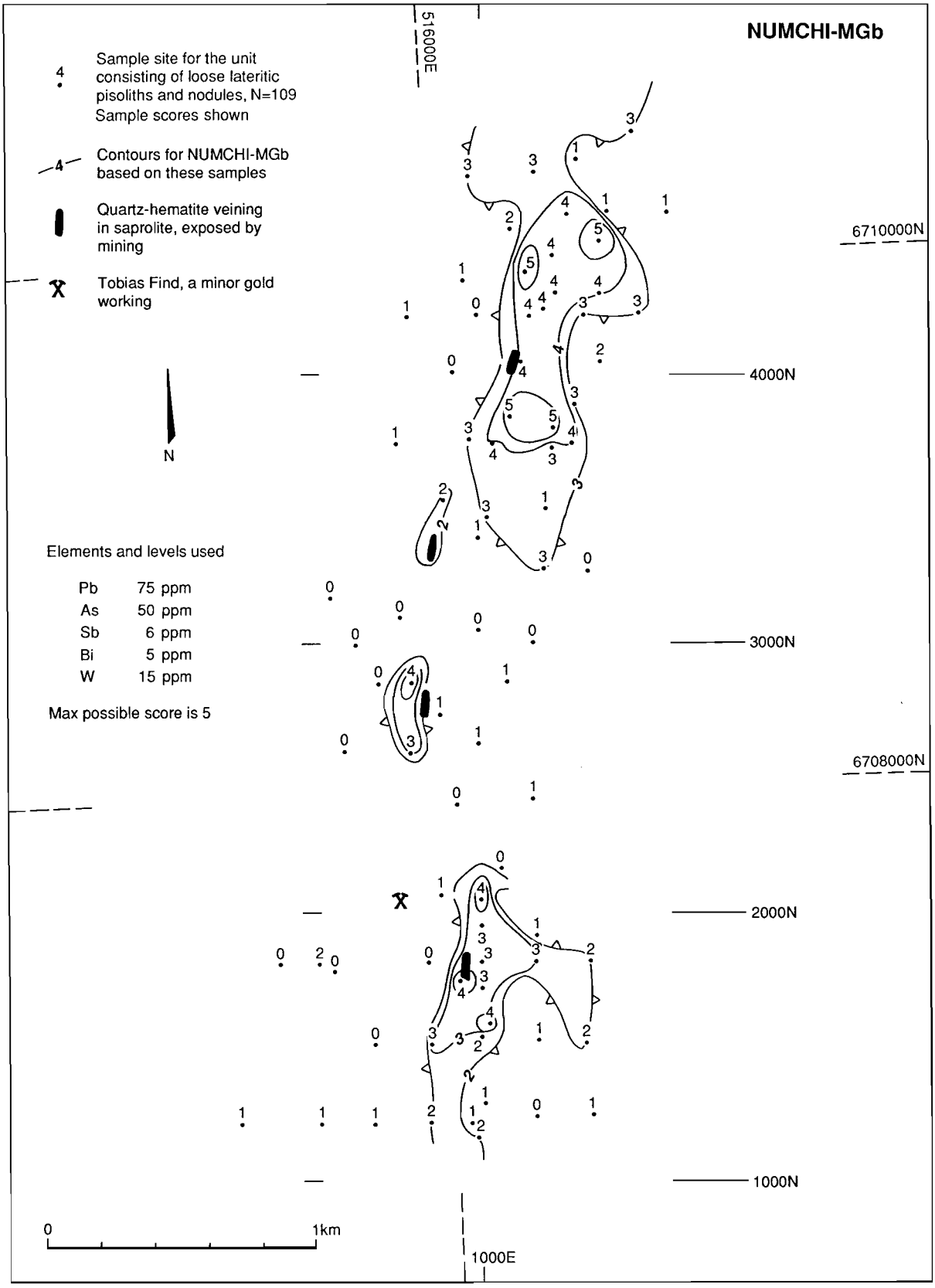

Fig. 35. Plan of the Mt. Gibson orientation area showing scores for a customized proximity index from which Au and Ag have been dropped.

The research highlights the critical importance of having a well-controlled and understood appreciation of the regolith/landform relationships when planning, executing, and interpreting an exploration geochemical survey in this style of deeply-weathered terrain.

The results show that, properly carried out, laterite geochemistry can provide large, internally-consistent geochemical haloes regardless of whether the lateritic unit is at surface or sub-surface.

The superimposition of anomalies of elements which may vary greatly in their geochemical mobility indicate that these elements are proximal to a genetically-related bedrock source, for example, the shear-hosted quartz-hematite veins within tuffaceous metasediments.

Generalizations on the dispersion processes are compounded by the existence of post-laterization authigenic carbonatization and development of thick buffering units of nodular calcrete and calcretized hardpan within the regolith profile. Groundwaters encountering these buffers will suffer a modification or even reversal of their transport characteristics in respect of some elements, e.g., Se.

Results from 37 duricrust samples analysed to date show similar element levels and associations to those in the overlying loose unit, Table 4. However, close comparisons, particularly on halo size and other aspects of geometry must await results from recent sampling which bring the total of duricrust samples to 90.

---oOo---

TABLE 4. Comparison of some element levels in loose pisolitic laterite and pisolitic nodular duricrust, Mt. Gibson orientation area. Values are in ppm.

	Samples of loose lateritic pisoliths, nodules N=109	Samples of lateritic duricrust N=37
Au	.005-12.75	.005-5.9
Ag	0.1-3.3	0.1-3
As	3-185	1-160
Sb	1-20	1-15
Bi	1-44	1-24
Sn	1-20	1-9
W	1-45	1-14
Se	1-14	1-5

4.0 OUTLOOK

- Regolith/landform relationships in the Mt. Gibson mining areas are now reasonably well understood. Reconnaissance at district-scale by mapping onto the 1:50,000 photomosaic will be completed in order to provide a broader perspective over the surrounding 30-km by 30-km area.

- Geochemical patterns based upon a broader range of samples of lateritic duricrust will be established and will enable comparisons with those presented in this report based largely on loose lateritic pisoliths and nodules. The previous 37 sample sites of duricrust were increased to a total of 90 in February providing a suitable network for comparisons. Sample preparation is advanced and analyses are scheduled for completion during April.

- Data sets on the loose pisolitic/nodular laterite unit are ready for statistical investigation. These will be coupled with investigation of duricrust samples mentioned above. This phase of research is scheduled for mid-year.

- Research into the siting and bonding of elements of interest in the lateritic materials, including the study of subdivided samples, has been underway since June, as a background activity.

- A component study commenced in February to provide control over the dominant groundwater regimes in the Mt. Gibson study area as well as to investigate the possibility of hydrogeochemical haloes. Some 50 water samples were taken by D. Gray and A. Giblin, the majority of which came from the main study area, with several sites providing reconnaissance coverage in the saline drainage sump for the district (including Lake Karpa). Results should be particularly pertinent to the formation and preservation/modification of multi-element geochemical haloes (Au, As, Sb, Bi, and Ag) in laterite and buried laterite profiles and to the correct application of interpretive methods.

- Most lateritic and other ferruginous materials at Mt. Gibson can now be placed comfortably in a genetic classification scheme. Some research still needs to be done on the origin of the goethite pods that occur within duricrusts in some locations.

- Integration of the various research components forming the orientation study at Mt. Gibson is well underway, having commenced last November, and is based upon the regolith/landform model presented in this report.

---o0o---

5.0 CONCLUSIONS

- Research in the Mt. Gibson orientation area shows that landscape evolution and geochemical dispersion can be understood in terms of the dynamics of formation, preservation, and dismantling of the undulating lateritic weathering mantle.

- Dismantling of the laterite mantle in local uplands has resulted in burial of the laterite profile in adjacent footslopes and lowlands.

- In the process, local erosional/depositional couples have resulted in colluvial/alluvial sequences, some of which show an inversion of the sequence of the former weathering profile, now dismantled. Gravelly detritus at the base of such colluvium is dominated by lateritic pisoliths and nodules, grading upwards to silty sandy detritus at the top, compatible with derivation by erosion of saprolite.

- The network of 109 orientation sample sites collected from the loose pisolitic nodular laterite unit which overlies duricrust delineates a multi-element Au Ag Pb As Bi Sb W association for the lateritic S, C, and N Au deposits. The geochemical anomaly is 1 km to 1.5 km wide and in excess of 4 km in length with a high degree of internal consistency, particularly for Au.

- A zonal pattern to the laterite anomaly was identified with Pb, Sb, and W characterizing the northern section located within the overall longer Au Ag As Bi anomaly.

- The coincidence of several typomorphic elements in laterite to form multi-element centres suggests that the anomaly is a secondary dispersion halo which has a close genetic link to bedrock sources. This is confirmed by some occurrences of Au-bearing quartz-hematite veining in saprolitic bedrock exposed by mining. However, detail relationships of laterite geochemistry to source areas must await more information on the distribution of mineralization in bedrock, particularly in local upslope areas.

- The size and consistency of the Au halo in laterite argues for either substantial Au resources in bedrock or very efficient precipitation and preservation of the Au geochemical halo.

- Replacement calcrete and carbonate cementation within hardpan are generally explained by an upslope source, transportation, and footslope deposition, though details are the topic of current research.

- The likely importance of pH buffering by carbonate on the geochemical cycle of Au in the lateritic units is recognized and is the topic of current research.

- An idealized regolith/landform facies model for the Mt. Gibson setting has been erected, acting as a framework and guide in prediction of regolith relationships in comparable areas elsewhere, as well as acting as a basis for planning, interpreting, and integrating follow-up research.

- Recognition and understanding of the dynamics of landform/regolith relationship is important in interpreting the origins of laterite.

---o0o---

6.0 ACKNOWLEDGEMENTS

We wish to thank the management and staff of the Mt. Gibson Gold Project, and of the joint venture partners Forsayth (Gibson) Ltd and Reynolds Australia Mines Pty Ltd for their co-operation and hospitality without which this study would not be possible. We also acknowledge the very substantial funding provided through AMIRA by the consortium of 24 sponsoring companies of the CSIRO/AMIRA Laterite Geochemistry Project.

Mr John Perdrix provided research support both in the field and laboratory and maintained the geochemical database, and was responsible for managing production of the report. Typing to a tight deadline was admirably carried out by Ms Cheryl Harris and Jenny Porter. Diagrams were drafted by Mr Angelo Vartesi under the supervision of Mr Colin Steel. Sample preparation, to demanding non-metallic standards, was carried out by Mr John Wass and Ms Angela Janes under supervision by Mr John Crabb.

---o0o---

7.0 REFERENCES

Ashley, P.M., Dudley, R.J., Lesh, R.H., Marr, J.M. and Ryall, A.W., 1988. The Scuddles Prospect Cu-Zn on Archaean Volcanogenic massive sulphide deposit, Golden Grove District, Western Australia, *Econ. Geol.* **83**, 918-951.

Barlow, B.A., 1981. The Australian Flora: its origin and evolution. In: *Flora of Australia*, Bureau of Flora and Fauna, Canberra, 25-75; Australian Government Publishing Service, Canberra, 200pp.

Baxter, J.L., 1978. Molybdenum, tungsten, vanadium and chromium in Western Australia. *Geol. Surv. West. Aust., Min. Resources Bull.* 11, 140pp.

Baxter, J.L. and Lipple, S.L., 1985. Perenjori, Western Australia. *Geol. Surv. West. Aust. 1:250 000 Geol. Series Explan. Notes*, 32pp.

Baxter, J.L., Lipple, S.L. and Marston, R.J., 1983. Kirkalocka, Western Australia. *Geol. Surv. West. Aust. 1:250 000 Geol. Series Explan. Notes*, 24pp.

Beard, J.S., 1976. *Vegetation Survey of Western Australia*. Vegmap Publications, 6 Fraser Road, Applecross, W.A.

Bettenay, E. and Churchward, H.M., 1974. Morphology and stratigraphic relationships of the Wiluna hardpan in arid Western Australia. *J. geol. Soc. Aust.*, **21**, 73-80.

Bettenay, E. and Mulcahy, M.J., 1972. Soil and landscape studies of Western Australia. *J. geol. Soc. Aust.*, **18**, 359-369.

Birrell, R.D. and Butler, I.K., 1987. Progress report on the laterite geochemical survey, Mt. Gibson Mine area, July 1987. Unpublished report of Geochemex Australia to Forsayth NL and Reynolds Australia Mines Pty Ltd (unpaginated).

Bisdom, E.B.A., Stoops, G., Deluigne, J., Curmi, P. and Altemuller, H.J., 1982. Micromorphology of weathering biotite and its secondary products. *Pedologie Gand* **32**, 225-252.

Browning, P., Groves, D.I., Blockley, J.G. and Rosman, K.J.R., 1987. Lead isotope constraints on the age and source of gold mineralization in the Archaean Yilgarn Block, Western Australia. *Econ. Geology*, **82**, 971-986.

Butt, C.R.M., 1985. Granite weathering and silicate formation on the Yilgarn Block, Western Australia, *Aust. J. Earth Sci.*, **32**, 415-432.

Campbell, A.S. and Schwertmann, V., 1984. Iron oxide mineralogy of placic horizons. *J. Soil Sci.*, **35**, 569-582.

Davy, R., Clarke, R., Sale, M. and Parker, M., 1988. The nature and origin of the gold-bearing laterite at Mount Gibson, Western Australia. *Proc. 2nd Int. Conference on Prospecting in Arid Terrain*, Perth, W. Aust., 45-47 (Abstract).

Frater, K.M., 1983a. Geology of the Golden Grove prospect, Western Australia: A volcanogenic massive sulphide-magnetite deposit: *Econ. Geol.*, **78**, 875-919.

Frater, K.M., 1983b. Effects of metasomatism and development of quartz "eyes" in intrusive and extrusive rocks at Golden Grove Cu-Zn deposit, Western Australia. *Trans. Instn Min. Metall.* **92**, Sect. B, 121-131.

Frater, K.M., 1985a. Mineralization at the Golden Grove Cu-Zn deposit, Western Australia I: Premetamorphic textures of the opaque minerals., *Can. J. Earth Sci.*, **22**, 1-14.

Frater, K.M., 1985b. Mineralization at the Golden Grove Cu-Zn deposit, Western Australia II: Deformation textures of the opaque minerals. *Can. J. Earth Sci.*, **22**, 15-26.

Gold Gazette, 1988. May Mellor bullish on Forsayth NL. 10 Oct., p.71.

Hallberg, J.A., 1976. A petrochemical study of a portion of the western Yilgarn Block. *CSIRO Div. of Mineralogy Rept. FP 13*, 38pp.

Jutson, J.T., 1950. The physiography (geomorphology) of Western Australia. *Geol. Surv. West. Aust. Bull.* **95**, (3rd ed.), 366pp.

Lipple, S.L., Baxter, L.J. and Marston, R.J., 1983. Ninghan, Western Australia, *Geol. Surv. West. Aust. 1:250 000 Geol. Series Explan. Notes*, 23pp.

Mabbutt, J., 1980. Weathering history and landform development. In: Butt, C.R.M. and Smith, R.E. (eds.), Conceptual Models in Exploration Geochemistry - Australia, *J. Geochem. Explor.*, **12**, 96-116.

Marston, R.J., 1979. Copper mineralization in Western Australia, *Geol. Surv. West. Aust. Min. Resources Bull.*, **13**, 208pp.

McFarlane, M.J., 1976. *Laterite and Landscape*, Acad. Press, London, 151pp.

Mining Journal, 1988. Vol.311, No.7982, August 19, 137, 139.

Muhling, P.C. and Low, G.H., 1973. Explanatory notes on the Yalgoo 1:250,000 geological sheet, Western Australia. *Geol. Surv. West. Aust. Record* 1973/6.

Muhling, P.C. and Low, G.H., 1977. Yalgoo, Western Australia, *Geol. Surv. W. Aust. 1:250,000 Geol. Series Explan. Notes*, 36pp.

Ollier, C.D., Chan, R.A., Craig, M.A. and Gibson, D.L., 1988. Aspects of landscape history and regolith in the Kalgoorlie region, Western Australia. *BMR J. Aust. Geol. and Geophys.*, **10**, 309-321.

Parker, M., 1988. Unpublished company report on regolith stratigraphy at S2 pit.

Phillips, G.N., 1985. Interpretation of Big Bell/Hemlo-type gold deposits: precursors, metamorphism, melting and genetic constraints. *Trans. geol. Soc. S. Afr.*, **88**, 159-173.

Pullan, R.A., 1967. A morphological classification of lateritic ironstones and ferruginised rocks in Northern Nigeria. *Niger. J. Sci.*, **1**, 161-174.

Schwertmann, V. and Kampf, N., 1985. Properties of geothite and hematite in kaolinitic soils of southern and central Brazil. *Soil Sci.*, **139**, 344-350.

Smith, R.E., 1987. Patterns in lateritic geochemistry Mt. Gibson, Western Australia. Progress report of Geochemex Australia to Forsayth NL, December, 37pp.

Smith, R.E. and Anand, R.R., 1988. The use of geochemistry in gold exploration with particular reference to work on the regolith - discussion paper, 47-50. *West. Australian School of Mines Symposium R & D for the Minerals Industry*, Kalgoorlie, 323pp.

Smith, R.E. and Perdrix, J.L., 1983. Pisolitic laterite geochemistry in the Golden Grove massive sulphide district, Western Australia. *J. Geochem. Explor.* **18**, 131-164.

Walker, R.J. (ed.), 1984. *Facies Models*. Geoscience Canada. Ainsworth Press Limited, Ontario, 211pp.

Watkins, K.P. and Hickman, A.H., 1988a. Geology of the Murchison Province: Locality Guide. *Geol. Surv. West. Aust., Centennial Field Excursion Guidebook*, 22pp.

Watkins, K.P. and Hickman, A.H., 1988b. Murchison Province: Stratigraphy, structure and mineralization. *Geol. Surv. West. Aust. Bull.*, **137**, Plate 2.

Watkins, K.P., Hickman, A.H., Davy, R. and Ahmat, A.L., 1989. Geological evolution and mineralization of the Murchison Province, Western Australia. *Geol. Surv. West. Aust. Bull.*, **137**, (in press).

---o0o---

APPENDICES

I Morphological descriptions of some typical vertical profiles

II Morphological description and chemical composition of three typical vertical profiles

III Analytical data

APPENDIX I

MORPHOLOGICAL DESCRIPTION OF SOME TYPICAL VERTICAL PROFILES

LOCATION: 1275 N, 1000 E (S1 Pit)

Depth in metres	Regolith Unit	Description	Remarks
0-0.4	Red clay soil	Red (10R 4/6, m)[1], friable, clay; black (2.5YR 3/0, d), ferruginous pellets (1-10 mm) with shiny surfaces (~25 volume %); few lithorelics; calcareous; moderate coarse roots; sharp boundary.	Transported
0.4-0.9	Hardpan in colluvium/alluvium	Red (2.5YR 4/6, m), firm, laminar, fine grained; few ferrugious pellets (~5 volume %); few lithorelics; powdery carbonate along partings; manganiferous staining on fracture surfaces; moderate very coarse roots; sharp boundary.	Transported
0.9+	Loose lateritic nodules and pisoliths	Dark reddish-brown (2.5YR 4/4, d) 5-30-mm nodules (~60 volume %); friable, clay matrix (~40 volume %); abundant manganese staining on outer surface of nodules and matrix; powdery carbonates in matrix and on surface of nodules (base of unit not exposed).	In situ

[1] Munsell colours in parentheses are given as moist, m, or dry, d.

LOCATION: 1470 N, 725 E (S1 Pit)

Depth in metres	Regolith Unit	Description	Remarks
0-0.4	Red clay soil	Red (2.5YR 4/8, m), friable, clay; black (2.5YR 3/0, d) ferruginous pellets (2-3 mm) and nodules (~25 volume %); calcareous; few fine roots; sharp boundary.	Transported
0.4-0.8	Silty hardpan in colluvium/alluvium	Red (2.5YR 4/6, m), firm, laminar, fine grained; black (2.5YR 3/0, d) nodules (~10 volume %) with thin yellow coatings; powdery carbonates along partings; manganiferous staining/ accumulations on fracture surfaces; gradational boundary.	Transported
0.8+	Hardpanized lateritic duricrust	Black (2.5YR 3/0, d), 4-10 mm nodules and pisoliths with thin yellow coatings; red (2.5YR 4/6, d), sandy clay, matrix (~70 volume %); calcareous.	In situ

LOCATION: 1525 N, 740 E (S1 Pit)

Depth in metres	Regolith Unit	Description	Remarks
0-0.3	Red clay soil	Reddish-brown (2.5YR 4/4, m), friable, clay; black (2.5YR 3/0, d), 2-10-mm ferruginous pellets and nodules (~30, volume %); calcareous; moderate coarse roots; sharp boundary.	Transported
0.3-0.45	Loose lateritic pisoliths in matrix	Black (2.5YR 3/0, d) and red (2.5YR 4/8, d) pisoliths; red, friable, clay, matrix; calcareous; sharp boundary.	Transported
0.45-1.2	Calcrete	Pink (5YR 3/4, m), firm, matrix (~50 volume %); carbonate coatings on nodules and pisoliths; sharp boundary.	Transported
1.2-1.50	Loose lateritic nodules and pisoliths in matrix	Red (10R 4/6, d) nodules and pisoliths (~70 volume %); red, firm, clay, matrix (~30 volume %); calcareous; sharp boundary.	Transported
1.5-1.8	Loose lateritic pisoliths	Black (2.5YR 3/0, d) and red (10R 4/6, d) 10-50-mm, pisoliths with 2-15 mm, yellow (10YR 7/6, d) and light red (2.5YR 4/6, d) coatings; silicified.	In situ
1.8+	Lateritic duricrust	Vermiform voids, 10-40 mm in length; light red (2.54R 4/6, d) infill; red (10R 4/6, d) sandy clay, matrix; quartz grains in voids.	In situ

LOCATION: 1530 N, 1100 E (S2 Pit)

Depth in metres	Regolith Unit	Description	Remarks
0-0.6	Red clay soils	Red (2.5YR 4/8, m), friable, clay; black (2.5YR 3/0, d) ferruginous pellets; calcareous; few fine roots; sharp boundary.	Transported
0.6-1.7	Red plastic clays	Red (10R 4/6, m), plastic, clays; calcareous; occasionally patches of carbonate in matrix; sharp boundary.	In situ
1.7+	Saprolite	Pale coloured, sandy clay.	In situ

LOCATION: 1900 N, 1100 E (S2 Pit)

Depth in metres	Regolith Unit	Description	Remarks
0-0.4	Red clay soil	Red (2.5YR 4/8, m), friable, clay; black (2.5YR 3/0, d) ferruginous pellets and nodules (~35 volume %); calcareous; few fine roots; sharp boundary.	Transported
0.4-0.8	Nodular calcrete	Light red (2.5YR 6/8, m), firm, clayey; black (2.5YR 3/0, d), 10-20 mm, ferruginous pellets and nodules; carbonate coatings on pellets and nodules; manganese staining on surface; gradational boundary.	Transported
0.8-1.2	Nodular calcrete	Red (2.5YR 5/6, m), firm, clayey; black (2.5YR 3/0, d) and red (2.5YR 5/6, d), 10-20 mm, nodules; carbonate coatings on nodules; sharp boundary.	Transported
1.2+	Mottled zone	Red (10R 4/6 m), sandy clay, matrix; yellow (10YR 7/8, m) mottles; few, black pisoliths; few lithorelics; calcareous.	In situ

LOCATION: 2050 S, 845 E (S2 Pit)

Depth in metres	Regolith Unit	Description	Remarks
0-0.3	Red clay soil	Red (2.5YR 4/8, m), friable, clay; black, (2.5YR 3/0, d) ferruginous pellets and nodules (~40 volume %) with reddish-brown (7.5YR 7/6, d) coatings; few litho-relics; acid; fine roots; sharp boundary.	Transported
0.3+	Hardpan in colluvium/alluvium	Red (2.5YR 5/8, m), firm, laminar, fine grained; black (2.5YR 3/0, d) nodules (~25 volume %); few lithorelics; calcareous manganiferous straining on fracture surfaces; rounded black vesicular goethite pods.	Transported

LOCATION: 3455 N, 1025 E (C3 Pit)

Depth in metres	Regolith Unit	Description	Remarks
0-0.4	Orange sandy clay soil	Reddish yellow (5YR 6/8, m), friable, sandy, clay loam; yellow (10YR 7/8, d), 2-10 mm, nodules and pisoliths (~35 volume %) with yellowish-brown (10YR 6/4, d) concretionary coatings; acid; fine roots; gradational boundary.	In situ
0.4-1.2	Loose lateritic nodules and pisoliths	Red (7.5R 4/6, d) and dark reddish brown (2.5YR 3/4, d), 2-15 mm, nodules and pisoliths (~80 volume %) with thin yellow and orange concretionary coatings; yellow (10YR 7/8, d), sandy clay, matrix (~20 volume %); acid; gradational boundary.	In situ
1.2+	Poorly indurated duricrust	Black (2.5YR 3/0, d) and dark red (2.5YR 3/6, d), 2-10 mm, nodules (~60 volume %) with thin yellow concretionary coatings; yellow (10YR 7/8, d) and red (2.5YR 4/6, d), sandy clay, matrix (~40 volume %); acid.	In situ

LOCATION: 3850 N, 1120 E (N2 Pit)

Depth in metres	Regolith Unit	Description	Remarks
0-0.4	Orange sandy clay loam soil	Reddish yellow (5YR 6/8, m), friable, sandy clay loam; black (2.5YR 3/0, d), 2-15 mm, nodules and pisoliths (~35 volume %) with yellowish brown (10YR 5/8, d) concretionary coatings; acid; few fine roots; gradational boundary	In situ
0.4-1.4	Loose lateritic nodules	Red (2.5R 4/6, d), 5-25 mm, nodules with thin yellowish brown (10YR 5/8, d) coatings; acid; sharp boundary.	In situ
1.4+	Silicified lateritic duricrust	Black (2.5YR 3/0, d) and red (2.5YR 4/6, d), 1-8 mm, pisoliths and nodules (~70 volume %); yellowish brown (10YR 5/8, d), sandy clay, matrix (~30 volume %); acid; silica in cracks and voids.	In situ

LOCATION: 3890 N, 1355 E (N2 Pit)

Depth in metres	Regolith Unit	Description	Remarks
0-0.3	Red clay soil	Red (2.5YR 4/8, m), friable, clay; black (2.5YR 3/0, d), 2-6 mm, ferruginous pellets and nodules (~25 volume %); acid; few fine roots; sharp boundary.	Transported
0.3-0.7	Loose lateritic pisoliths, nodules in matrix	Dark reddish brown (2.5YR 3/4, d) and yellow (10YR 7/8, d), 5-15 mm, nodules and pisoliths (~60 volume %) with yellow (10YR 7/8, d) concretionary coatings; red (2.5YR 4/6, d), friable, sandy clay, matrix (~40 volume %); acid; gradational boundary.	Transported
0.7-1.0	Silty hardpan in colluvium/alluvium	Red (10R 4/6, m), firm, laminar, fine grained; lithorelics (~20 volume %); powdery carbonates along partings; manganiferous staining on fracture surfaces; gradational boundary.	Transported
1.0-1.5	Nodular hardpan in colluvium/alluvium	Red (2.5YR 4/6, m), firm, laminar, fine grained; reddish brown (2.5YR 4/4, d) and black (2.5YR 3/0, d), 5-10 mm nodules and pisoliths (~25 volume %) with thin yellow (10YR 7/6, d) concretionary coatings; few lithorelics; powdery carbonates along partings; manganiferous staining on fracture surfaces; sharp boundary.	Transported
1.5+	Hardpanized lateritic duricrust	Red (2.5YR 4/6, d) and black (2.5YR 3/0, d) , 2-10 mm nodules (~60 volume %) with thin yellow concretionary coatings; yellow (10YR 7/6, d), matrix (~40 volume %); hardpan laminations.	In situ

LOCATION: 4280 N, 1260 E (N2 Pit)

Depth in metres	Regolith Unit	Description	Remarks
0-0.5	Red clay soil	Red (10R 4/6, m), friable, clay; black (2.5YR 3/0, d), 2-7 mm, ferruginous pellets and nodules (~25 volume %); calcareous; moderate fine roots; sharp boundary.	Transported
0.5-1.5	Hardpan in colluvium/alluvium	Red (2.5YR 4/8, m), firm, laminar, fine grained; red (2.5YR 4/4, d), 5-10 mm, nodules and pisoliths (~30 volume %) with yellow (10YR 7/8, d) concretionary coatings; few lithorelics; calcareous; manganiferous staining on fracture surface; sharp boundary.	Transported
1.5+	Lateritic duricrust	Red (10R 4/6, d), 2-5 mm, pisoliths and nodules (~40 volume %); yellowish brown (10YR 5/8, d) and dark red (7.5R 3/4, d) sandy clay, matrix (~60 volume %); few lithorelics, calcareous.	In situ

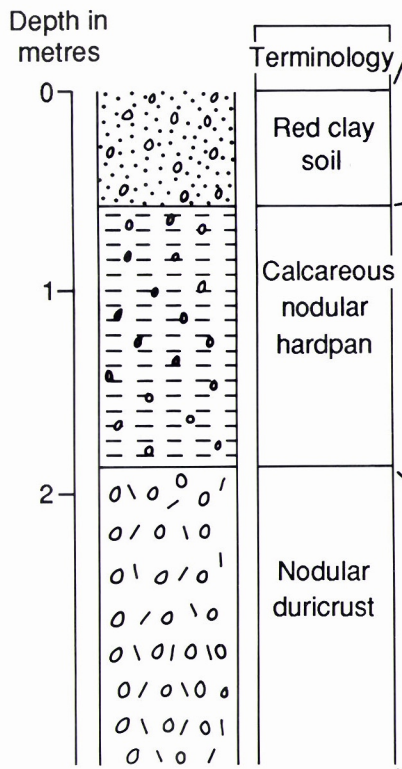

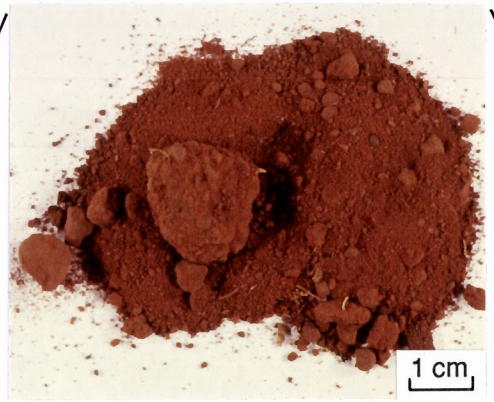

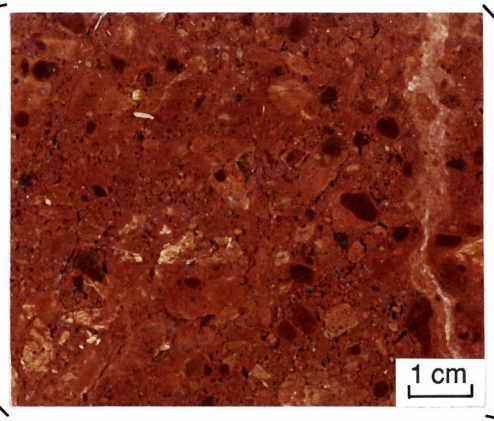

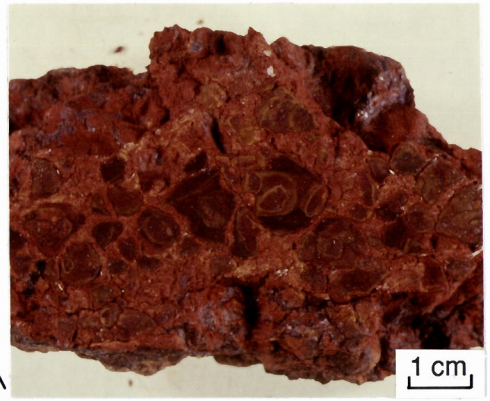

CHEMICAL COMPOSITION (wt %)

Sample No.	SiO_2	Al_2O_3	Fe_2O_3	MgO	CaO	Na_2O	K_2O	TiO_2	LOI	TOTAL
07-0536	40.21	18.30	31.03	0.136	0.192	0.059	0.268	1.851	9.8	101.84
07-0537	42.57	16.09	9.18	0.877	12.507	0.170	0.358	0.497	21.5	103.74
07-0539	38.93	18.78	28.26	0.708	0.862	0.253	0.304	1.491	13.2	102.78

Vertical profile at 3825N, 1050E, N2 pit

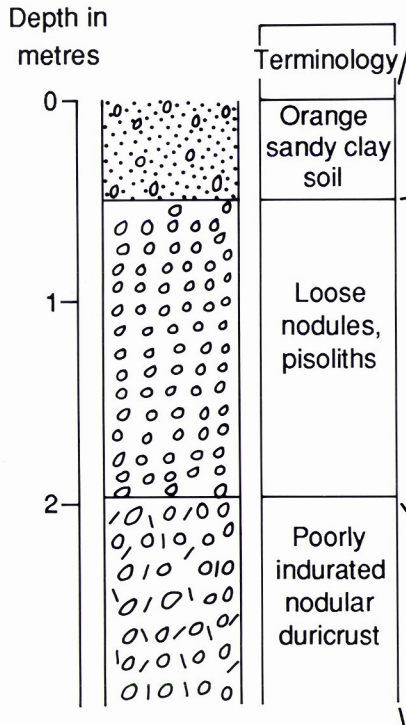

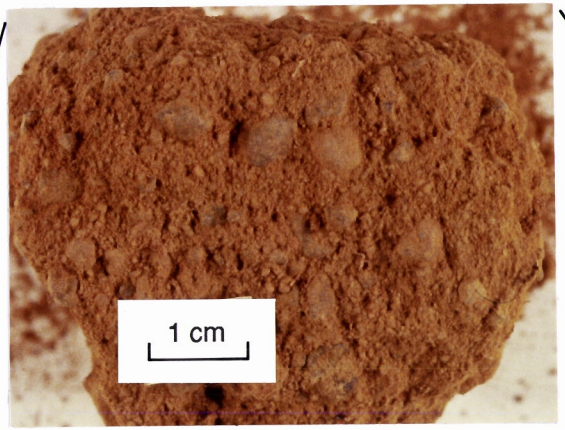

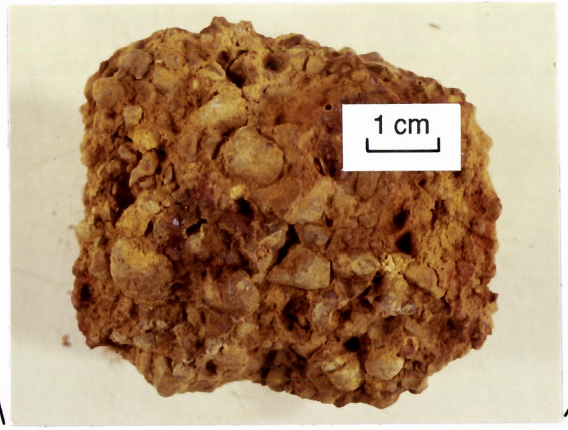

CHEMICAL COMPOSITION (wt %)

Sample No.	SiO_2	Al_2O_3	Fe_2O_3	MgO	CaO	Na_2O	K_2O	TiO_2	LOI	TOTAL
07-0296	59.25	11.90	26.74	0.076	0.077	0.077	0.217	1.059	5.10	104.53
07-0295	21.39	14.22	57.77	0.055	0.029	0.022	0.093	1.623	4.92	100.15
07-0295	20.53	20.02	49.62	0.058	0.029	0.034	<0.050	1.239	8.52	100.08

Vertical profile at 3475N, 1025E, C3 pit

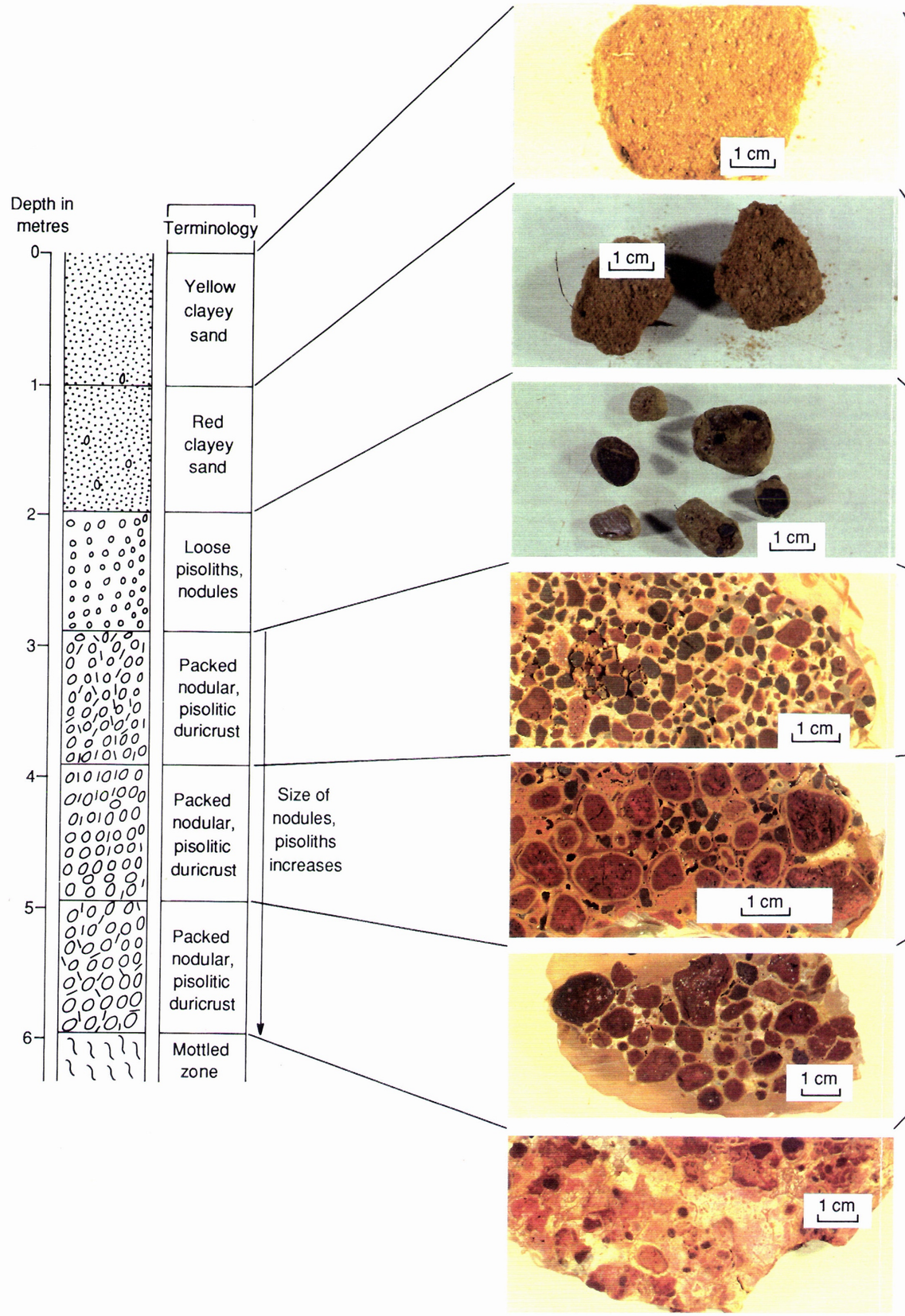

CHEMICAL COMPOSITION (wt %)

Sample No.	SiO_2	Al_2O_3	Fe_2O_3	MgO	CaO	Na_2O	K_2O	TiO_2	LOI	TOTAL
07-0326	85.35	7.29	3.19	0.040	0.038	0.034	0.164	0.394	3.35	99.85
07-0327	81.92	9.05	3.96	0.051	0.042	0.036	0.230	0.497	3.66	99.45
07-0589	32.08	18.59	40.04	0.096	0.062	0.073	<0.060	1.304	9.1	101.35
07-0328	21.60	15.02	56.48	0.096	0.074	0.102	0.080	1.218	5.46	100.15
07-0333	36.36	22.29	30.74	0.126	0.101	0.158	0.102	1.189	9.84	100.14
07-0329	31.23	22.67	34.46	0.098	0.084	0.163	0.075	1.513	9.05	100.13
07-0334	33.80	30.04	22.02	0.126	0.027	0.324	0.084	2.002	11.60	100.03

Vertical profile at 2850N, 825E, CI pit

APPENDIX III

CSIRO/AMIRA Laterite Geochemistry Project P240

Mt. Gibson Orientation Study, Analytical Data

Regolith unit consisting of loose pisoliths and nodules, analyses to 31 March 1989.

Samples were analysed in four batches as the project developed. Analytical methods were chosen to be either identical or compatible, according to the analytical codes listed below.

Batch 4 consists of 26 samples from the GEOCHEMEX survey which lay within the orientation area. The samples have a more restricted element suite because they were exploration rather than research samples. Analyses on GEOCHEMEX samples have been kindly made available for inclusion in the CSIRO/AMIRA orientation study by the management of the Mt. Gibson Gold Project.

Sample numbers	Batch	Number of Samples
07-0262 to 07-0341	1	11
07-0502 to 07-0620	2	27
02-2883 to 02-2943	3	56
MGN0002 to MGN0039	4	26
	TOTAL	120

LEGEND, ANALYTICAL METHODS

Laboratory	Code
CSIRO	1
AMDEL	2
ANALABS	3
Not analysed	0

Method	Code
X-ray fluorescene	X
Atomic absorption	A
Inductively coupled plasma	I
Not analysed	O

LEGEND, SAMPLE TYPE

LP	Loose lateritic pisoliths
LN	Loose lateritic nodules
PKD	Packed pisolitic or nodular duricrust
PNM	Pisoliths or nodules in matrix

Mt. Gibson Loose Lateritic Pisoliths & Nodules

ANALYSES

Sample Type (Laboratory)) (Method)) (det. limit))	AMG Coordinates Easting	Northing	Sheet	Weight percent SiO2 3320 III0 (0.1)	Al2O3 3320 III0 (0.02)	Fe2O3 3320 III0 (0.01)	MgO 3320 III0 (.01)	CaO 3320 III0 (.01)	Na2O 3320 III0 (.01)	K2O 3320 III0 (0.06/ 0.01)	TiO2 3320 III0 (.003)
Batch 1											
07-0262 LN	516206	6707623	SH-50-07	**30.16**	27.20	29.17	.048	.027	.089	<.060	1.051
07-0266 LP	516006	6707628	SH-50-07	29.95	18.02	43.19	.068	.042	.063	.090	1.393
07-0268 LP	516006	6707625	SH-50-07	**35.08**	21.91	33.03	.068	.024	.059	<.060	1.164
07-0290 LN	515973	6708914	SH-50-07	26.52	19.08	42.18	.046	.031	.043	<.060	.652
07-0295 LN	516216	6709048	SH-50-07	21.39	14.22	**57.77**	.055	.029	.022	.093	**1.623**
07-0300 LP	516068	6709117	SH-50-07	24.38	19.65	46.62	.192	.158	.084	.188	**2.402**
07-0328 PKD	515950	6708404	SH-50-07	21.60	15.02	**56.48**	.096	.074	.102	.080	1.218
07-0329 PKD	515950	6708404	SH-50-07	**31.23**	22.67	34.46	.098	.084	.163	.075	**1.513**
07-0333 PKD	515950	6708404	SH-50-07	**36.36**	22.29	30.74	.126	.101	.158	.102	1.189
07-0335 LN	516023	6708327	SH-50-07	**44.71**	23.99	22.02	**.789**	.253	**.394**	**.361**	1.019
07-0341 LN	516012	6708273	SH-50-07	23.96	**30.41**	27.03	**.895**	**1.144**	**.303**	.113	**1.648**
Batch 2											
07-0505 PNM	515883	6707106	SH-50-07	**30.35**	20.27	35.12	.478	**1.186**	.088	**.324**	**2.302**
07-0506 PNM	515883	6707106	SH-50-07	26.31	27.24	19.59	**2.006**	**4.855**	**.333**	.125	**1.818**
07-0507 LN	515882	6707096	SH-50-07	24.38	22.16	38.28	.264	.193	**.305**	<.060	**3.870**
07-0508 LP	515917	6707090	SH-50-07	18.61	**30.13**	31.60	.288	.152	**.284**	<.060	**3.636**
07-0510 LP	515902	6707067	SH-50-07	23.10	23.61	36.89	.371	.375	**.293**	<.060	**4.237**
07-0526 PNM	516136	6706849	SH-50-07	**38.93**	22.72	10.77	**.933**	**8.562**	**.329**	**.333**	.927
07-0527 PNM	516136	6706849	SH-50-07	**31.23**	24.93	20.33	**.650**	**4.827**	**.305**	.114	**3.086**
07-0534 LN	516321	6709420	SH-50-07	27.81	17.30	45.76	.058	.036	.022	.071	1.421
07-0542 LN	516248	6709322	SH-50-07	28.19	18.19	43.33	.101	.111	.062	.102	**1.668**
07-0546 LN	516473	6709296	SH-50-07	23.96	19.04	46.33	.056	.034	.049	<.060	1.096
07-0547 LN	516473	6709296	SH-50-07	21.99	19.66	47.19	.045	.024	.027	<.060	1.002
07-0548 LN	516473	6709296	SH-50-07	23.51	17.74	49.91	.058	.029	.023	.067	1.416
07-0551 PNM	516557	6709454	SH-50-07	**36.79**	12.11	44.33	.058	.045	.024	.161	1.476
07-0552 PNM	516557	6709454	SH-50-07	**32.94**	15.92	42.04	.085	.062	.036	.166	**1.580**
07-0561 PNM	516310	6709611	SH-50-07	**40.85**	20.17	26.31	.169	.036	**.210**	.166	**2.218**
07-0577 LN	516416	6708848	SH-50-07	23.96	23.73	40.33	.290	.106	**.256**	.076	**2.552**
07-0578 LN	516416	6708848	SH-50-07	26.72	25.05	33.60	**.589**	**.993**	**.345**	.106	**2.552**
07-0585 LN	515920	6708180	SH-50-07	**40.00**	22.42	25.74	.098	.106	.044	.149	1.326
07-0586 PNM	515920	6708180	SH-50-07	**37.22**	**31.00**	17.00	.055	.049	.034	.000	1.231
07-0589 LP	516053	6708327	SH-50-07	**32.08**	18.59	40.04	.096	.062	.073	<.060	1.306
07-0592 LP	515926	6708430	SH-50-07	**33.26**	14.26	41.04	.048	.043	.120	<.060	**2.869**
07-0606 LN	516073	6707316	SH-50-07	**34.44**	19.53	35.03	.048	.043	.024	<.060	1.198
07-0611 LN	515976	6708429	SH-50-07	**41.07**	15.30	35.61	.095	.067	.043	.161	1.124
07-0613 LP	515976	6708429	SH-50-07	23.83	15.21	**53.91**	.073	.043	.032	.077	1.233
07-0618 LN	516233	6707722	SH-50-07	27.81	24.50	34.61	.033	.031	.016	<.060	1.041
07-0619 LN	516233	6707722	SH-50-07	27.38	19.91	40.33	.050	.041	.042	<.060	.939
07-0620 LN	516233	6707722	SH-50-07	27.17	14.56	44.62	.051	.057	.073	<.060	1.151
Batch 3											
02-2883 PNM	515235	6706797	SH-50-07	**58.80**	13.98	13.71	.030	.060	.021	.090	.290
02-2884 PNM	515534	6706790	SH-50-07	**56.53**	13.95	16.25	.020	.050	.016	.020	.380
02-2885 PNM	515734	6706785	SH-50-07	**35.54**	18.67	26.27	.020	.030	.017	.030	.610
02-2886 PNM	515934	6706780	SH-50-07	18.90	15.71	43.33	.010	.050	.010	.020	.830
02-2887 PNM	516084	6706776	SH-50-07	**34.37**	25.84	20.51	<.010	<.010	<.010	.020	.540
02-2888 PNM	516108	6706725	SH-50-07	16.52	17.24	41.68	.050	.060	.021	.020	1.070
02-2889 PNM	516335	6706795	SH-50-07	20.55	19.09	32.98	.150	.200	.038	.020	.560
High light levels				**30.00**	**30.00**	**50.00**	**.500**	**.500**	**.200**	**.200**	**1.500**
Percentile (see notes)						75th					

Mt. Gibson Loose Lateritic Pisoliths & Nodules

ANALYSES

PPM

Sample Type	Mn	Cr	V	Cu	Pb	Zn	Ni	Co	As	Sb	Bi
(Laboratory >)	3320	1122	1120	1122	3322	1122	1122	1122	1222	1222	1222
(Method >)	III0	XXIX	XXI0	XXAA	AIXX	XXAA	XXAA	XXAA	XXXX	XXXX	XXXX
(det. limit >)	(15)	(10)	(10)	(10)	(5)	(5)	(10)	(5)	(2)	(2)	(2/5/1)
Batch 1											
07-0262 LN	34	754	1201	32	66	<5	32	16	43	4	4
07-0266 LP	132	954	1419	42	70	10	30	10	47	<2	6
07-0268 LP	76	832	1121	33	64	9	31	<5	35	2	4
07-0290 LN	128	657	1082	375	53	22	29	10	19	3	7
07-0295 LN	167	1416	1744	55	78	12	19	16	24	4	12
07-0300 LP	213	1192	1580	78	110	12	49	6	3	5	10
07-0328 PKD	108	908	1235	34	72	6	36	11	19	<2	<2
07-0329 PKD	40	854	1333	36	83	12	36	11	10	6	8
07-0333 PKD	65	673	935	37	67	9	40	9	10	4	5
07-0335 LN	227	464	602	123	65	15	79	31	16	<2	3
07-0341 LN	130	682	960	68	57	10	69	19	15	4	4
Batch 2											
07-0505 PNM	390	483	1005	52	55	24	43	11	32	4	9
07-0506 PNM	118	324	504	42	36	6	48	21	<2	9	<5
07-0507 LN	190	589	1277	38	46	6	28	8	19	5	4
07-0508 LP	54	566	1474	40	72	<5	32	6	20	4	5
07-0510 LP	84	572	1659	37	66	5	18	22	26	3	2
07-0526 PNM	231	552	469	67	44	21	53	13	17	4	11
07-0527 PNM	84	1151	1213	73	58	11	45	6	10	3	5
07-0534 LN	114	1211	1465	32	104	6	23	<5	50	9	8
07-0542 LN	107	971	1480	31	122	9	29	6	48	7	8
07-0546 LN	30	733	723	90	163	<5	27	<5	40	7	<5
07-0547 LN	28	945	1082	108	179	<5	38	28	55	6	<5
07-0548 LN	124	1275	1323	34	125	11	34	25	62	8	3
07-0551 PNM	166	954	1114	14	88	12	25	<5	20	7	<5
07-0552 PNM	126	1180	1199	41	108	15	35	<5	34	9	5
07-0561 PNM	117	1405	1582	56	109	14	42	20	36	8	7
07-0577 LN	121	999	1762	64	81	12	50	30	38	3	15
07-0578 LN	245	791	1301	68	87	7	48	<5	6	<3	<5
07-0585 LN	107	622	906	76	64	17	46	12	9	5	<5
07-0586 PNM	67	649	861	44	58	7	48	15	8	3	<5
07-0589 LP	72	855	1184	16	97	8	50	74	38	<2	4
07-0592 LP	37	747	1581	45	86	11	25	44	22	6	7
07-0606 LN	62	781	1721	18	86	9	20	<5	64	10	5
07-0611 LN	104	692	1002	38	84	14	38	13	15	<3	<5
07-0613 LP	98	1050	1462	19	111	5	32	<5	52	<2	<2
07-0618 LN	187	2092	719	107	61	15	25	21	22	2	<2
07-0619 LN	134	1650	442	134	49	43	50	11	15	6	<5
07-0620 LN	106	206	525	106	48	29	<10	13	40	6	5
Batch 3											
02-2883 PNM	105	622	413	26	41	15	28	<5	45	<2	14
02-2884 PNM	40	1116	447	18	24	8	49	5	33	2	5
02-2885 PNM	123	629	897	37	43	13	40	8	46	<2	6
02-2886 PNM	199	471	1570	42	68	22	27	7	185	<2	6
02-2887 PNM	25	664	792	42	62	10	39	7	39	5	8
02-2888 PNM	93	1346	1934	32	111	15	25	8	38	2	12
02-2889 PNM	121	1355	1332	167	15	15	42	9	37	<2	<1
High light levels	200	1000	1000	100	75	31	75	41	50	7	5
%ile (see notes)	83th	77th	80th	85th	95th	75th	80th	95th	85th	95th	98th

Mt. Gibson Loose Lateritic Pisoliths & Nodules

ANALYSES

ppm

Sample Type	Cd	In	Mo	Ag	Sn	Ge	W	Zr	Nb	Se	Au
(Laboratory >)	1100	1100	1122	3322	3322	1022	1122	1120	1120	1322	3322
(Method >)	XX00	XX00	XXXX	AAAA	XXXX	X0XX	XXXX	XXX0	XXX0	XXXX	AAAA
(det. limit >)	(1)	(1)	(2)	(0.1)	(3/1)	(2/1)	(5)	(4)	(3)	(2/3/2)	(.001)
Batch 1											
07-0262 LN	<1	<1	3	1.5	6	<2	<5	184	9	8	2.440
07-0266 LP	<1	<1	5	.5	6	<2	<5	266	8	11	2.590
07-0268 LP	<1	<1	4	.5	8	<2	12	259	6	9	1.370
07-0290 LN	<1	<1	<2	.5	<3	<2	17	129	<3	4	2.220
07-0295 LN	1	<1	3	1.0	6	2	24	283	8	3	1.440
07-0300 LP	<1	<1	4	1.0	8	<2	14	295	16	3	1.950
07-0328 PKD	<1	2	4	.5	3	3	13	246	7	3	.530
07-0329 PKD	1	<1	5	1.0	9	<2	5	259	12	2	1.260
07-0333 PKD	<1	<1	3	.5	6	2	8	255	10	6	.310
07-0335 LN	1	<1	2	1.0	3	2	8	245	11	<2	1.570
07-0341 LN	<1	<1	<2	2.5	5	2	5	290	11	6	2.650
Batch 2											
07-0505 PNM	1	1	4	.6	15	0	13	355	23	3	1.760
07-0506 PNM	<1	<1	4	.5	9	0	8	279	17	4	1.050
07-0507 LN	1	<1	4	.8	20	0	24	470	40	3	3.780
07-0508 LP	1	<1	5	1.1	10	0	19	462	28	3	6.000
07-0510 LP	<1	<1	6	.8	15	0	20	502	29	5	1.290
07-0526 PNM	<1	1	4	1.1	5	0	<5	82	8	<3	1.080
07-0527 PNM	<1	<1	4	2.3	9	0	<5	274	20	4	.930
07-0534 LN	1	<1	2	.5	6	0	15	245	6	7	3.300
07-0542 LN	2	<1	5	.7	8	0	15	293	10	<3	3.480
07-0546 LN	1	<1	2	.4	3	0	8	175	3	3	3.270
07-0547 LN	2	<1	2	.6	<3	0	9	172	6	6	.500
07-0548 LN	1	1	3	.5	3	0	8	289	10	<3	.450
07-0551 PNM	<1	<1	5	.4	4	0	14	312	13	<3	.082
07-0552 PNM	<1	1	6	.4	8	0	22	287	11	<3	.690
07-0561 PNM	1	<1	3	.3	7	0	14	280	10	<3	1.040
07-0577 LN	<1	2	3	1.3	<3	0	21	276	9	3	1.540
07-0578 LN	1	<1	<2	.6	<3	0	15	275	10	<3	2.000
07-0585 LN	<1	<1	6	.7	5	0	<5	313	9	4	6.280
07-0586 PNM	<1	<1	4	.9	<3	0	7	246	6	<3	1.900
07-0589 LP	<1	<1	4	.3	7	0	<5	268	12	<3	3.560
07-0592 LP	1	<1	4	2.2	8	0	25	320	16	3	4.490
07-0606 LN	<1	1	3	.3	4	0	6	258	8	7	3.260
07-0611 LN	<1	1	3	.3	10	0	<5	301	11	<3	.410
07-0613 LP	<1	<1	5	.4	7	0	17	238	10	3	.870
07-0618 LN	<1	<1	<2	1.1	4	0	<5	142	8	4	.970
07-0619 LN	<1	<1	<2	.4	4	0	14	100	6	3	.340
07-0620 LN	<1	2	2	.4	<3	0	11	92	7	3	.640
Batch 3											
02-2883 PNM	0	0	16	<.1	<1	<1	14	275	11	4	.009
02-2884 PNM	0	0	10	<.1	2	<1	12	329	16	<2	.005
02-2885 PNM	0	0	5	.7	1	<1	<5	269	12	2	.160
02-2886 PNM	0	0	2	.1	2	3	5	297	16	8	.112
02-2887 PNM	0	0	7	1.1	4	<1	<5	184	9	6	1.449
02-2888 PNM	0	0	4	.6	11	2	11	305	15	5	1.535
02-2889 PNM	0	0	1	1.7	3	1	<5	391	9	6	.033
High light levels	0	0	9	.5	7	2	15	300	28	9	.030
%ile (see notes)			95th	95th	95th	98th	95th		95th	98th	95th

Mt. Gibson Loose Lateritic Pisoliths & Nodules

ANALYSES

Sample	Type (Laboratory>) (Method >) (det. limit >)	AMG Coordinates Easting	Northing	Sheet	Weight percent SiO2 3320 III0 (0.1)	Al2O3 3320 III0 (0.02)	Fe2O3 3320 III0 (0.01)	MgO 3320 III0 (.01)	CaO 3320 III0 (.01)	Na2O 3320 III0 (.01)	K2O 3320 III0 (0.06/ 0.01)	TiO2 3320 III0 (.003)
02-2890	PNM	516535	6706790	SH-50-07	20.37	15.29	38.83	.040	.030	.012	.030	.620
02-2891	PNM	516517	6707065	SH-50-07	**36.66**	24.99	18.41	<.010	.030	.011	.010	.550
02-2892	PNM	516342	6707080	SH-50-07	29.16	12.01	13.03	**2.840**	**15.810**	.078	.110	.350
02-2893	PNM	516142	6707100	SH-50-07	29.67	13.70	23.67	**.690**	**7.810**	.049	.090	.450
02-2894	PNM	515942	6707080	SH-50-07	14.59	12.97	45.12	.180	.270	.012	.020	1.310
02-2895	PNM	515742	6707085	SH-50-07	22.80	19.49	31.86	.080	.070	.018	.010	.730
02-2896	LP	515399	6707393	SH-50-07	**40.30**	24.80	35.50	.060	.050	<.010	.010	.440
02-2887	LN	515599	6707358	SH-50-07	22.61	19.90	29.81	.050	.050	.013	.010	.680
02-2898	PNM	515549	6707389	SH-50-07	15.24	14.90	42.88	.050	.040	<.010	.010	1.340
02-2899	PNM	515949	6707379	SH-50-07	26.98	18.26	27.07	.170	.070	.027	.070	.700
02-2900	PNM	516088	6707350	SH-50-07	**30.11**	24.00	24.20	.030	.010	<.010	.010	.900
02-2903	LN	516149	6707374	SH-50-07	**30.81**	22.93	24.78	.020	.020	<.010	.010	.760
02-2904	PNM	516349	6707369	SH-50-07	23.57	15.81	35.11	.060	.030	.018	.020	.890
02-2905	PNM	516549	6707364	SH-50-07	**38.00**	22.50	49.90	.030	.030	<.010	.010	.450
02-2906	PNM	515919	6708180	SH-50-07	15.12	25.39	34.10	.090	.360	.035	.010	**1.890**
02-2907	LP	515669	6708187	SH-50-07	**31.52**	18.38	26.57	<.010	.010	<.010	.010	**1.730**
02-2908	LN	516169	6708204	SH-50-07	**33.79**	18.48	26.16	.220	.030	**.244**	.040	.840
02-2909	PNM	516169	6708174	SH-50-07	**32.38**	17.45	27.46	.170	.130	.101	.030	.770
02-2911	LN	516189	6708974	SH-50-07	29.17	24.86	22.25	.090	.030	<.010	.030	.680
02-2912	LN	516023	6708928	SH-50-07	12.76	25.86	30.56	.270	.330	.186	.030	**2.040**
02-2913	LN	516092	6709076	SH-50-07	25.54	24.21	23.45	.260	.420	.123	.020	**1.630**
02-2914	LN	516586	6708839	SH-50-07	**36.70**	21.37	22.00	.040	.030	<.010	.020	.440
02-2916	LP	516258	6709312	SH-50-07	**30.80**	22.90	21.58	.180	**1.190**	.117	.030	.670
02-2917	LN	515898	6709331	SH-50-07	6.01	**36.57**	24.18	.150	.320	.015	.030	**1.640**
02-2918	PNM	516548	6709315	SH-50-07	**30.14**	14.07	32.51	.070	.070	.012	.030	.740
02-2919	LP	516173	6709334	SH-50-07	10.81	9.14	49.58	.170	.350	.016	.020	**1.740**
02-2920	LP	516474	6709367	SH-50-07	18.97	14.36	39.51	.050	.030	<.010	.020	.820
02-2921	PNM	516365	6709620	SH-50-07	25.56	24.21	24.23	.010	.010	<.010	.010	.930
02-2922	PNM	515960	6709805	SH-50-07	5.35	**36.20**	24.71	.090	.230	.011	.010	**1.530**
02-2923	PNM	516210	6709799	SH-50-07	7.90	21.58	39.95	.030	.040	<.010	.010	1.380
02-2924	PNM	516410	6709794	SH-50-07	17.03	16.68	37.18	.020	.040	.011	.020	1.160
02-2925	PNM	516610	6709789	SH-50-07	13.28	14.67	43.35	.020	.030	<.010	.010	1.080
02-2926	PNM	516810	6709784	SH-50-07	12.04	14.27	47.77	<.010	.020	<.010	.010	1.070
02-2927	PNM	516460	6709817	SH-50-07	10.22	13.73	47.53	.010	.040	<.010	.010	1.210
02-2928	PNM	515892	6708681	SH-50-07	**57.17**	15.35	13.09	.020	.020	.021	.020	.440
02-2929	PNM	515634	6708763	SH-50-07	26.62	18.91	30.19	.010	.020	.033	.010	1.170
02-2930	PNM	516180	6708624	SH-50-07	**52.98**	14.04	16.53	.030	.030	.016	.020	.430
02-2931	PNM	515947	6707279	SH-50-07	**35.81**	22.05	19.50	<.010	<.010	<.010	.020	.710
02-2932	PNM	516147	6707274	SH-50-07	**32.49**	23.36	20.46	<.010	.010	<.010	.010	1.040
02-2933	PNM	516297	6707296	SH-50-07	**30.06**	24.00	23.18	.040	.070	.035	.010	.730
02-2934	LN	516053	6707542	SH-50-07	**35.85**	14.28	27.41	.030	.030	.016	.010	1.460
02-2935	PNM	516153	6707510	SH-50-07	17.95	11.99	41.77	.020	.050	<.010	.020	.960
02-2936	LN	516352	6707469	SH-50-07	25.04	19.22	29.92	.070	.130	.088	.020	.630
02-2937	PNM	516056	6707637	SH-50-07	15.00	12.10	45.80	.040	.030	<.010	.010	1.310
02-2938	PNM	516155	6707614	SH-50-07	17.00	13.20	43.40	.050	.030	<.010	.010	1.040
02-2939	PNM	516257	6707672	SH-50-07	20.83	15.70	32.88	<.010	.020	<.010	.010	.790
02-2940	PNM	516379	6708569	SH-50-07	29.81	12.93	32.48	.040	.030	.021	.020	.650
02-2942	LN	516184	6707174	SH-50-07	**40.37**	16.83	13.78	<.010	<.010	.029	.060	.430
High light levels					**30.00**	**30.00**	**50.00**	**.500**	**.500**	**.200**	**.200**	**1.500**
Percentile (see notes)							75th					

Mt. Gibson Loose Lateritic Pisoliths & Nodules

ANALYSES

ppm

Sample Type	Mn	Cr	V	Cu	Pb	Zn	Ni	Co	As	Sb	Bi
(Laboratory >)	3320	1122	1120	1122	3322	1122	1122	1122	1222	1222	1222
(Method >)	III0	XXIX	XXI0	XXAA	AIXX	XXAA	XXAA	XXAA	XXXX	XXXX	XXXX
(det. limit >)	(15)	(10)	(10)	(10)	(5)	(5)	(10)	(5)	(2)	(2)	(2/5/1)
02-2890 PNM	132	**1655**	**1373**	24	69	16	25	7	47	<2	**6**
02-2891 PNM	58	**1060**	**1399**	35	62	11	30	7	**76**	<2	**8**
02-2892 PNM	177	382	539	76	57	**31**	20	6	47	<2	3
02-2893 PNM	**250**	550	849	64	68	28	24	<5	**50**	<2	**6**
02-2894 PNM	105	677	**2192**	47	**79**	14	18	<5	28	<2	**8**
02-2895 PNM	143	288	**1592**	30	51	16	17	<5	31	<2	1
02-2896 LP	40	**2500**	**1020**	43	23	8	63	8	35	<2	<1
02-2897 LN	104	231	633	29	30	13	14	<5	18	2	1
02-2898 PNM	125	732	**1669**	10	**90**	13	12	6	23	2	**6**
02-2899 PNM	125	721	**1444**	73	52	**35**	10	<5	27	4	<1
02-2900 PNM	61	621	**1971**	20	**97**	13	42	<5	**69**	5	**8**
02-2903 LN	26	**1452**	**2394**	27	60	8	33	<5	**88**	6	**44**
02-2904 PNM	82	**1590**	**1749**	29	**89**	20	47	7	**76**	5	**15**
02-2905 PNM	50	**1300**	**1310**	15	31	12	41	<5	63	5	**6**
02-2906 PNM	124	**1231**	**1623**	27	**78**	18	32	<5	15	**9**	**13**
02-2907 LP	34	585	**1761**	14	59	12	16	<5	34	<2	<1
02-2908 LN	92	677	**1183**	50	59	13	39	5	38	**9**	2
02-2909 PNM	162	573	**1183**	63	52	13	37	5	31	<2	<1
02-2911 LN	77	888	**1208**	37	42	14	53	8	40	<2	**12**
02-2912 LN	**388**	**1088**	**1532**	46	37	**31**	37	9	43	3	**9**
02-2913 LN	**253**	**1099**	**1358**	95	42	28	59	8	19	<2	3
02-2914 LN	116	646	717	25	22	10	33	7	37	<2	3
02-2916 LP	39	697	902	**108**	52	11	55	8	40	**8**	**9**
02-2917 LN	**960**	829	942	65	48	23	34	20	17	<2	1
02-2918 PNM	107	902	892	33	**90**	**15**	40	7	**55**	**15**	**5**
02-2919 LP	137	949	**2722**	53	72	19	8	<5	33	**20**	**7**
02-2920 LP	145	**1392**	**1495**	30	**89**	17	37	5	**65**	**10**	**11**
02-2921 PNM	45	1769	**1377**	28	**93**	15	42	7	**51**	3	**5**
02-2922 PNM	**1327**	431	899	50	10	20	36	20	14	<2	1
02-2923 PNM	**244**	807	**1437**	17	38	17	24	7	18	<2	<1
02-2924 PNM	134	**1423**	**1788**	27	**93**	18	34	7	**56**	**7**	**10**
02-2925 PNM	184	**1797**	**1419**	21	**77**	23	27	<5	**69**	**12**	**4**
02-2926 PNM	126	**1744**	**1423**	16	55	21	30	<5	**62**	**9**	**4**
02-2927 PNM	**208**	**2156**	**1935**	27	**90**	21	16	5	**70**	5	**13**
02-2928 PNM	45	409	418	21	29	11	32	<5	23	<2	3
02-2929 PNM	106	609	**1710**	26	34	22	46	8	17	3	<1
02-2930 PNM	57	525	527	37	48	16	34	<5	35	<2	3
02-2931 PNM	57	473	**1151**	27	39	12	20	<5	**84**	<2	**4**
02-2932 PNM	102	753	**1694**	42	**79**	16	18	<5	**116**	4	**16**
02-2933 PNM	29	784	**1016**	35	**80**	12	42	5	49	<2	1
02-2934 LN	62	**1144**	**2083**	28	28	10	25	<5	39	4	**19**
02-2935 PNM	185	**1368**	**2139**	29	53	19	18	<5	**125**	**7**	**13**
02-2936 LN	104	**1362**	868	76	38	24	34	6	**83**	<2	**4**
02-2937 PNM	160	**1580**	**2700**	22	42	17	15	6	**116**	2	**7**
02-2938 PNM	160	**1500**	**2500**	27	**78**	18	24	6	**130**	6	**3**
02-2939 PNM	120	**1122**	**1534**	38	53	25	26	6	**112**	4	**10**
02-2940 PNM	**222**	392	892	62	58	29	34	8	31	4	2
02-2942 LN	49	436	606	33	32	15	37	<5	47	6	**10**
High light levels	**200**	**1000**	**1000**	**100**	**75**	**31**	**75**	**41**	**50**	**7**	**5**
%ile (see notes)	83th	77th	80th	85th	95th	75th	80th	95th	85th	95th	98th

Mt. Gibson Loose Lateritic Pisoliths & Nodules

ANALYSES

Sample Type	Cd	In	Mo	Ag	Sn	Ge	W	Zr	Nb	Se	Au
						ppm					
(Laboratory >)	1100	1100	1122	3322	3322	1022	1122	1120	1120	1322	3322
(Method >)	XX00	XX00	XXXX	AAAA	XXXX	X0XX	XXXX	XXX0	XXX0	XXXX	AAAA
(det. limit >)	(1)	(1)	(2)	(0.1)	(3/1)	(2/1)	(5)	(4)	(3)	(2/3/2)	(.001)
02-2890 PNM	0	0	2	<.1	7	<1	<5	320	9	11	.021
02-2891 PNM	0	0	3	<.1	3	<1	<5	207	8	4	.953
02-2892 PNM	0	0	<1	<.1	<1	<1	15	134	3	2	2.080
02-2893 PNM	0	0	2	<.1	<1	<1	13	185	4	<2	1.085
02-2894 PNM	0	0	6	.3	4	<1	25	332	15	3	2.652
02-2895 PNM	0	0	3	.1	7	<1	9	257	6	<2	.050
02-2896 LP	0	0	4	<.1	4	<1	<5	295	10	2	.033
02-2897 LN	0	0	<1	.5	<1	2	<5	221	4	8	1.187
02-2898 PNM	0	0	3	<.1	2	<1	11	405	16	4	.530
02-2899 PNM	0	0	2	<.1	<1	1	13	185	5	10	.425
02-2900 PNM	0	0	2	2.0	<1	2	11	287	5	<2	11.705
02-2903 LN	0	0	1	.4	3	<1	5	245	7	12	12.615
02-2904 PNM	0	0	2	.2	1	1	5	285	11	7	1.099
02-2905 PNM	0	0	5	<.1	3	<1	9	212	10	<2	.013
02-2906 PNM	0	0	<1	.4	5	<1	11	378	16	<2	1.681
02-2907 LP	0	0	3	.3	6	2	9	420	18	<2	.125
02-2908 LN	0	0	9	<.1	6	<1	5	265	8	<2	.078
02-2909 PNM	0	0	1	.1	3	<1	9	264	8	3	.190
02-2911 LN	0	0	4	.6	6	<1	7	250	9	8	4.707
02-2912 LN	0	0	<1	1.7	<1	<1	15	370	14	3	9.910
02-2913 LN	0	0	<1	1.7	<1	4	6	286	14	<2	1.704
02-2914 LN	0	0	2	.1	2	<1	<5	252	13	4	.034
02-2916 LP	0	0	1	2.6	1	2	17	210	7	<2	2.104
02-2917 LN	0	0	1	3.3	2	<1	31	327	12	3	.583
02-2918 PNM	0	0	1	.5	6	2	<5	259	10	<2	.311
02-2919 LP	0	0	3	1.6	1	<1	45	378	14	<2	.858
02-2920 LP	0	0	1	.7	8	2	25	282	8	<2	.870
02-2921 PNM	0	0	1	.9	8	3	16	246	7	7	3.185
02-2922 PNM	0	0	2	1.1	4	<1	15	266	10	<2	.059
02-2923 PNM	0	0	2	1.9	<1	1	9	306	12	<2	.579
02-2924 PNM	0	0	2	1.5	2	3	12	285	14	5	6.633
02-2925 PNM	0	0	3	1.2	7	3	13	283	9	<2	.396
02-2926 PNM	0	0	4	.5	<1	2	36	318	12	6	.050
02-2927 PNM	0	0	7	2.3	5	1	22	273	11	<2	2.197
02-2928 PNM	0	0	<1	.1	2	<1	<5	261	8	<2	.397
02-2929 PNM	0	0	1	.4	<1	<1	8	282	11	2	.047
02-2930 PNM	0	0	3	.7	1	<1	12	230	10	8	.733
02-2931 PNM	0	0	<1	.1	2	2	<5	236	8	14	5.771
02-2932 PNM	0	0	2	.5	3	<1	<5	274	8	3	12.757
02-2933 PNM	0	0	2	1.5	1	<1	<5	189	10	4	4.779
02-2934 LN	0	0	<1	1.5	3	3	8	340	17	3	.941
02-2935 PNM	0	0	5	.1	1	<1	<5	324	11	5	2.625
02-2936 LN	0	0	5	.7	<1	<1	10	196	8	2	1.757
02-2937 PNM	0	0	2	.3	8	<1	6	378	7	4	1.558
02-2938 PNM	0	0	3	.8	<1	<1	18	354	14	6	3.004
02-2939 PNM	0	0	5	.6	<1	3	<5	271	11	4	1.665
02-2940 PNM	0	0	2	.6	7	1	<5	222	10	<2	.060
02-2942 LN	0	0	2	.1	2	<1	<5	233	10	6	.756
High light levels	0	0	9	.5	7	2	15	300	28	9	.030
%ile (see notes)			95th	95th	95th	98th	95th		95th	98th	95th

Mt. Gibson Loose Lateritic Pisoliths & Nodules

ANALYSES

Sample Type (Laboratory)) (Method)) (det. limit))	AMG Coordinates Easting	Northing	Sheet	Weight percent SiO2 3320 III0 (0.1)	Al2O3 3320 III0 (0.02)	Fe2O3 3320 III0 (0.01)	MgO 3320 III0 (.01)	CaO 3320 III0 (.01)	Na2O 3320 III0 (.01)	K2O 3320 III0 (0.06/ 0.01)	TiO2 3320 III0 (.003)
02-2943 LP Batch 4	516184	67071	SH-50-07	18.69	12.54	28.01	<.010	<.010	.020	.020	.490
MGN0002 LP	516087	6707976	SH-50-07	.00	.00	.00	.000	.000	.000	.000	.000
MGN0003 LP	516362	6707969	SH-50-07	.00	.00	.00	.000	.000	.000	.000	.000
MGN0004 LP	515823	6708432	SH-50-07	.00	.00	.00	.000	.000	.000	.000	.000
MGN0005 LP	516272	6708421	SH-50-07	.00	.00	.00	.000	.000	.000	.000	.000
MGN0006 LP	515736	6708584	SH-50-07	.00	.00	.00	.000	.000	.000	.000	.000
MGN0007 LP	516181	6708799	SH-50-07	.00	.00	.00	.000	.000	.000	.000	.000
MGN0010 LN	516297	6709071	SH-50-07	.00	.00	.00	.000	.000	.000	.000	.000
MGN0011 LN	516447	6709068	SH-50-07	.00	.00	.00	.000	.000	.000	.000	.000
MGN0012 LN	516617	6710364	SH-50-07	.00	.00	.00	.000	.000	.000	.000	.000
MGN0013 LP	516446	6710318	SH-50-07	.00	.00	.00	.000	.000	.000	.000	.000
MGN0014 LP	516216	6710323	SH-50-07	.00	.00	.00	.000	.000	.000	.000	.000
MGN0015 LP	516563	6710165	SH-50-07	.00	.00	.00	.000	.000	.000	.000	.000
MGN0016 LN	516362	6710120	SH-50-07	.00	.00	.00	.000	.000	.000	.000	.000
MGN0018 LP	516585	6710062	SH-50-07	.00	.00	.00	.000	.000	.000	.000	.000
MGN0019 LP	516509	6710016	SH-50-07	.00	.00	.00	.000	.000	.000	.000	.000
MGN0020 LP	516408	6709969	SH-50-07	.00	.00	.00	.000	.000	.000	.000	.000
MGN0021 LN	516177	6709924	SH-50-07	.00	.00	.00	.000	.000	.000	.000	.000
MGN0024 LN	516506	6709866	SH-50-07	.00	.00	.00	.000	.000	.000	.000	.000
MGN0025 LP	516681	6709862	SH-50-07	.00	.00	.00	.000	.000	.000	.000	.000
MGN0026 NP	516675	6709612	SH-50-07	.00	.00	.00	.000	.000	.000	.000	.000
MGN0027 LP	516500	6709617	SH-50-07	.00	.00	.00	.000	.000	.000	.000	.000
MGN0028 LP	516350	6709620	SH-50-07	.00	.00	.00	.000	.000	.000	.000	.000
MGN0030 LP	516125	6709585	SH-50-07	.00	.00	.00	.000	.000	.000	.000	.000
MGN0035 LP	516820	6710459	SH-50-07	.00	.00	.00	.000	.000	.000	.000	.000
MGN0038 LP	516713	6710163	SH-50-07	.00	.00	.00	.000	.000	.000	.000	.000
MGN0039 LN	516943	6710156	SH-50-07	.00	.00	.00	.000	.000	.000	.000	.000
High light levels				30.00	30.00	50.00	.500	.500	.200	.200	1.500
Percentile (see notes)						75th					

Mt. Gibson Loose Lateritic Pisoliths & Nodules

ANALYSES

ppm

Sample Type	Mn	Cr	V	Cu	Pb	Zn	Ni	Co	As	Sb	Bi
(Laboratory >)	3320	1122	1120	1122	3322	1122	1122	1122	1222	1222	1222
(Method >)	III0	XXIX	XXI0	XXAA	AIXX	XXAA	XXAA	XXAA	XXXX	XXXX	XXXX
(det. limit >)	(15)	(10)	(10)	(10)	(5)	(5)	(10)	(5)	(2)	(2)	(2/5/1)
02-2943 LP	109	704	1084	38	86	39	36	9	82	<2	14
Batch 4											
MGN0002 LP	0	680	0	40	58	18	17	8	14	<2	4
MGN0003 LP	0	770	0	50	60	19	28	8	39	8	2
MGN0004 LP	0	460	0	37	68	13	40	<5	12	3	3
MGN0005 LP	0	770	0	59	80	27	21	<5	24	3	7
MGN0006 LP	0	710	0	25	46	14	30	<5	24	2	<1
MGN0007 LP	0	1420	0	34	62	23	27	<5	49	8	<1
MGN0010 LN	0	890	0	31	26	12	29	<5	31	<2	5
MGN0011 LN	0	620	0	28	42	9	23	<5	32	<2	5
MGN0012 LN	0	1060	0	53	52	12	13	9	11	3	8
MGN0013 LP	0	1180	0	39	120	17	17	<5	80	7	<1
MGN0014 LP	0	1440	0	22	76	17	14	<5	22	3	14
MGN0015 LP	0	1620	0	38	130	25	28	<5	68	11	7
MGN0016 LN	0	830	0	45	68	19	28	<5	31	7	8
MGN0018 LP	0	1840	0	42	125	25	17	<5	74	19	10
MGN0019 LP	0	1840	0	54	115	30	18	<5	44	15	7
MGN0020 LP	0	1680	0	24	135	14	18	<5	155	27	7
MGN0021 LN	0	375	0	315	46	42	20	<5	30	2	5
MGN0024 LN	0	690	0	47	54	29	25	<5	56	8	<1
MGN0025 LP	0	1600	0	69	94	30	16	<5	60	10	9
MGN0026 LN	0	2240	0	36	64	12	19	<5	64	12	<1
MGN0027 LP	0	1220	0	38	62	13	35	<5	39	3	5
MGN0028 LP	0	1480	0	27	42	21	19	<5	21	10	4
MGN0030 LP	0	730	0	49	12	22	15	17	6	3	3
MGN0035 LP	0	1620	0	46	66	22	25	7	35	11	11
MGN0038 LP	0	1140	0	52	42	27	24	8	34	8	<1
MGN0039 LN	0	1720	0	35	24	15	<5	<5	14	<2	<1
High light levels	200	1000	1000	100	75	31	75	41	50	7	5
%ile (see notes)	83th	77th	80th	85th	95th	75th	80th	95th	85th	95th	98th

Mt. Gibson Loose Lateritic Pisoliths & Nodules

ANALYSES

Sample Type	Cd	In	Mo	Ag	Sn	Ge	W	Zr	Nb	Se	Au
						ppm					
(Laboratory >)	1100	1100	1122	3322	3322	1022	1122	1120	1120	1322	3322
(Method >)	XX00	XX00	XXXX	AAAA	XXXX	X0XX	XXXX	XXX0	XXX0	XXXX	AAAA
(det. limit >)	(1)	(1)	(2)	(0.1)	(3/1)	(2/1)	(5)	(4)	(3)	(2/3/2)	(.001)
02-2943 LP	0	0	4	.7	<1	1	16	270	8	2	1.205
Batch 4											
MGN0002 LP	0	0	3	.4	3	<1	6	0	0	2	.840
MGN0003 LP	0	0	<1	.5	3	1	<5	0	0	<2	.840
MGN0004 LP	0	0	2	.6	1	<1	12	0	0	<2	.150
MGN0005 LP	0	0	1	<.1	3	<1	14	0	0	<2	.210
MGN0006 LP	0	0	1	<.1	2	<1	<5	0	0	4	.340
MGN0007 LP	0	0	3	.3	3	1	10	0	0	3	.330
MGN0010 LN	0	0	3	<.1	3	1	<5	0	0	<2	.540
MGN0011 LN	0	0	3	1.5	3	<1	8	0	0	<2	.110
MGN0012 LN	0	0	3	.5	3	<1	14	0	0	<2	.060
MGN0013 LP	0	0	12	.2	3	<1	32	0	0	<2	.190
MGN0014 LP	0	0	3	.5	<1	<1	60	0	0	<2	.350
MGN0015 LP	0	0	4	<.1	5	1	20	0	0	<2	1.500
MGN0016 LN	0	0	<1	.5	1	<1	8	0	0	3	2.700
MGN0018 LP	0	0	4	.9	6	<1	8	0	0	5	.460
MGN0019 LP	0	0	5	.6	3	2	18	0	0	<2	.400
MGN0020 LP	0	0	9	.4	5	<1	18	0	0	2	1.350
MGN0021 LN	0	0	1	<.1	2	<1	<5	0	0	6	.360
MGN0024 LN	0	0	3	2.0	2	<1	8	0	0	2	.800
MGN0025 LP	0	0	4	1.2	2	<1	16	0	0	4	1.400
MGN0026 LN	0	0	1	1.6	6	<1	8	0	0	<2	.240
MGN0027 LP	0	0	3	.5	3	<1	10	0	0	3	1.050
MGN0028 LP	0	0	4	.2	6	4	12	0	0	3	.130
MGN0030 LP	0	0	2	1.0	7	<1	12	0	0	<2	.100
MGN0035 LP	0	0	2	1.0	2	<1	22	0	0	7	.700
MGN0038 LP	0	0	5	1.2	<1	1	8	0	0	<2	.240
MGN0039 LN	0	0	1	.1	<1	<1	36	0	0	2	.054
High light levels	0	0	9	.5	7	2	15	300	28	9	.030
%ile (see notes)			95th	95th	95th	98th	95th		95th	98th	95th